

On the dehydration of lactic acid in near- and supercritical water



TECHNISCHE
UNIVERSITÄT
DARMSTADT

Vom Fachbereich Chemie
der Technischen Universität Darmstadt

zur Erlangung des akademischen Grades eines
Doktor-Ingenieurs (Dr.-Ing.)
genehmigte

Dissertation

vorgelegt von

Horea Stefan Szedlacsek, Inginer Diplomat
aus Bukarest (Rumänien)

Referent: Prof. Dr.-Ing. H. Vogel
Korreferent: Prof. Dr. rer. nat. P. Claus
Tag der Einreichung: 09.11.2012
Tag der mündlichen Prüfung: 21.01.2013

Darmstadt 2013

D 17

*Für eine Liebe,
die mir die Kraft und Begeisterung gegeben hat,
diese Arbeit zu Ende zu bringen*



Die vorliegende Arbeit wurde im Zeitraum vom 01. Dezember 2006 bis 01. April 2011 am Ernst-Berl-Institut für Technische und Makromolekulare Chemie der Technischen Universität Darmstadt unter Leitung von Herrn Prof. Dr.-Ing. G. H. Vogel durchgeführt.



Acknowledgements

I would like to thank Professor Herbert Vogel for the given opportunity to work in his group as well as for the supervision of my research activity.

I am grateful to Professor Frieder Lichtenthaler for his helpful advice along the time, but much more for his friendship for which I feel deeply endowed.

I thank Professor Alfons Drochner and Nina Blickhan for their help with Presto simulation software.

Many thanks to Dr. Stefan Immel for his advice regarding reaction mechanisms and to Dr. Reinhard Meusinger for the helpful discussions concerning the NMR analyses.

Thanks to my colleagues Heiner Busch and Andrea Soler for the productive discussions concerning the reaction network of lactic acid dehydration.

I would like to thank the employees of the workshops, especially to Harald Jung for the fine execution of the ordered technical equipment.

I wish to thank Walter David for his willingness to help and major contribution in appending an UV-Spectrometer to the installation on which the experimental work has been carried out.

Thanks to Renate Clemens and Kornelia Thomalla for their good vibes and support.

Besides, I wish to thank to a number of persons, all with special powers, for their precious support:

To Gabriela Viorica Ghimpeteanu (Găbica) for her patience with me and too-long-lasting support, for her congenial presence and sometimes wise if not brilliant ideas.

To my university colleagues and good friends Balázs László (Jegosu') and Ramona Veér for their cheering and unconditional support through hard times.

To Stephan Urfels (Meserie) for his solid friendship, for the good times spent together, for the fine philosophical walks through the Odenwald and for his thorough and sometimes brutal correction of my dissertation.

To Dr. Cosmin Conțiu (Jacksy - whose excellence in the chemical industry, in my opinion, nears perfection) for his perplexing good-witted remarks and for some warm-hearted words which helped me a lot.

To Dr. Michael Sarlea (Tiger) for introducing me to a new work environment and for the demonstration of his "golden hand" ability to make chemical equipment obey the user.

To the magnificent three Tudor Vasiliu, Theodor-Ovidiu Pârvu and Mihai Dragu for their (useless) efforts to bring me to normality and for the late nights out in Bucharest, London, Paris, Berlin, Darmstadt or Lindau.

To Irina Dulgheru (la muse des écrivains), Adriana Șola, Claudia Cîrlig, Cristina Șerbănescu, Aura-Eliza Statina, Joy-Antoinette Aselmann and Anna-Dorothee Arnold for their cheering presence during my PhD at times of loneliness.

To Nadine and Michael Dürr for their warm friendship.

To Péter Katona, a renowned Colchester-based Psychologist, Freud scholar and explorer of the Far-East: for his freudian ideas (most of which I reject from all my heart), for the endless hours we have spent trying to explore the psyche and for his deep wisdom which confirmed that a bath in December in the North Sea is absolutely necessary.

To my family for their inexhaustible loving support and especially to my father with his slow, deep and rigorous thinking which always brought me invaluable insight and optimism in whatever problem I was confronted with.



CONTENTS

1. INTRODUCTION	4
2. STATE OF THE ART IN LACTIC ACID DEHYDRATION	8
2.1. REACTION NETWORK.....	9
2.1.1. <i>Pathway I – Decarbonylation</i>	10
2.1.2. <i>Pathway II – Decarboxylation</i>	10
2.1.3. <i>Pathway III – Dehydration</i>	11
2.2. EFFECT OF REACTION PARAMETERS.....	12
2.2.1. <i>Effect of pH</i>	12
2.2.2. <i>Influence of Different Acid Catalysts</i>	12
2.2.3. <i>Influence of Na₂HPO₄</i>	12
2.2.4. <i>Effect of the Initial Concentration</i>	12
2.2.5. <i>Effect of Temperature</i>	13
2.2.6. <i>Effect of Pressure and Solvent Density</i>	15
2.2.7. <i>Reactor Aging</i>	16
2.3. ALTERNATIVE METHODS INVOLVING DEHYDRATION OF LACTIC ACID TO ACRYLIC ACID.....	16
2.3.1. <i>Heterogeneous Catalysis – Reaction of Lactic Acid over Supported Phosphate Catalysts</i>	16
2.3.2. <i>Reaction of Lactic Acid Catalysed by Group VIII Metal Complexes</i>	17
2.3.3. <i>Biotechnological Pathways</i>	17
2.4. PATENTS.....	18
2.5. OUTLINE OF THE RESEARCH ACTIVITY.....	19
3. FUNDAMENTALS IN NEAR- AND SUPERCRITICAL WATER	20
3.1. PHASE EQUILIBRIA AND EQUATIONS OF STATE.....	20
3.1.1. <i>The Phase Diagram</i>	20
3.1.2. <i>Density, Dielectric Constant and Dissociation Constant</i>	21
4. BINARY MIXTURES OF NEAR- AND SUPERCRITICAL WATER	24
4.1. PHASE BEHAVIOUR AND SOLUBILITY OF ELECTROLYTES IN SCW.....	24
4.2. MICROSCOPIC EFFECTS.....	27
4.3. ACIDS AND BASES IN SCW.....	32
5. EXPERIMENTAL PART	36
5.1. DESCRIPTION OF THE EXPERIMENTAL APPARATUS.....	36
5.2. DESIGN AND CONSTRUCTION OF THE REACTORS.....	37
5.2.1. <i>Pipe Reactor</i>	37
5.2.2. <i>Continuously Stirred Tank Reactor</i>	38
5.2.3. <i>Temperature Control</i>	38
5.3. OPERATION OF THE INSTALLATION.....	40
5.4. METHODS OF ANALYSIS.....	42
5.4.1. <i>HPLC Analysis</i>	42
5.4.2. <i>Quantification of 3-Hydroxypropionic acid</i>	43
5.4.3. <i>FTIR Measurements</i>	48
5.4.4. <i>Enzymatic Analysis of L-lactic Acid</i>	49
5.4.5. <i>Preparation of 2-methoxy-propionic Acid</i>	50
6. RESULTS AND DISCUSSION	51
6.1. MEASUREMENTS IN PURE WATER.....	51
6.1.1. <i>Influence of the Residence Time</i>	51
6.1.2. <i>Influence of the Pressure</i>	53
6.1.3. <i>Influence of the Temperature</i>	55
6.1.4. <i>Influence of the Lactic Acid initial Concentration</i>	57

6.1.5.	<i>Influence of the Reactor Aging</i>	58
6.1.6.	<i>Stability of Acrylic Acid</i>	60
6.2.	ANALYSIS OF THE GAS PHASE	63
6.3.	DEHYDRATION OF SUBSTANCES SIMILAR TO LACTIC ACID	65
6.3.1.	<i>Lactic Acid Methyl Ester</i>	65
6.3.2.	<i>2-Methoxy-propionic Acid</i>	67
6.3.3.	<i>3-Hydroxypropionic Acid</i>	68
6.3.4.	<i>2-Hydroxy-isobutyric Acid</i>	70
6.3.5.	<i>2-Hydroxy-3-methylbutyric acid</i>	71
6.4.	INFLUENCE OF PHOSPHATES	73
6.4.1.	<i>Preliminary Experiments for Catalyst Screening</i>	73
6.4.2.	<i>Influence of Acetic and Phosphoric Acid</i>	76
6.4.3.	<i>Phosphates: The H₃PO₄/KOH Ratio</i>	78
6.4.4.	<i>Phosphates: Effect of Different Concentrations</i>	79
6.4.5.	<i>Phosphates: Effect of Different Cations</i>	80
6.4.6.	<i>Phosphates: Effect on the Stability of Acrylic Acid</i>	82
7.	REACTION KINETICS AND MECHANISMS	84
7.1.	DESCRIPTION OF THE KINETIC MODEL	84
7.2.	ESTIMATION OF THE REACTION RATE CONSTANTS WITH PRESTO KINETICS® SOFTWARE	87
7.3.	THE MECHANISM OF THE ACETALDEHYDE FORMATION.....	92
7.4.	THE REACTION NETWORK AND PROPOSED ELEMENTARY REACTIONS	93
8.	SUMMARY AND OUTLOOK	95
9.	BIBLIOGRAPHY	101
10.	APPENDIX	105



1. Introduction

At the beginning of the 19th century the production of chemicals was based almost entirely on renewable raw materials. Starting from the 1850's the chemical industry came to depend increasingly on coal. Later, from the 1940's on, mineral oil and natural gas became to be increasingly important, eventually reaching the status of major feedstock as they still are nowadays. In the 1970's the oil crises brought the concern about the limited availability of fossil resources. Since then, there is an increasing interest about processes based on renewable raw materials [Bau-1988]. Nowadays, the use of natural gas and oil peaks and it will presumptively decrease in the near future, while the use of renewable feedstock displays a steady increase (Figure 1-1).

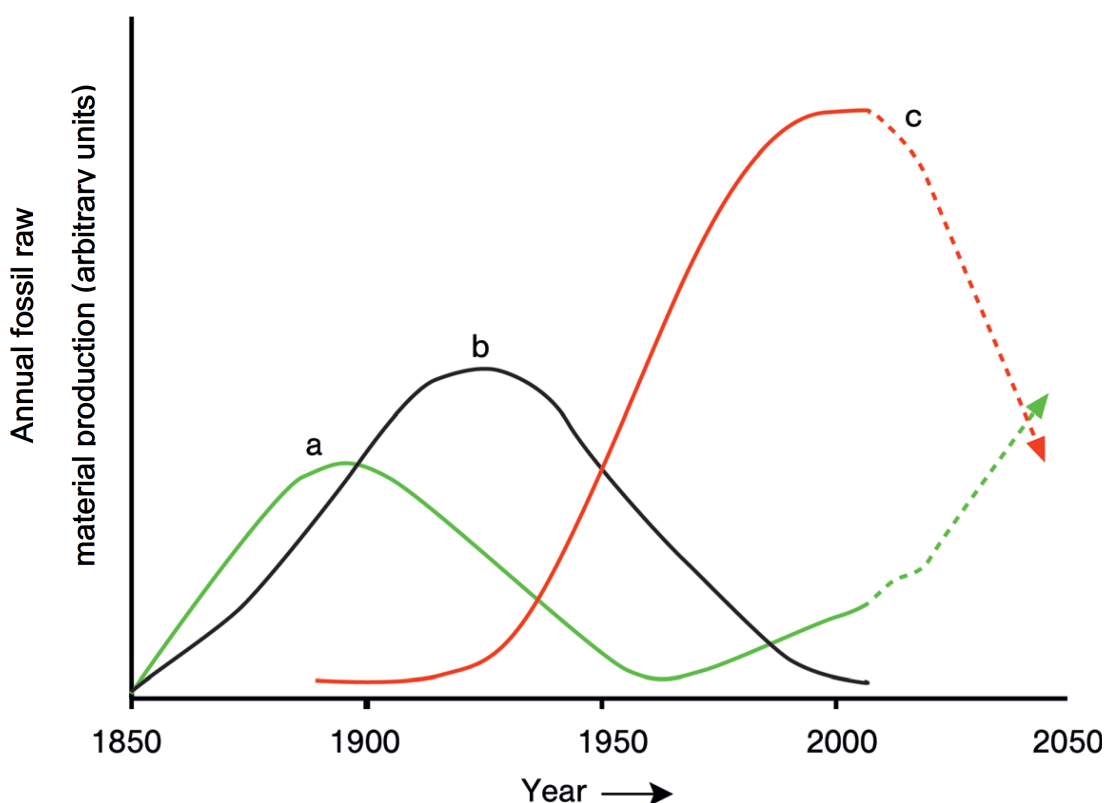


Figure 1-1 Historical perspective over the use of raw materials by the chemical industry a) renewable feedstocks; b) coal; c) natural gas, oil [Lic-2010]

Vegetable biomass, from which carbohydrates represent a major part, is produced in vast amounts (170 Millions of Tons/Year) by natural photosynthesis. Only a minor 3 % of this biomass is cultivated and used for food or non-food applications [Cla-2008]. Apart from ethical limitations which include the urge for rational deforestation and the satisfaction of local food demands, this percent could be extended in an effort to avoid the use of fossil feedstock for industrial applications. This effort is partly motivated by the limited availability of fossil resources, but not only. It belongs to a general trend towards a more sustainable living.

By the 1980's the environmental reputation of the chemical industry was at stake. Tragic accidents such as Seveso (1976) and Bhopal (1984) or the realisation of more subtle anthropogenic influences on the environment such as the atmospheric ozone layer thinning, sensitized the public opinion about the health hazards and the negative effects over the ecosystem caused by the man-made chemistry. As a consequence, the environmental regulations became increasingly stringent for the chemical companies aiming to discourage the generation of hazardous wastes and to make the chemical industry cleaner, environment-friendlier [Sig-1996]. Thus, in 1991 the concept of *Green Chemistry* emerged which can be explained in terms of sustainability: making the industrial chemistry safer, cleaner; designing products which are more energy efficient throughout their life cycle; using renewable feedstocks whenever this is possible [San-2011].

Another concept belonging to this new, avant-garde chemistry is *Biorefinery* [Kam-2004] with a tight connection to Green Chemistry, describing industrial ensembles which transform renewable raw materials into valuable chemicals, fuels or energy. In a first separation step (Figure 1-1) the biomass is converted to intermediates such as biopolymers (starches, cellulose, proteins, etc.), oils, etc. In a second step, a chemical or biochemical processing transforms the intermediates into valuable chemical commodities.

Intensive research has been carried out concerning the efficiency and possibilities of transforming biomass into valuable chemicals by the means of biorefineries [Cor-2007, Cla-2006, Gal-2007].

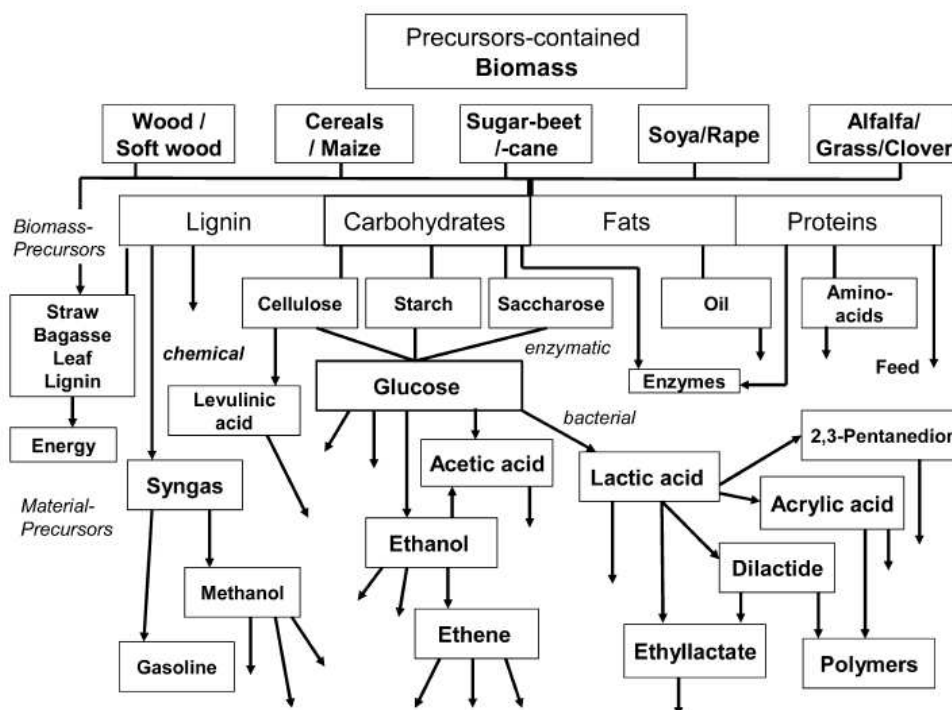


Figure 1-2 The general scheme of a biorefinery with focus on the carbohydrates [Kam-2004].

Despite the great diversity of products which can be obtained from biomass, many of them find nowadays no industrial application from economical reasons and the respective production processes are characterized in the literature by their future attractiveness [Gal-

2007]. Nevertheless, some of these processes like the production of bio-ethanol are implemented on an industrial scale. Many of them involve the fermentation of carbohydrates and the subsequent use of the so-called platform molecules which are those derivatives which are potential building blocks for the chemical synthesis (see Figure 1-3).

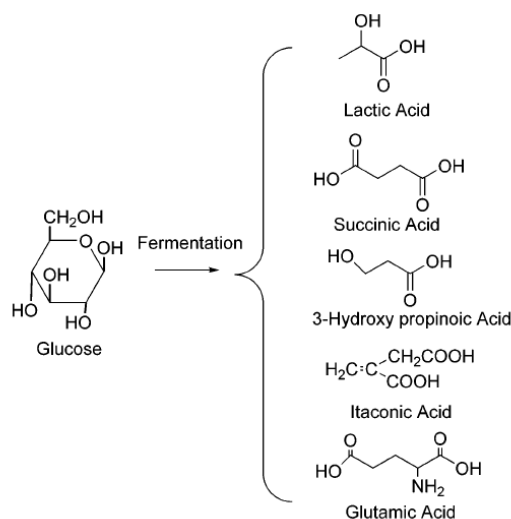


Figure 1-3 Important platform molecules obtained by the fermentation of glucose [Cor-2007].

Except for lactose which is a platform molecule from the milk industry, the most important other platform molecules are obtained through fermentation of carbohydrates [Gal-2007]. Some of the important platform molecules are presented in Figure 1-2. From these platform molecules only lactic acid will be discussed. Its annual production lies around 350 000 Tons [Was-2004]. An important use of it is the production of the biodegradable poly-lactic acid polymer (Figure 1-4). A great advantage of the use of lactic acid as feedstock is its relatively low price.

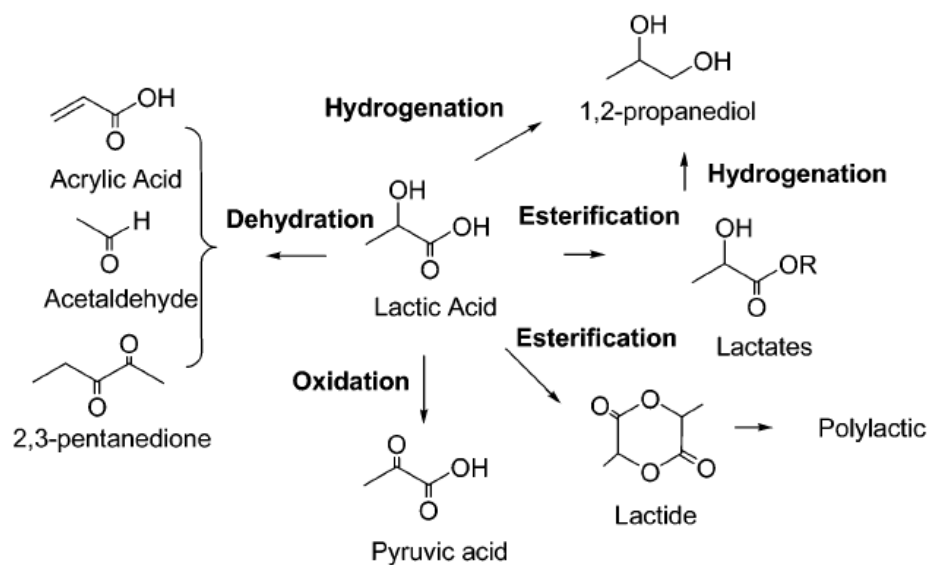


Figure 1-4 The lactic acid platform [Cor-2007].

An important product among the derivatives which can be obtained from lactic acid is acrylic acid with a capacity of around 4 million tons/year. It is an important intermediate in the production of surface coatings, fibres, adhesives, etc. It is almost entirely obtained by a process involving the catalytic oxidation of propene, which is a product of natural gas refining.

The great availability of lactic acid and its low price makes the production of acrylic acid using this renewable feedstock very attractive. Additionally, the two molecules have a relatively similar structure and the transformation succeeds through elimination of a water molecule from lactic acid and formation of the C1-C2 double bond.

Unfortunately, there are major hindrances in developing such a process, like the low product yields, the need of an appropriate catalyst, derivatisation of the lactic acid or extreme reaction conditions (high temperatures and pressures), making the transformation more complex than it initially appears to be.

At least, concerning the high temperature and pressure needed for the reaction, a clean and elegant method for converting lactic acid to acrylic acid is to use water as a solvent at temperatures and pressures which near its critical point.

Aim of the present work, in the *Green Chemistry* context which has been hitherto outlined, is the study of the reaction of lactic acid in near- and supercritical water, a better understanding of its mechanism and the investigation of various means to improve the acrylic acid yield. In this respect, an important focus will be set on homogeneous catalysis which can bring a significant contribution to the distribution of reaction products. In the following section, the literature dealing with the dehydration of lactic acid and its derivatives will be reviewed in order to elaborate an outline for the experiments needed to better understand the behaviour of lactic acid in near- and supercritical water and find conditions where the yields in acrylic acid are higher.

2. State of the Art in Lactic Acid Dehydration

This chapter covers the information found in the literature about the different methods of converting lactic acid or its derivatives to acrylic acid. A greater emphasis has been put on the scientific literature, but patents are also briefly discussed.

There are several pathways by which lactic acid can be dehydrated to acrylic acid. The most yielding process is a gas-phase pyrolysis and uses α -acetoxy-methyl-propionate as starting material [Rat-1944]. The reaction is shown in Figure 2-1:

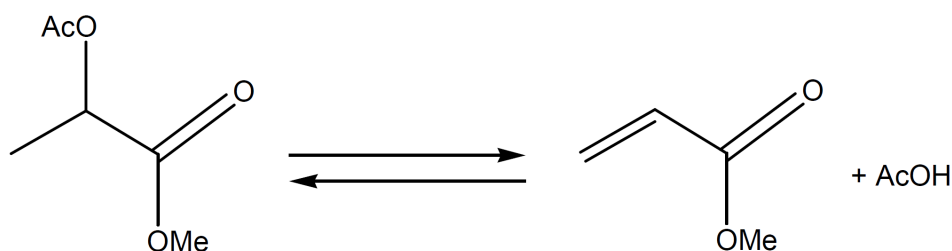


Figure 2-1 Pyrolysis of α -acetoxy-methyl-propionate leading to methyl acrylate in high yields

The authors studied the influence of several factors such as temperature, residence time, contact material and initial feed concentration on the outcome of the reaction. The highest yields of methyl acrylate were obtained (Figure 2-2) at 550 °C, a residence time of 8 seconds and a packing material for the reactor consisting of carborundum crystals.

Since the curves in Figure 2-2 representing short reaction times do not have an inflection point even at temperatures as high as 580 °C, it can be concluded that the highest yield for the reaction would be achieved at higher temperatures and very short residence times (1-4 seconds).

The packing material has probably no catalytic role but that of favouring the heat and mass transfer, that is, supplying the necessary heat to the reactant through a large contact surface and also allowing a fast replacement of the reaction product by new quantities of reactant at the reaction sites, making short reaction times possible. Thus, those inert materials possessing the highest surface and a high thermal conductivity as well as a geometry that facilitates an efficient mass exchange between reactant and product are the best suited for the reaction. The preparation of the α -acetoxy-methyl-propionate feed requires acetic anhydride, which is to be regenerated from the acetic acid resulting from the pyrolysis. Probably due to these expenses, this process has not been yet scaled-up for industrial production of acrylate. Recently, a new method has been developed, which avoids the use of acetic anhydride and uses acetic acid for the acetylation at 70 °C and 150 mm Hg [Lil-2004].

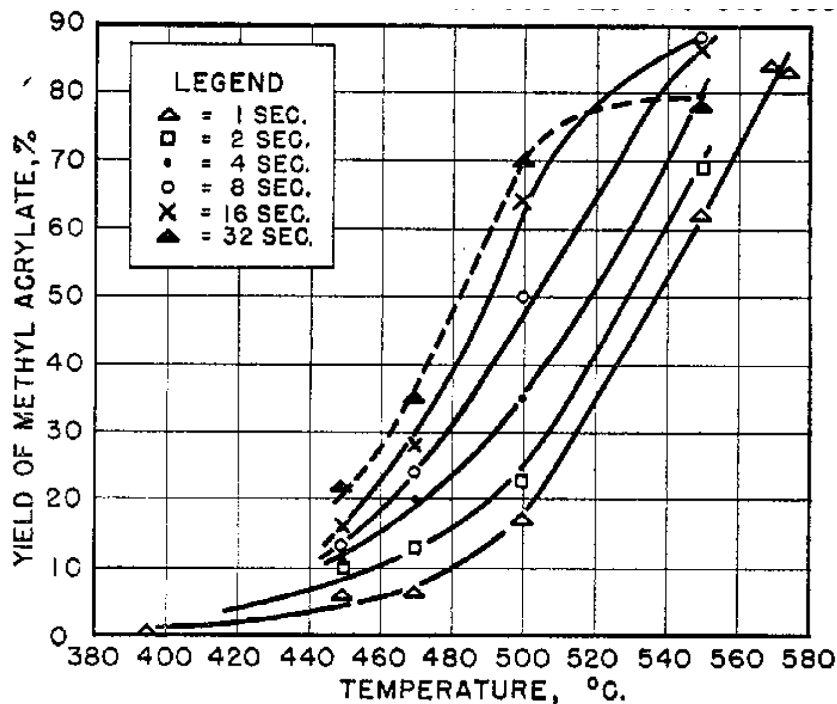


Figure 2-2 Dependence of methyl acrylate yield on the temperature at various residence times [Smi-1942].

Mok *et al.* [Mok-1989] thoroughly studied the dehydration of lactic acid in near- and supercritical water. A reaction network has been described, based on various theoretical considerations and experiments using isotope-labelled lactic acid as reactant. Also, the influence of important parameters such as the initial concentration of the reactant, temperature, pressure, reaction time, pH of the feed solution, etc. on the reaction has been studied.

2.1. Reaction Network

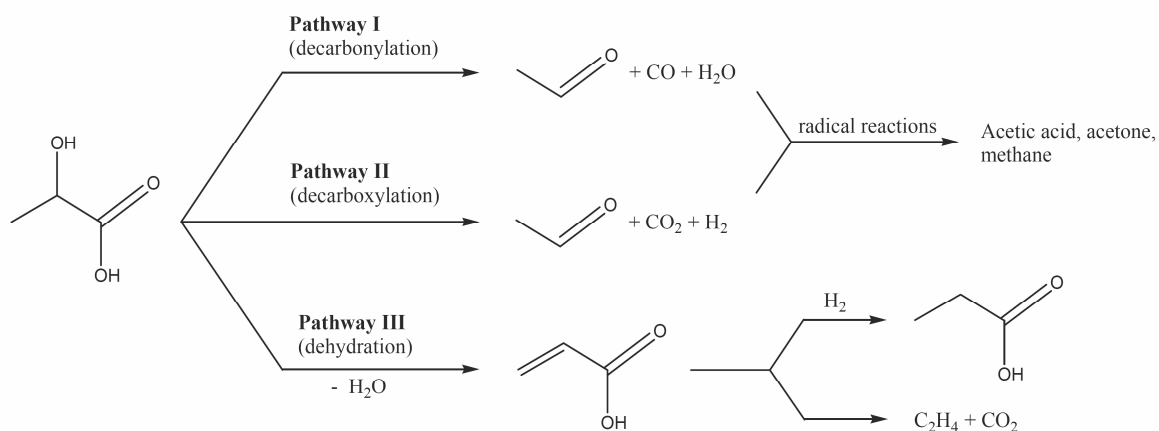


Figure 2-3 Reaction network of lactic acid in near- and supercritical water [Mok-1989].

2.1.1. Pathway I – Decarbonylation

By decreasing the pH of the feed solution, the major product of the reaction of lactic acid in supercritical water becomes acetaldehyde. Evidence for the decarbonylation is also provided by experiments with isotope-labelled lactic acid: using $\text{CH}_3\text{CHOH}^{13}\text{COOH}$ instead of lactic acid in an acidic medium produces no labelled acetaldehyde whereas ^{13}CO has been detected by GC-MS.

The proposed mechanism for this pathway is shown in Figure 2-4.

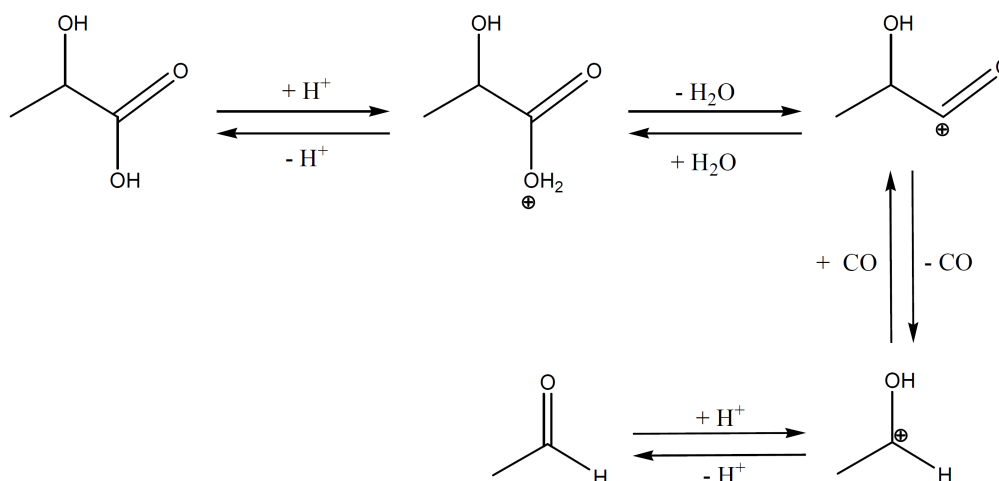


Figure 2-4 Decarbonylation path for the reaction of lactic acid in near- and supercritical water [Mok-1989].

In accordance with the proposed mechanism, decreasing the pH of the feed solution by addition of acids increases the yield of acetaldehyde by favouring the addition of a proton to the carboxylic group. Further on, it is reported that addition of salt increases the reaction rate by stabilizing the charged transition state. Nevertheless, as it will be discussed later, the effect of the addition of salts strongly depends on their properties in supercritical water. Some species like phosphates can inhibit the formation of acetaldehyde [Lir-1993].

2.1.2. Pathway II – Decarboxylation

$^{13}\text{CO}_2$ has also been detected from the experiments with labelled lactic acid, indicating that decarboxylation also takes place. There is, however, no clear mechanism to explain this pathway, because ethanol, the obvious product of decarboxylation has not been detected although it should be stable at the given conditions [Xu-1990]. Instead, among the reaction products only acetaldehyde has been detected along with the labelled $^{13}\text{CO}_2$ and H_2 . Ionic species like H^+ , OH^- or salts are reported to have little influence on the decarboxylation rate (characterized by the CO_2 amount) suggesting a radical mechanism. The observation that pressure suppresses this pathway, probably through a cage effect, supports the idea of a radical mechanism.

2.1.3. Pathway III – Dehydration

Since there is no explanation for the formation of acrylic acid based on the two previously described pathways, there must be a third pathway corresponding to lactic acid dehydration.

Propionic acid is a secondary product of this pathway together with ethene. The formation of ethene can be simply judged as a decarboxylation product of acrylic acid. To render an explanation the formation of propionic acid as a hydrogenation product of acrylic acid, an experiment has been carried out involving a mixture of formic and acrylic acid as a feed. Separately taken, formic acid has been found to decompose instantly to CO_2 and H_2 therefore allowing the adjustment of the H_2 quantities in the reactor by means of the added formic acid. The mixture of acrylic and formic acids yields significant amounts of propionic acid in supercritical water. Hence a first hint for the propionic acid as a hydrogenation product. Further, acetaldehyde has been found to react to acetic acid and H_2 and since acetaldehyde is produced in significant amounts during the reaction of lactic acid in supercritical water, at least one source of H_2 has been found. Thus, the propionic acid also belongs to the products of pathway III [Mok-1989].

There are two proposed mechanisms for the dehydration:

The first proposed mechanism involves a concerted elimination with the carbonyl group playing the role of the attacking base in the elimination.

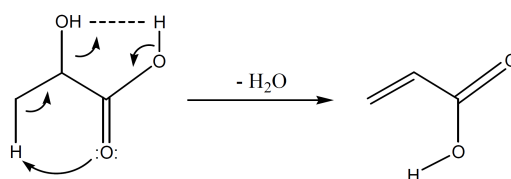


Figure 2-5 Mechanism for the dehydration of lactic acid involving an attack on the β -carbon atom from the carbonyl group [Mok-1989].

The second proposed mechanism involves the formation of an α -lactone which further dehydrates to acrylic acid.

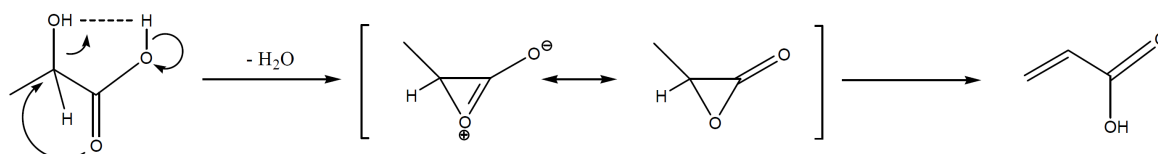


Figure 2-6 Mechanism for the dehydration of lactic acid involving the formation of a α -lactone intermediate [Mok-1989].

Important supporting information for these mechanistic considerations which led to the separation of the reaction of lactic acid in supercritical water into pathways is provided by parameters such as initial concentration of the reactant, temperature, pH of the feed solution, or the use of different catalysts which have been found to induce important changes in the course of the reaction. Some of these effects will be presented further on.

2.2. Effect of Reaction Parameters

2.2.1. Effect of pH

As mentioned in Section 2.1.1, decreasing the pH favours the decarbonylation pathway while the dehydration pathway is inhibited. Increasing the pH in feed above 7 inhibits both pathway I and III. Neutralizing the lactic acid with NaOH in feed inhibits the dehydration as well as the formation of CO via decarbonylation. There is a clear trend showing that increasing pH favours the formation of CO₂ [Mok-1989 Lir-1993]. These results are in accordance with the observation that the dehydration is most successful without pH shift by bases or acids [Mok-1989]. The overall conversion of lactic acid is inhibited by increasing the pH and enhanced at lower pH values as compared to a feed where no pH adjustment has been made.

2.2.2. Influence of Different Acid Catalysts

A more subtle effect than a simple pH shift is provided by the general acid catalysis. The influence of H₃PO₄, HNO₃ and H₂SO₄ has been studied [Lir-1993]. It has been found that, at very small concentrations (1.6 mM; pH = 2.8) H₃PO₄ inhibits the formation of acetaldehyde although an acidic medium should favour at least pathway I. The yield of acrylic acid in the presence of low concentrations of phosphoric acid is comparable to the yield without any catalyst. At higher concentrations, however, the formation of acetaldehyde is favoured, probably due to the protonation of the carboxylic acid. This hints to the significance of the phosphate anion for the reaction.

2.2.3. Influence of Na₂HPO₄

A further evidence for the importance of the phosphate anion as a catalyst rather than the phosphoric acid itself is given by experiments where sodium monohydrogen phosphate has been added. Within a concentration range between 4 and 80 mM Na₂HPO₄ the highest acrylic acid to acetaldehyde ratio is obtained when the highest concentration of phosphate is used. Na₂HPO₄ effectively suppresses the other pathways favouring dehydration.

2.2.4. Effect of the Initial Concentration

At very small lactic acid concentrations (below 25 mM) pathways I and III are favoured while pathway II is slightly inhibited. Increasing the lactic acid concentration in feed inhibits significantly the decarboxylation while the decarbonylation rate slightly increases. The dehydration is apparently not influenced by the initial lactic acid concentration. The curves in

Figure 2-7 representing the productivity as sum of the yields of the products which are specific for a pathway (CO for decarbonylation, CO₂ for decarboxylation and acrylic acid, ethene and propionic acid for dehydration), can be roughly represented by a linear trend, suggesting a first order reaction for pathway I and III. It is difficult, however, to consider the dependence of productivity for path II with the increasing initial concentration as linear. There is no straightforward explanation for the decrease of yields with increasing initial concentration. However, if the productivities of pathway I and II (corresponding to decarbonylation and decarboxylation) are added and considered together, a quasi-linear dependence of the productivity on the initial concentration is obtained. This addition of productivities could be justified by the fact that both pathways produce acetaldehyde.

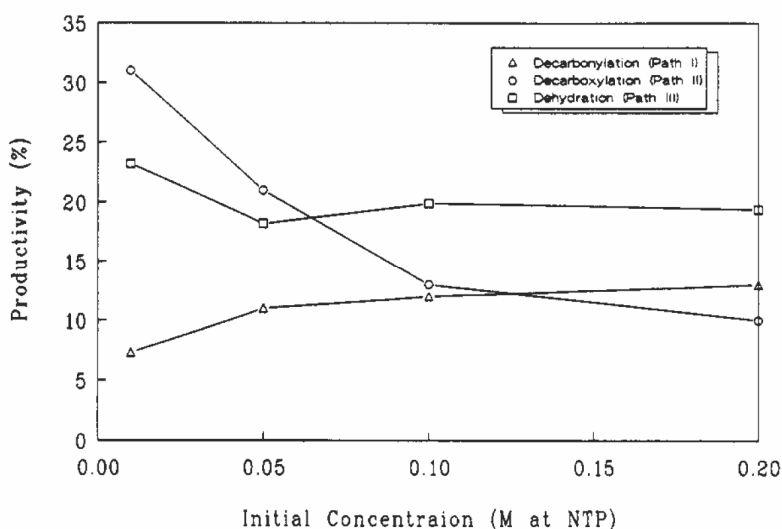


Figure 2-7 Effect of the initial concentration on the productivity (sum of the yields of path-products) [Mok-1989].

2.2.5. Effect of Temperature

The degradation of the lactic acid molecule requires high inputs of energy. Therefore it is not surprising that an increase in temperature favours the absolute yields for all pathways; that is, the concentration of all analyzed reaction products increase with temperature, at least between 320 and 400 °C [Mok-1989, Lir-1993]. Since the carbon balance does not change significantly, this implies that no significant decomposition reactions interfere with the main reactions for the considered products and within the mentioned temperature range temperature range.

To avoid confusion with regard to the term “selectivity”, the selectivity towards a reaction product and the selectivity of a reaction path will be defined in order to compare the data in the literature. For the studied reaction network where all mentioned products have the same stoichiometric coefficients as the reactants, it can be written:

$$S_{\text{product}} = \frac{C_{\text{product}}}{C_{\text{iLA}} - C_{\text{fLA}}} \cdot 100 \quad (2-1)$$

$$S_{\text{pathway}} = \frac{\sum C_{\text{product}}}{C_{\text{iLA}} - C_{\text{fLA}}} \cdot 100 \quad (2-2)$$

S_{product}	selectivity towards a reaction product /%
S_{pathway}	global selectivity for a reaction pathway /%
C_{iLA}	initial theoretical concentration of lactic acid /mol l ⁻¹
C_{fLA}	concentration of lactic acid after the reaction /mol l ⁻¹
C_{product}	concentration of a specific product /mol l ⁻¹
$\sum C_{\text{product}}$	sum of concentrations of the products determining a path /mol l ⁻¹

Similarly, the yield represents the percentual ratio between the molarity of product and the molarity of the reactant.

Although a clear comparison is not possible due to difference in other reaction parameters, Figure 2-8 gives an overview of the dependence of selectivity on temperature.

First of all, it is to be mentioned that the measurements by Lira *et al.* are made in the presence of sodium phosphate which makes a direct comparison with the results of Mok *et al.* impossible. Secondly, the reaction times and pressures diverge between the two studies. However, from both sets of data it can be concluded that the selectivity toward acrylic acid peaks in the near-critical region between 340 - 360 °C.

There is little difference between the dehydration pathway selectivity and the acrylic acid selectivity when phosphate is present indicating that the catalyst inhibits the side reactions of acrylic acid along the entire studied temperature range. Concerning the dependence of acrylic acid yield on temperature there is little difference between the data provided by the two considered papers.

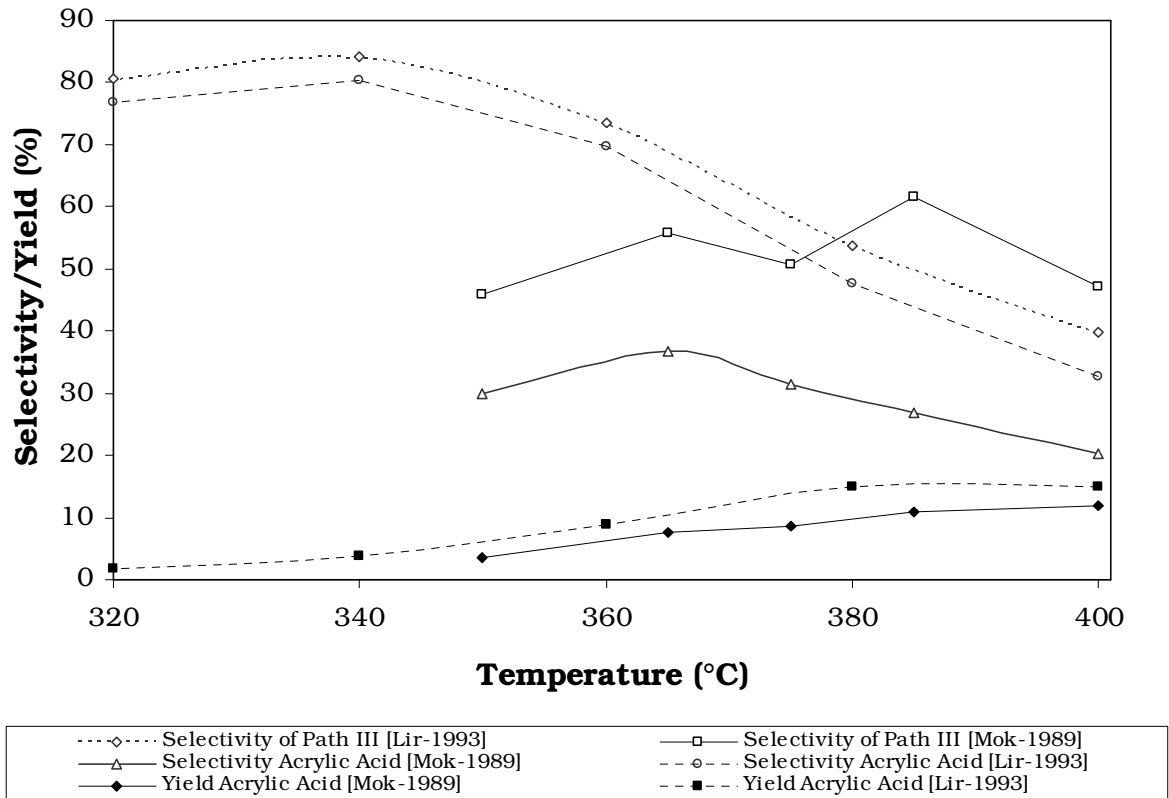


Figure 2-8 Dependence of selectivity and yield on temperature, according to two sources from the literature.

2.2.6. Effect of Pressure and Solvent Density

Increasing the pressure seems to slightly disfavour all three pathways. As illustrated by the figures Figure 2-9 and Figure 2-10, the pressure, like the initial concentration of the lactic acid in feed, only have a significant effect on the decarboxylation. On the other hand, density has a more pronounced effect, at least on the dehydration and acrylic acid yield.

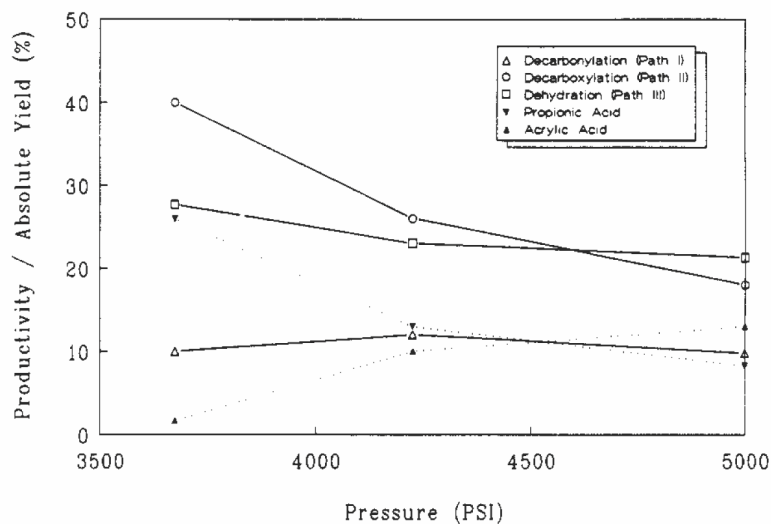


Figure 2-9 Effect of pressure on the reaction network [Mok-1989].

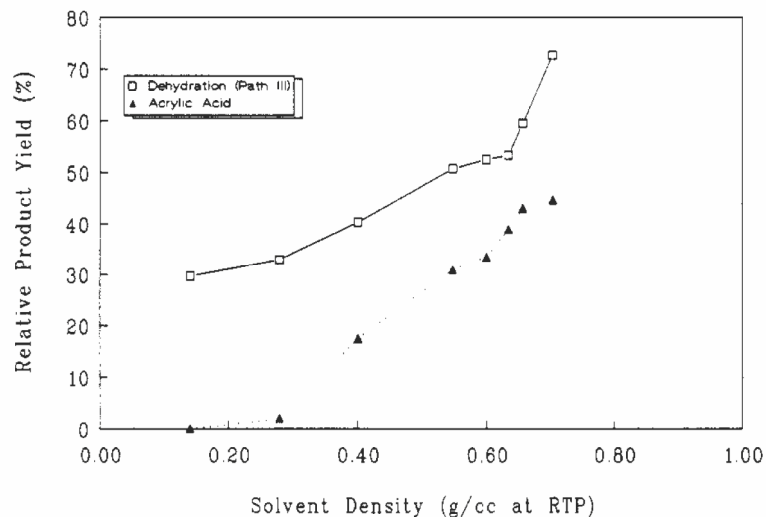


Figure 2-10 Effect of solvent density on the reaction network [Mok-1989].

2.2.7. Reactor Aging

The subcritical water is a corrosive medium. This effect is due to the increased value of the dissociation constant of water in the vicinity of its critical point. At longer contact times between the corrosive medium and the steel surface of the reactor, a protective layer, is formed. Its stability strongly depends on the temperature, pressure and the species dissolved in water [Kri-2004]. The experiments by Lira *et al.* refer to the influence of the "fresh" and passivated metal surface on the reaction of lactic acid. It was found that the overall conversion is higher when using aged reactors. The carbon dioxide yield decreased with aging while the carbon monoxide yield is largely unaffected by this process. The dehydration pathway is also unaffected by the aging but the acrylic acid yield *per se* is higher in an aged reactor [Lir-1993]. The studied material was always Hastelloy C-276.

2.3. Alternative Methods Involving Dehydration of Lactic Acid to Acrylic Acid

2.3.1. Heterogeneous Catalysis – Reaction of Lactic Acid over Supported Phosphate Catalysts

Gunter *et al.* [Gun-1995] used a reactor with silica-alumina supported sodium phosphates to convert lactic acid. The reaction is carried out in the gas phase. Helium has been used as a carrier gas to enhance the transport of lactic acid which hardly vaporizes and tends to dimerize or polymerize. The highest yield (9.8 molar percent based on feed) and the highest selectivity (29 %) towards acrylic acid were obtained at a temperature of 350 °C, a pressure of

5 bar and a residence time of 0.3 sec, using Na_3PO_4 . Their study focuses mainly on the formation of 2,3-pentanedione for which they propose a reaction mechanism [Tam-1997]. Another work by the same authors uses FTIR and ^{31}P -NMR spectroscopic analyses in order to determine the transformations undergone by the phosphate species. They also investigate the role of these phosphates present on the catalyst surface as well as that of the sodium lactate on the formation of 2,3-pentanedione and acrylic acid. Sodium lactate has been found to be formed through exchange between lactic acid and phosphates (especially sodium triphosphate and pyrophosphate). Their results suggest that sodium lactate is either catalyst or intermediate in the formation of 2,3-pentanedione and acrylic acid.

Wadley *et al.* [Wad-1997] used NaNO_3 instead of phosphates, under similar conditions as Gunter *et al.* (370 °C, 6 bar, 0.3 sec residence time) and obtained a yield of 20 - 25 % for acrylic acid. Their analysis using FTIR spectroscopy also point out that sodium lactate, which is formed by exchange with the nitrate and forms a molten layer on the surface of the catalyst particles, should play an important role as a reaction intermediate in the formation of 2,3-pentanedione and acrylic acid.

2.3.2. Reaction of Lactic Acid Catalysed by Group VIII Metal Complexes

Odell and Earlam [Ode-1985] reports the conversion of lactic acid in aqueous solutions, in sealed glass ampoules, to various products in the presence of group VIII metal complexes. Acrylic acid is also obtained. Yields as high as 3.3 - 3.4 % are obtained in the presence of $[\text{Ni}(\text{CO})_2(\text{PEt}_3)_2]$ or $[\text{PtH}(\text{PEt}_3)_3]^+$ at about 230 °C and a residence time of 2 - 4 hours.

2.3.3. Biotechnological Pathways

The biotechnological production of acrylic acid from lactic acid is relatively well researched, with the potential for an industrial scale production of acrylic acid from renewable raw materials [Str-2005].

Clostridium propionicum is a bacterium capable of transforming lactate ions into propionate ions through its metabolic pathways. It has been found that acrylate is an intermediate [Bri-1990] in the reduction of lactate to propionate. In the presence of an electron donor in the medium, methylene blue in this case, acrylate accumulates in the medium via oxidation of propionate. A yield of 0.133 mmol acrylate/ g wet cell has been obtained and the reaction conditions were a temperature of 35 - 45 °C and 6 hours reaction time. The impediments towards industrial scale development of the process are the short productive time for these cells (a maximum of acrylic acid production at a cell age of 14 hours), the inhibition in the metabolic pathway through excessive accumulation of acrylate favouring the reverse reactions in the metabolic pathway (as acrylate is not the final product of the metabolism), poisoning by methylene blue and cell death. To hinder the inhibition of the process through acrylic acid accumulation, acrylate should be removed from the reaction site either through physical or

(bio)chemical methods thus providing a driving force for the conversion of lactate to acrylate. A yield of up to 18.5 % of propionate to acrylate has been obtained.

2.4. Patents

The patents concerning the dehydration of lactic acid were briefly reviewed chronologically by Corma *et al.* [Cor-2007].

In 1958 Holmen [Hol-1958] was the first to report a dehydration of lactic acid in the gas phase at 400 °C over a mixture of Na₂SO₄ and CaSO₄ obtaining a 68 % yield in acrylic acid. By treating an AlPO₄ catalyst with an ammonia solution, Papparizos *et al.* [Pap-1985] obtained acrylic acid with a yield of 43 % at 340 °C. Under the same conditions, but using ammonium lactate instead the yield was 61 %. Sawicki [Saw-1988] used Na₂HPO₄ supported on silica and NaHCO₃ as a acidity regulator of the catalyst at a temperature of 350 °C. He reported a yield of 58 % and 65 % selectivity towards acrylic acid. Walkup *et al.* [Wal-1991] reports a process for converting lactic acid esters into acrylic acid and acrylic esters at 350 – 410 °C, a residence time less than 30 sec the use of a fixed bed reactor with CaSO₄ as a catalyst and Na₂HPO₄ as buffering agent. The maximum acrylate/acrylic acid yield was 45 %. Finally, Abe *et al.* [Abe-1993] used zeolites of NaY and NaX types at 240 °C and dehydrated methyl lactate with a yield in acrylic acid/acrylate as high as 94 %. These catalysts can not be used in experiments involving supercritical water due to their short life times at these conditions.

2.5. Outline of the research activity

This chapter has covered most of the literature concerning the dehydration of lactic acid. Of the utmost importance for the scientific work presented hereinafter are the two papers by Mok *et al.* and Lira *et al.* [Mok-1989, Lir-1993]. These constitute for the core of the experimental research a very useful starting point.

The main objectives of this research work are the following:

- Development of a robust HPLC analytic method capable of separating and quantifying all major species found in the reaction mixture occurring during the experimental assays.
- Design and execution of the appropriate installation containing a pipe- or a continuously stirred tank reactor to carry out the experiments, whereby the latter is to be used for the kinetic measurements due to its uniform temperature and concentration distribution.
- Investigation of the effect of reaction parameters: temperature, pressure, residence time and initial concentration on the unfolding of the reaction of lactic acid in near- and supercritical water.
- Investigation of the stability of acrylic acid in near- and supercritical water.
- Study of the behaviour of relevant substances other than lactic acid at given supercritical conditions aiming to a better understanding of the dehydration mechanism.
- Study of the gaseous products emerging from the reaction of lactic acid as indicators of the different reaction pathways.
- Investigation of various additives (catalysts) with a focus on phosphates, which influence the outcome of the reaction.
- Elaboration of a kinetic model for the main reactions involving lactic and acrylic acid in near- and supercritical water and estimation of the reaction rates using a simulation software.

3. Fundamentals in Near- and Supercritical Water

Water is an inexpensive environmental friendly solvent and therefore was subject to intensive research concerning its potential as reaction medium. Some of the important properties of water over a large range of temperatures and pressures are presented further on. As a rule of thumb, near- and supercritical water has “borderline” behaviour, sharing physical and chemical properties with both liquid and gaseous water.

3.1. Phase Equilibria and Equations of State

Temperature and pressure are parameters that dramatically influence the properties of water. If at 1 atm and 25 °C water is a well-characterized liquid; increasing both temperature and pressure results in remarkable changes in properties such as density, dielectric constant and dissociation constant making it suitable for reactions that do not take place in aqueous systems under normal conditions [Brö-1999]. Besides, relatively large variations can be obtained by small adjustments of pressure and temperature.

3.1.1. The Phase Diagram

The interdependences of state variables of a thermodynamic system are described by an equation of state. The phenomena to be described are related to changing the state parameters such as pressure, temperature and volume. An overview of the phase behavior of water in the temperature range between 200 and 700 K and pressures varying from 10^{-5} to 10^4 MPa is provided by the diagram of the phase equilibrium (Figure 3-1).

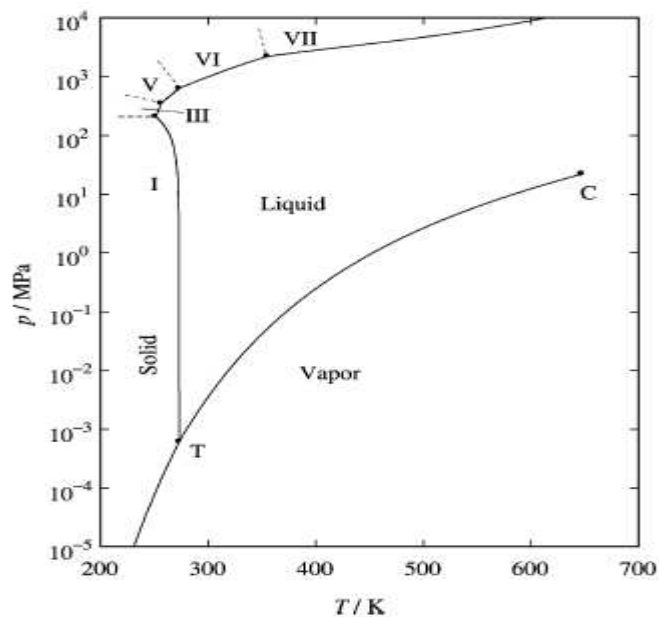


Figure 3-1 Phase diagram of water over a wide range of pressures and temperatures (p,T). On the diagram the *triple point T* and the *critical point C* are marked [Har-2004].

In the T (triple) point (at 0.01 °C and around 0.006 bar) three phases, vapor, solid and liquid coexist. In the C (critical) point (at 373.95 °C and 220.6 bar) the separation between liquid and gas ceases to exist and only one phase (supercritical water) is to be noticed. The regions limited on the diagram by the TC curve are to be discussed. At temperatures below that of the point T, depending on the pressure, gas phase or solid phase is to be found or an equilibrium of the two (if the pressure and temperature are those of a point from the separation line between the two phases). At higher temperatures than that of the T point, also depending on the pressure, the system consists either of liquid or vapor or of a mixture of the two. Remarkably, at very high pressures (10^3 - 10^4 bar) despite its relative incompressibility, the liquid is converted to solid, even at temperatures as high as 600 K.

The present work limits itself in characterizing water or aqueous systems with temperatures and pressures in the vicinity of the critical point C, that is, in the near-critical region.

In order to understand the behavior of the thermodynamic system and to successfully plan experiments, it is desirable to know the interdependence of the state parameters as accurately as possible. Several *equations of state* have been developed along the time, in order to describe the behavior of gases. Liquids and solids are here not been taken into consideration due to their high incompressibility. Some useful equations of state will be presented in the following section.

3.1.2. Density, Dielectric Constant and Dissociation Constant

Near the critical point the properties of water suffer dramatic changes. Its density decreases with temperature while increasing with pressure (Figure 3-2). These variations are sufficiently high and with minimal changes in these two parameters a wide range of densities can be obtained.

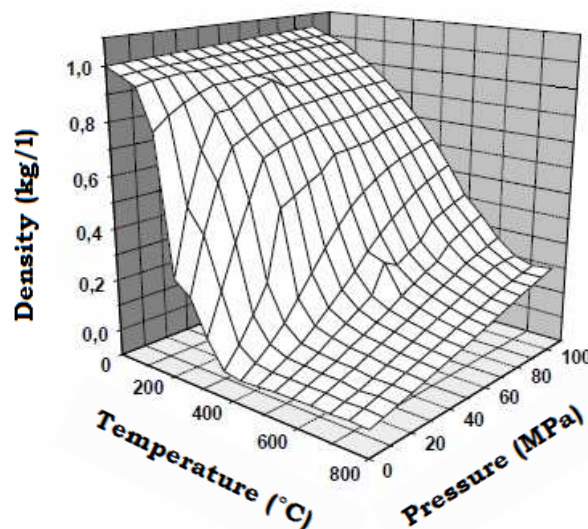


Figure 3-2 Temperature and pressure dependence of density for water [Leh-2008].

Most of physical chemical and thermodynamical properties of water are related to the density and are thus indirectly influenceable by varying temperature and pressure.

One such important property is the relative dielectric constant, ϵ_r , which is a measure of the polarity of a substance. At 25 °C and 1 atm $\epsilon_r = 78$ and decreases steadily reaching 20 in the vicinity of the critical point as it is illustrated in Figure 3-3.

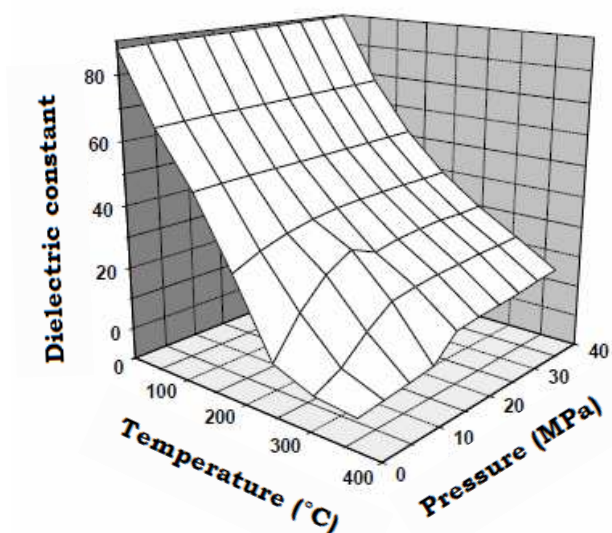


Figure 3-3 Representation of the relative dielectric constant for water as a function of temperature and pressure [Leh-2008].

This behaviour is due to the decreasing number of hydrogen bonds in the critical region [Brö-1999], making water comparable to slightly polar organic solvents (acetone has $\epsilon_r = 20.7$). At higher temperatures and pressures the dielectric constant of water becomes even smaller, with values comparable with those of unpolar solvents. This behaviour is due to the increase in internal energy of the system, making thermal agitation to prevail increasingly upon the dipole structures created by electrostatic forces.

Another property which is to be discussed in this section is the dissociation constant of water, K_w , defined as:

$$K_w = c_{\text{H}_3\text{O}^+} \cdot c_{\text{OH}^-} \quad (3-7)$$

where $c_{\text{H}_3\text{O}^+}$ and c_{OH^-} are the molar concentrations of the hydronium and hydroxyl ions in the aqueous system. Since changes in the system only occur at large changes in the concentrations of the above mentioned species, it is convenient to work with the logarithmic measure $\text{p}K_w = -\lg K_w$. The dependence of $\text{p}K_w$ with temperature and pressure is represented in Figure 3-2.

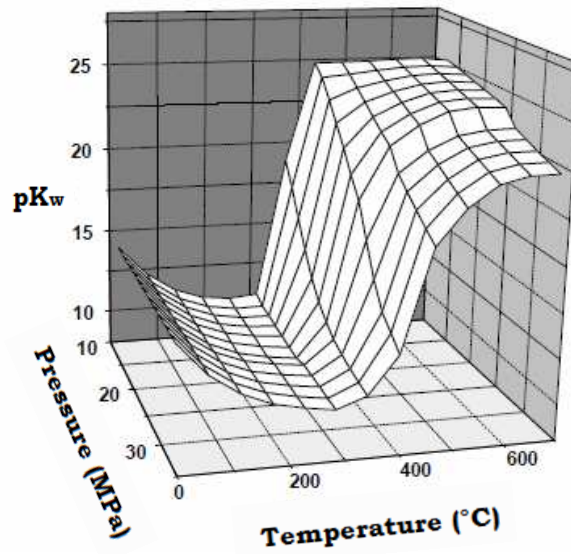


Figure 3-2 Dependence of pK_w with temperature and pressure [Leh-2008].

In the proximity of the critical point, the concentrations of the H^+ and OH^- are a few orders of magnitude higher than at normal conditions, making water suitable for acid/base catalysis.

4. Binary Mixtures of Near- and Supercritical Water

4.1. Phase Behaviour and Solubility of Electrolytes in SCW

In the previous section some important properties of SCW have been briefly described. In the critical region the polarity of water is low and ranges from that of a slightly polar solvent to that of an unpolar organic solvent. This is one of the key factors which influence chemical reactions in SCW and which can be relatively easily regulated by adjusting temperature or pressure. A very short review of some important properties of water as solvent is made in this chapter.

The phase behaviour of the mixtures is to be taken in consideration especially when dealing with reactions in near- and supercritical water. Separation of binary mixtures into two phases of different concentrations (mostly one with a low concentration and one with a high concentration) are to be taken into account with regard to corrosion effects caused by the solute species (because corrosion depends on the concentration of species dissolved in the aqueous system) [Wei-2005]. On the other hand, solubilities in SCW differ strongly from those in water at ambient conditions. For example, while K_3PO_4 , which is relatively soluble in water at supercritical conditions, Na_3PO_4 is practically insoluble [Wei-2005]. These effects are to be known prior to any experiments to be carried out in aqueous systems at high temperatures and pressures.

When a solute is present in SCW, the critical point is shifted and a locus of critical points is formed, depending on the concentration of the solute. The characterisation of the phase behavior of binary mixtures is not trivial, requiring data about the interaction of the two species which can hardly be predicted theoretically and are rather collected experimentally for every particular case. Several classifications of binary mixtures have been proposed, based on the van der Waals equation of state for mixtures [Sco-1970 Val-2004]. Phase separation often occurs like the liquid-liquid immiscibility region in the case of $KH_2PO_4 - H_2O$ system [Mar-1985].

Approaches that describe the phase behavior exist especially for the $NaCl-H_2O$ system which is among the most extensively studied [Arm-1993]. Thermodynamic models for this system have been developed exploiting the deviation from ideal gas behavior of the Helmholtz energy of the system [And-1993]. These models were generalised for other systems as well [Dja-2010].

As an example in Figure 4-1 and Figure 4-2, a T-x projection of $NaCl-H_2O$ mixture is given below together with a complete p-T-x diagram (pressure, temperature, composition) for the better visualization of the phase behavior of this system. The surface represents the vapour pressure curve (the $NaCl$ saturated gas pressure) for the gas-solid-liquid equilibrium. An interesting property of this system is the evolution of the critical point as a function of the concentration of the solute. Even at concentrations of $NaCl$ as high as 26 % (weight) there is a critical point at 700 °C and 1237 bars above which all phases are merged into one. Another interesting feature is that the concentration of $NaCl$ in saturated gas abruptly increases above a temperature of 550 - 600 °C and above 800 bars.

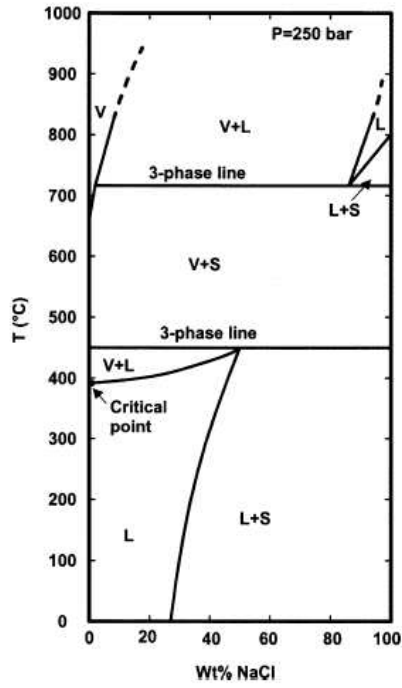


Figure 4-1 T-x projection for the NaCl-H₂O system at 250 bar. The lines delimitate regions of one or two phase equilibria (L-liquid S-solid V-vapor) [Hod-2004].

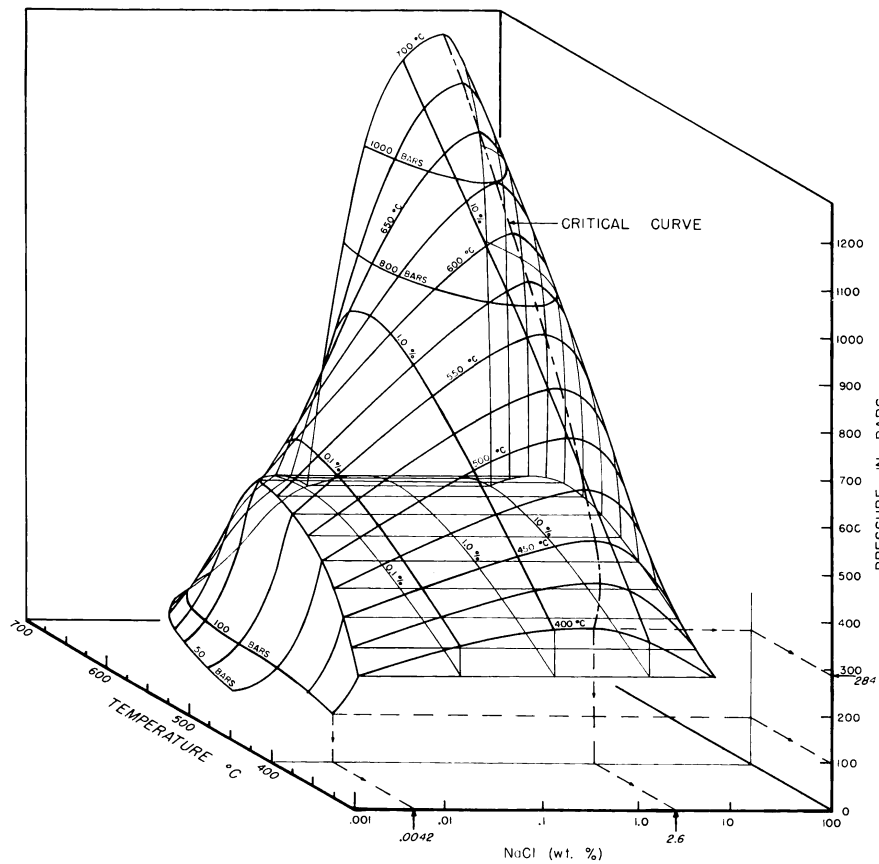


Figure 4-2 p-T-x diagram of a NaCl-H₂O system [Sou-1962].

A quantitative approach for the characterization of solubility in SCW is given by Leusbrock *et al.* [Leu-2010] and will be described below. Considering the equilibrium reaction for the solvation of a MeX salt:



the equilibrium constant for this reaction can be written as:

$$K_s = \frac{a_{\text{MeX}\cdot n\text{H}_2\text{O(aq)}}}{a_{\text{MeX(s)}} \cdot a_{\text{H}_2\text{O}}^n} \quad (4-2)$$

where “*a*” are the activity coefficients of each species and *n* the coordination number (number of solvent molecules involved in the solvation). Since the activity coefficients of MeX(s) are considered equal to unity the concentration of the species can be used instead of the activities. In case of water its concentration changes only because of the variations of density with temperature and pressure. A new equilibrium constant is used with respect to these assumptions:

$$K_s^* = \frac{c_{\text{MeX}\cdot \text{H}_2\text{O(aq)}}}{\rho_{\text{H}_2\text{O}}^n} \quad (4-3)$$

$c_{\text{MeX}\cdot \text{H}_2\text{O(aq)}}$ the molar concentration of the dissolved salt /mol l⁻¹

$\rho_{\text{H}_2\text{O}}$ the molar density of water /mol l⁻¹

This constant can also be written using a van't Hoff-like expression:

$$K_s^* = \exp\left(-\frac{\Delta G_{\text{solv}}}{RT}\right) = \exp\left(-\frac{\Delta H_{\text{solv}}}{RT} + \frac{\Delta S_{\text{solv}}}{R}\right) \quad (4-4)$$

By combining (4-3) and (4-4):

$$\ln c_{\text{MeX}\cdot \text{H}_2\text{O(aq)}} = -\frac{\Delta H_{\text{solv}}}{RT} + \frac{\Delta S_{\text{solv}}}{R} + n \ln \rho_{\text{H}_2\text{O}} \quad (4-5)$$

From a set of given experimental solubility data, ΔH_{solv} , ΔS_{solv} and *n* can be fitted and then equation (4-5) can be used, within a limited range of temperatures and densities to predict solubility.

4.2. Microscopic effects

Ion-water interactions are very strong even in the region of the critical point of the system. This results in large local density inhomogeneities around the solute.

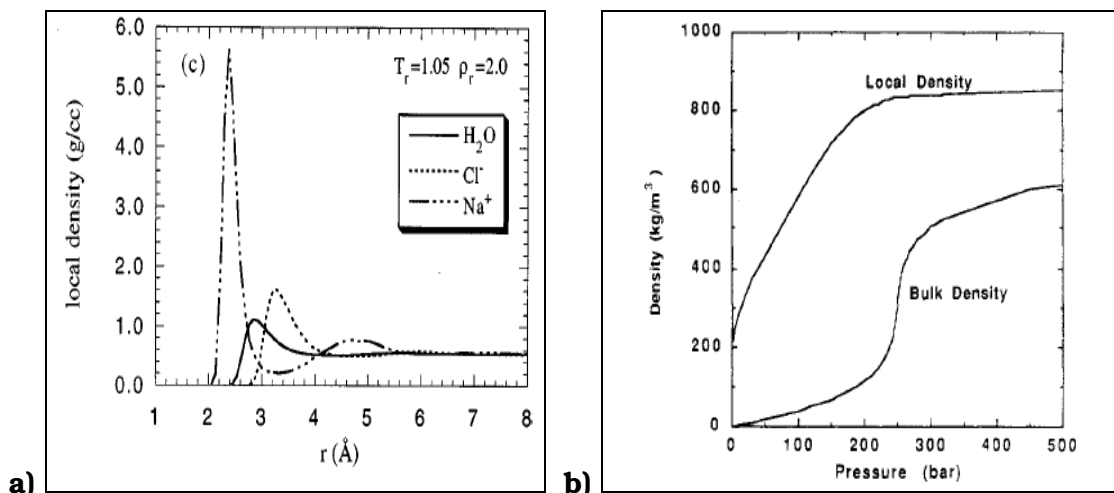


Figure 4-3 a) Comparison of the density inhomogeneities in supercritical water (temperature of 393 °C and bulk density of 0.644 g/cm³) for Na⁺, Cl⁻ and H₂O [Chi-1999]. b) Comparison of bulk density with local density around a monovalent ion at 2.2 Å from its center and at 385 °C [Fla-1989].

From Figure 4-3 it can be seen that local density differ significantly from the bulk density and is around 20 times higher than the bulk density in the case of the Na⁺ cation.

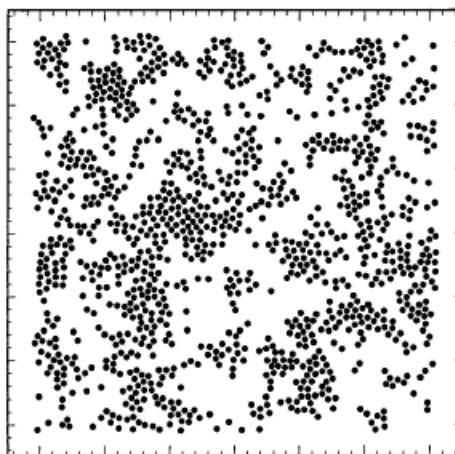


Figure 4-4 Density inhomogeneities in a two dimensional fluid at near-critical conditions [Tuc-1998].

Figure 4-4 illustrates the typical configuration of molecules with emphasis on density inhomogeneities near the critical point. These are related to the solute structure. According to Debendetti *et al.* [Deb-1989], there are three types of solvent-solute interactions in the vicinity of the critical point. These are: **repulsive**, corresponding to a solvent deficient region around the solute, **weakly attractive** and **attractive**, both corresponding to an increase in solvent density around the solute.

An aqueous solution of an electrolyte is an attractive mixture forming both a dense shell around the solute and being characterized by attractive solvent solute interactions. Further insight at this level can be gained through X-ray absorption experiments [Pfu-1994] and molecular simulation of the local environment around the solute. An estimation of the local density enhancement is by these means available.

As in the case of the phase behaviour studies, the NaCl-H₂O system has been most extensively researched and used for the theoretical modelling of the solute-solvent interactions in SCW [Chi-1999]. These simulations bring to light some important ideas about the solvation effects in SCW. Both at room temperature and supercritical conditions, the local density is orders of magnitude higher than the bulk density. The local environment of ionic species is liquid-like and not even extreme variations in temperatures or pressure can alter the density in this so-called first solvation shell [Fla-1997; Tuc-1998]. This relative insensitivity can be understood from Figure 4-5.

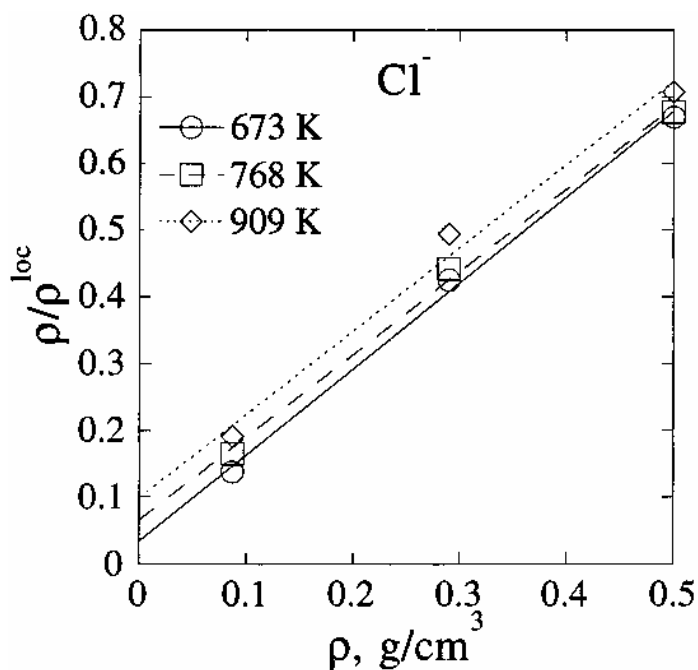


Figure 4-5 Relation between the bulk and the local density around the chloride ion in SCW at three temperatures [Fla-1997].

The ratio between bulk and local density ρ/ρ^{loc} is linearly dependent with ρ at all the represented temperatures, which means that ρ^{loc} is constant. Furthermore, the volume to charge ratio also plays a role on the density around the solvated species. Thus, the local density around Cl⁻ for example is lower than that surrounding OH⁻ both in ambient water and in SCW.

A characterization of the local environment around a solute can also be given in terms of coordination number (number of solvent molecules surrounding the solute or the first solvent

shell) and number of hydrogen bonds. In Table 4-1 this information is provided for a number of ions and for two neutral species (H₂O and HCl).

Table 4-1 Coordination numbers (n_{XO}) and number of hydrogen bonds (n_{HB}) for some ions and molecules at different temperatures and densities [Bal-1996].

ion/molecule	density / g cm ⁻³	T/K	n_{XO}	n_{HB}
OH ⁻	0.997	298	6.6	6.25
	0.29	673	7	5.3
	0.087	673	6.5	5
	0.29	768	6.6	4.85
Cl ⁻	0.997	298	7.4	6.7
	0.29	673	8.1	4.5
	0.087	673	7.5	4.4
	0.29	768	7.8	4.5
HCl	0.997	298	24.9	-
	0.29	673	6.4	-
	0.087	673	2.2	-
H ₂ O	0.997	298	5.1	3.8
	0.29	673	3.1	1.4
	0.087	673	1.6	0.6

ion/molecule	density / g cm ⁻³	T/K	n_{XO}
Na ⁺	0.997	298	5.2
	0.29	673	4.5
	0.087	673	4.6
K ⁺	0.997	298	5.9
	0.29	673	5.7
	0.087	673	4.8
	0.29	768	5.3
Rb ⁺	0.997	298	5.5
	0.29	673	5.5
	0.087	673	5.3
	0.29	768	4.6
Ca ²⁺	0.997	298	8
	0.29	673	7.2
	0.087	673	7.1
	0.29	768	7
Sr ²⁺	0.997	298	7.9
	0.29	673	7.3
	0.087	673	7.4
	0.29	768	7.4

Starting from this data some ideas should be emphasized:

For the anions and neutral species discussed the coordination number and the number of hydrogen bonds, differ. Since these two numbers are evaluated using a geometric criterion [Bal-1996], this difference is to be interpreted in terms of the stability of the hydrogen bond: in order to participate to a hydrogen bond with a solute, the solvent molecule must be from the first coordination shell of the solute and the O-H...X angle should not exceed 30° (where X is the solute) because of the librations that tend to break the bond [Luz-1996, Kon-2001, Laa-2007]. The coordination number for neutral molecules strongly decreases from ambient water to SCW compared to a minimal decrease for ions. This difference is due to the fact that ion-water interactions are stronger than molecule-water interactions.

The same considerations are valid for the hydrogen bonds and although these results are based on a geometrical criterion, they are consistent with the data obtained from nuclear magnetic resonance experiments, indicating the decrease in hydrogen bonding in water at increased temperatures [Mat-1997].

Charge transfer also occurs between ions and water and the lower the absolute charge of an ion, the higher the degree of solvation. In gas phase the ions are considered “fully” charged. The dependence of charge with temperature is described in Figure 4-6 based on a quantum mechanical and molecular mechanical method (QM/MM) and simulating on 1000 molecules (999 molecules of water and 1 molecule of solute) [Yag-2005].

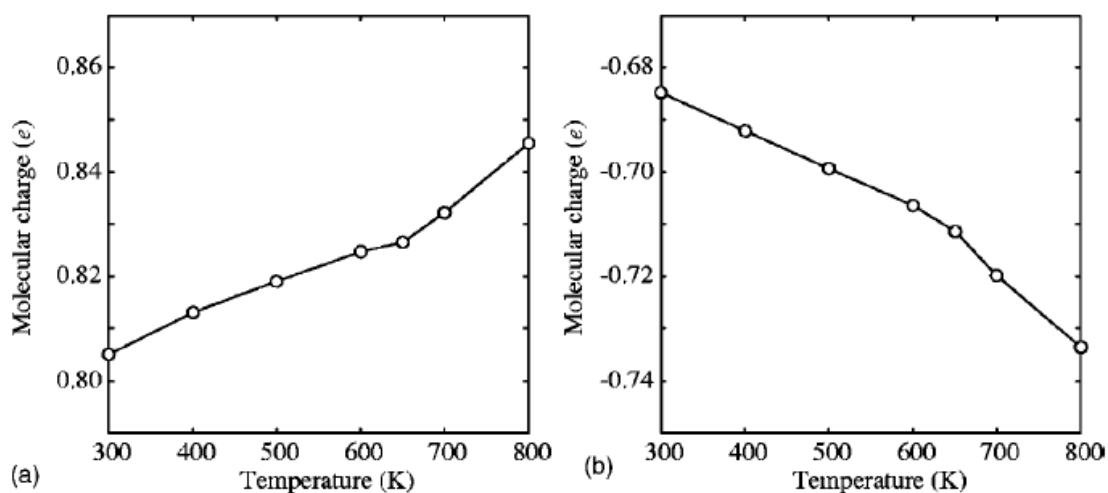


Figure 4-6 Dependence of charge for a) H₃O⁺ and b) OH⁻ with temperature (absolute charge for both ions is 1 e in gas phase) [Yag-2005].

As a last matter at microscopical level, ion pairing will be briefly discussed. Ion pairing refers to the partial association of oppositely charged ions in solutions of electrolytes [Mar-2006]. Three main types of ion pairs can be distinguished: solvent separated ion pairs, solvent shared ion pairs and contact ion pairs (Figure 4-7).

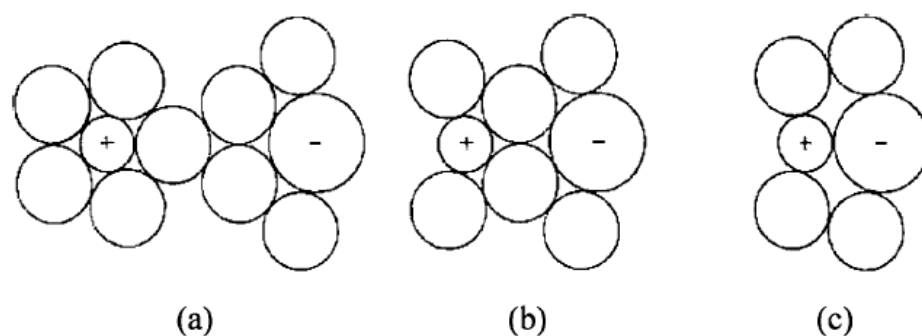


Figure 4-7 Types of ion pairs: a) solvent separated (2SIP); b) solvent shared (SIP); c) contact (CIP) [Mar-2006].

The phenomenon of ion pairing is augmented in SCW due the decrease in the solvation power of water. At higher temperatures, the association constant increase by 3-4 orders of magnitude even for substances that are strong electrolytes in ambient solutions [Chi-2000]. This phenomenon is invoked to explain some effects in SCW like the precipitation of salts in SCW [Cui-1995; Fla-1989], the diminished dissociation of acids and bases [Tre-2004], the prevalence of ionic mechanisms in the hydrolysis of *tert*-butyl chloride [Wes-2001; Joh-2001] or the peculiar effect of NaCl on the hydrolysis of diphenylether which will be discussed briefly hereinafter as a suggestive exemplification of salt effect in supercritical water.

Dilute solutions of NaCl in supercritical water (up to 3.1 % wt.) causes the rate of hydrolysis of diphenylether to decrease. A protonated diphenylether is an intermediate for this reaction,

postulated to follow a SN1 mechanism. At low concentrations, the decrease in the reaction rate is explained by the formation of $\text{H}^+ \text{Cl}^-$ ion pairs as a subsequent step to NaCl dissociation, thus by the removal from the solution of protons (formed through water self-dissociation) which were necessary for the formation of the protonated diphenylether intermediate. Cl^- exerts a stronger attraction on H^+ than on Na^+ . Hence the reaction rate decreases at small concentrations of NaCl due to the reduced availability of H^+ . At higher concentrations of the salt, the effect is reversed. The solvent separated Na^+Cl^- ion pairs transfers enough charge to the surrounding water mantle and the $\text{Na}^{\delta+}\cdots\text{OH}^-\cdots\text{H}^{\delta+}$ species, whose concentration increases with the NaCl concentration, are now likely to transfer the proton to the diphenylether molecules, thus accelerating the rate determining step and the overall reaction rate of the hydrolysis [Pen-2000].

As a general remark for the microscopic effects described, a good knowledge of the behaviour of the solutes in the high temperature and pressure aqueous systems can bring precious information about the unfolding of the reactions at those conditions.

4.3. Acids and Bases in SCW

The dissociation of acids requires charge separation for which the polarity of the solvent plays an important role as a measure of its ability to solvate these charges. Since water approaching its critical point is rather unpolar, acids which are strong in ambient water are rather weak in SCW.

With the increase in temperature water loses part of its hydrogen bonding network and by that the ease to solvate protons. At ambient temperature water consists of extended hydrogen bond networks which become increasingly fragmented as temperature increases, influencing parameters such as the compressibility which becomes infinite in the critical point. A straightforward correlation with the acidity of the solvated species is, however, not possible. These ideas can not explain directly the augmenting of the dissociation constant for many species including water in a temperature region between 273 and 573 K (see Figure 4-8). A quantitative study of this effect needs to consider the thermodynamic parameters which influence the dissociation constant. An expression of the latter is written below [Tre-2004]:

$$\lg K_{T,p} = \frac{1}{2,303R} (\lg K_{T_r,p_r} + \Delta H_{T_r,p_r}^0 (\frac{1}{T_r} - \frac{1}{T})) + \int \frac{\Delta C_p^0}{T} dT - \frac{1}{T} \int \Delta C_p^0 dT - \int \frac{\Delta V^0}{T} dp \quad (4-6)$$

T temperature

p pressure

T_r reference temperature

p_r reference pressure

ΔC_p^0 standard partial molar heat

ΔH^0 standard molar enthalpy of formation

ΔV^0 standard partial molar volume

$K_{T,p}$ dissociation constant at the given conditions

R gas constant

the indices T_r and p_r refer to quantities at the reference temperature and pressure

As it is seen in equation (4-6) there are several parameters which influence the dissociation constant making its dependence on temperature more complex than explained by the solvation power of water alone. By increasing temperature, the ability of water to solvate protons decreases, but the proton transfer increases. Therefore, there is an intermediate region between ambient temperature and the critical temperature, where proton transfer reaches a maximum and thus acidity increases. Nevertheless, at temperatures which are high enough, above the intermediate temperature region of increased acidity (200 - 350 °C), the value dissociation constant for any acid drops dramatically due to the above-mentioned inability of water to solvate the protons which therefore remain attached to the respective anion.

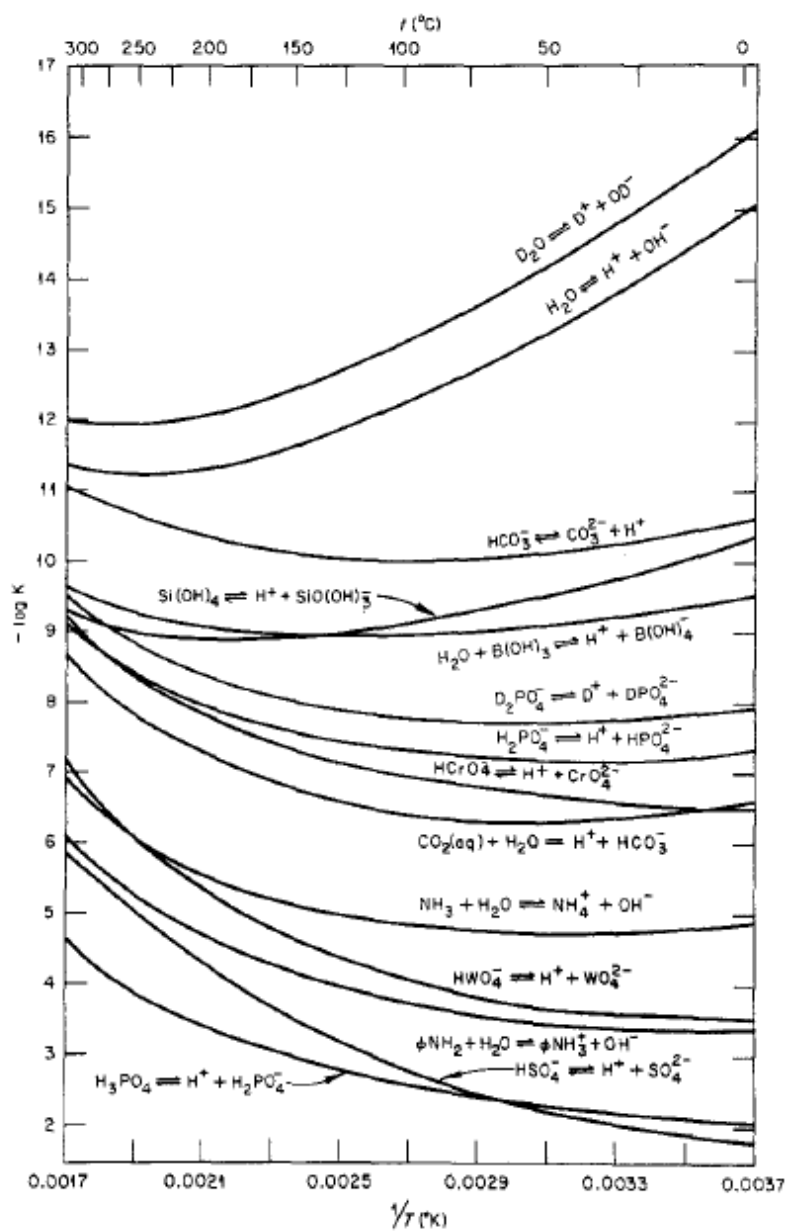


Figure 4-8 Temperature dependence of dissociation constants for weak acids and bases. The symbol ϕ represents cyclohexyl- [Mes-1988].

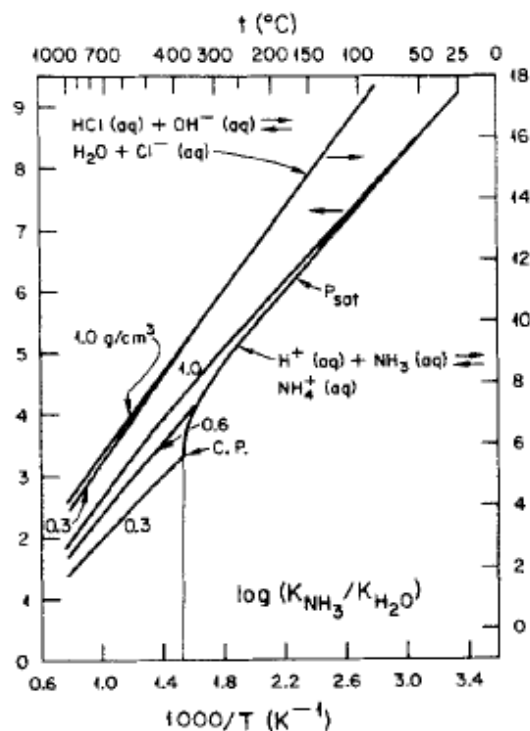


Figure 4-9 Relative acidity (to water) $\lg(K_s/K_w)$ for $\text{HCl}(\text{aq})$ and $\text{NH}_3(\text{aq})$ as a function of temperature [Mes-1988].

Mesmer *et al.* [Mes-1988] compared the acidity of HCl to that of water and found that at temperatures of about 1000 K the dissociation constant of hydrochloric acid is only two orders of magnitude higher than that of water while at room temperature the ratio is significantly higher (Figure 4-9). The strength of acids and bases decreases with temperature approaching that of water. An investigation of this effect based on molecular simulation has been carried out by Johnston *et al.* [Joh-1996]. The following equilibria were taken into account:



The equilibrium representing the relative acidity of hydrochloric acid to water in (4-9) is almost completely shifted to the right at both room temperature and above the critical temperature of water. A solvation effect of minor importance moves the equilibrium in (4-9) to the left: water as a polar solvent with $\epsilon = 80$ solvates better the small OH^- than the Cl^- anion due to the larger charge to volume ratio; at higher temperatures, as the dielectric constant of water decreases this difference diminishes bringing a minor increase in the acidity of HCl relative to water. The theoretical study concluded that the dissociation free energy is almost constant for the two compared species (water and HCl) and the driving force for the decrease of HCl acidity relative to water is temperature:

$$\Delta pK_a = \frac{\Delta\Delta A^{\text{diss}}}{2.3RT} \quad (4-10)$$

where $\Delta pK_a = pK_a - pK_w = -\lg K_w + \lg K_a$

and $\Delta\Delta A^{\text{diss}}$ is the difference in the free energy of dissociation for the two acids (hydrochloric acid and water). Since $\Delta\Delta A^{\text{diss}}$ is almost constant, the decreasing difference in acidity is proportional to an increase in $1/T$.

A decrease in acidity with temperature has been observed for carboxylic acids as well. Data for the calculation of dissociation constant for several aliphatic carboxylic acids up to 350 °C and 23 MPa are available in the literature [Sue-2004].

The acidity of β -naphthoic acid has been studied by the *in-situ* measurement of the UV-absorption of the acid (dissociated and undissociated form) in pure water and in a solution where NH_3 was also present [Xia-1997]. The dissociation of the acid is favoured by the presence of NH_3 which is a stronger base than water even at supercritical conditions. Another important conclusion of the study is that the density plays a minor role in the isocoulombic reaction between β -naphthoic acid and the OH^- from water but has an increased importance in an ionogenic reaction like the one between β -naphthoic acid and ammonia since the higher solvent density favours the solvation of ions.

Regardless if the medium is ambient water or SCW, the strength of acids and bases is determined by the balance between the energy release through solvation of the species and the energy required for the proton-anion bond break. This factor should be taken into account when acidity is to be determined. This balance also determines if the solvation process is exothermic or endothermic.

5. Experimental Part

5.1. Description of the Experimental Apparatus

For the experiments in near and supercritical water two types of reactors have been used. For the experiments where no precise temperature control was necessary, a pipe reactor was used. For all other experiments a continuously stirred tank reactor (CSTR) was used. A flow-chart of the reactor system is given in Figure 5-1.

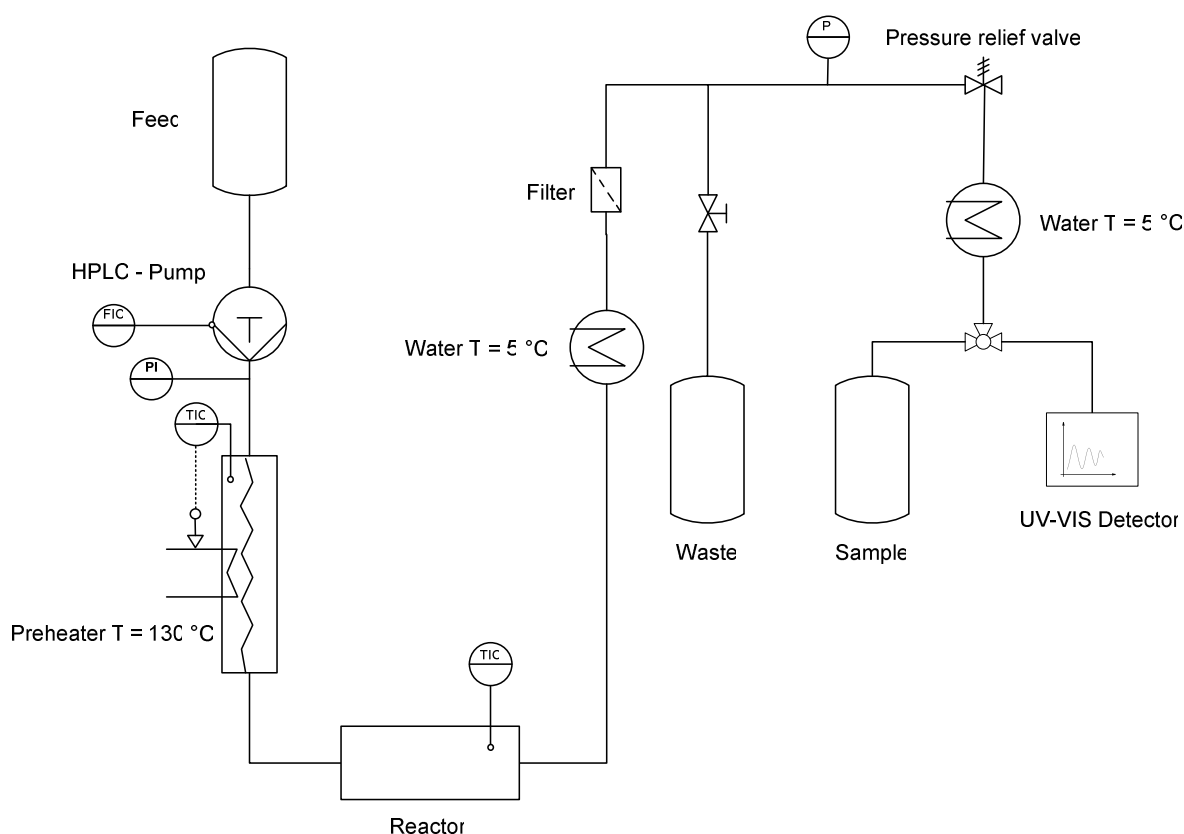


Figure 5-1 Scheme of the reactor system used for experiments in near- and supercritical water.

The feed solution is pumped through the system by a HPLC-Pump (Kontron Instruments HPLC Pump 422; max. flow 10 ml min^{-1} ; $p_{\text{max}} = 400 \text{ bar}$). The two reactor types used will be described in the next section. The preheater consists of a pipe reactor made of stainless steel. The temperature control succeeds here by a temperature controller (Julabo LC 5-E) connected with Pt100 thermocouples. The temperature in the reactor is controlled similarly using a Eurotherm temperature controller and NiCr/Ni thermocouples. The reaction medium is then cooled by a double pipe heat exchanger with water at $5 - 10 \text{ °C}$ as a cooling medium. An inline filter with sintered stainless steel filter elements ($20 - 100 \mu\text{m}$ porosity) is used to protect the subsequent components from solids and accumulations thereof, which lead to deterioration. The pressure control succeeds manually by a pressure relief valve. The solution

emerging from the reactor is cooled again (also by a double pipe heat exchanger with water at 5 °C as a cooling medium) in order to keep volatile components in the liquid phase. A three way valve is used to switch between a sampling collection line and a line leading to an UV/VIS Spectrometer (Perkin-Elmer Lambda 14P) used to check that the concentration among the reaction products remains constant with the time. Another use of this device is for determining the residence time distribution in the reactor with the help of tracers.

5.2. Design and Construction of the Reactors

5.2.1. Pipe Reactor

The pipe reactor consists of a stainless steel type 1.4301 or 1.4541 with 1/8” outer diameter and 1 or 2 mm inner diameter. The volume of the reactor is 3 ml. The pipe is coiled around an aluminium cylinder core which is heated by a 500 W heating cartridge. Two aluminium jackets covering the aluminium cylinder and the coiled pipe are used for a uniform heat distribution. Two axial bore holes are made, in the jacket and in the cylinder for inserting the thermocouples used for temperature control. The reactor isolation is made of glass wool.

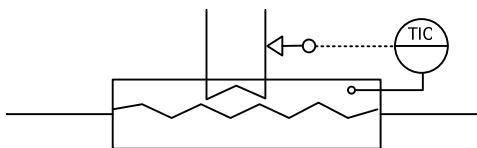


Figure 5-2 Scheme of a pipe reactor used for some preliminary experiments.

5.2.2. Continuously Stirred Tank Reactor

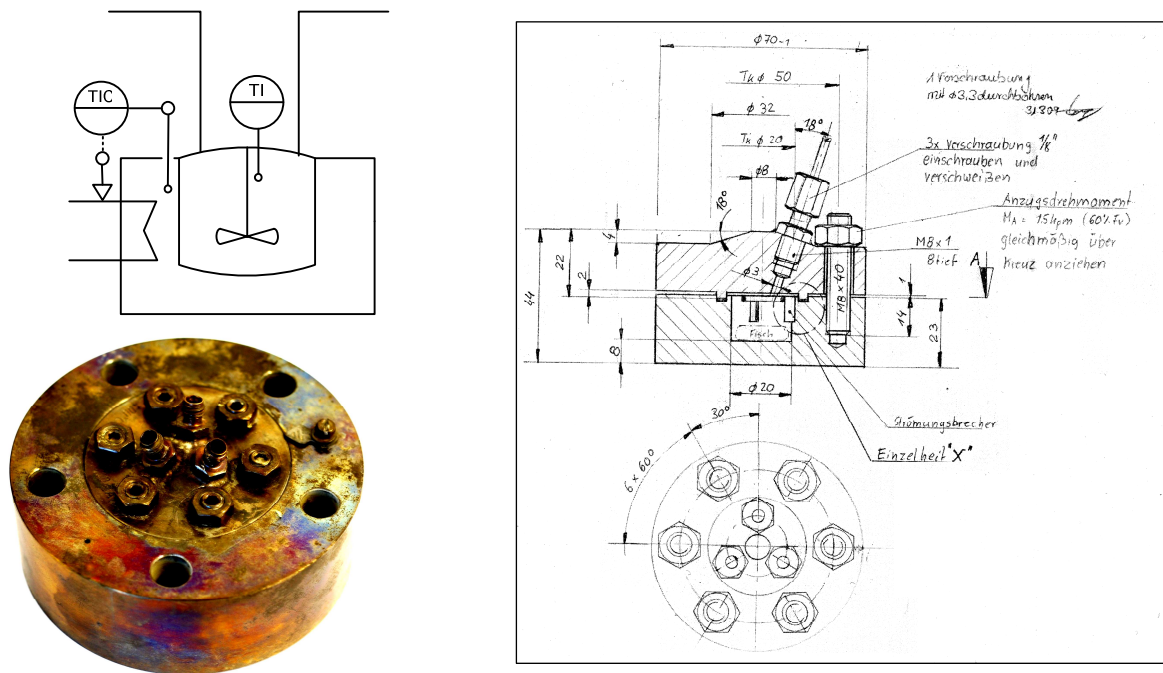


Figure 5-3 Scheme and execution drawing of the CSTR used for experiments in near- and supercritical water.

As in the case of the pipe reactor (Figure 5-2) the isolation is made with glass wool. The free volume in the reactor is 4.5 ml. The material of construction is stainless steel type 1.4571. The closure head has three outlets, two for the circulation of the reaction fluid and one for the insertion of a thermo couple for temperature control. The two reactor parts, the reactor body and the closure head are assembled with the help of screws and then sealed with a graphite gasket. In order to ensure a good mixing in the reactor, a flow breaker and a magnetic stir bar of AlNiCo type (*Curie*-Temperature of about 850 °C), mantled in stainless steel are used. The stir bar is rotated by an external magnetic stirrer equipped with strong Neodymium magnets. These are cooled by a cooler fan. The reactor is inserted into a steel jacket with bore holes for heating cartridges. The limiting conditions for the use of the reactor are a pressure of 400 bars and a temperature of 430 °C.

5.2.3. Temperature Control

In this section, the temperature control inside the CSTR will be discussed. The temperature is controlled with the help of a **temperature controller**. Two NiCr/Ni thermocouples are used for measuring the temperature in the reactor. One measures the temperature in the reactor and the other in the heating jacket. The thermocouple which measures the actual temperature in reactor can not be used for controlling temperature. The reason is the following: the feed enters the reactor from the preheater at a temperature of 130 °C which is significantly below the temperature in the reactor. This inflow of low temperature substance causes the

temperature controller to increase the heating rate of the reactor. By this phenomenon the reactor is overheated and the temperature oscillates around the set point. The amplitude of these oscillations is directly correlated to the flow rate. Thus, at higher flow rates and reduced residence times, the oscillations of the temperature in reactor are quite significant.

A method of avoiding this behaviour is to use the temperature of the heating jacket for temperature control. The temperature set in the jacket is higher than the temperature which must be obtained in the reactor. This difference is dependent on the flow rate. The higher the flow rate, the larger is the difference between the two temperatures. For a constant flow rate, a fine adjustment of the temperature in the heating jacket eventually provides a constant temperature in the reactor. With flow rates in the range 0-10 ml min⁻¹ the deviation from the set temperature in the reactor is ±1 °C.

It has been noticed that there is a linear dependence between the temperature to be set in the jacket and the flow rate. This behaviour is illustrated in Table 5-1.

Table 5-1 Temperatures in heating jacket and reactor as a function of the flow rate, at a pressure of 350 bar.

T _{heating jacket} /°C	481	433	412	403	398	395
Fl. rate /ml min ⁻¹	8.951	4.662	2.2985	1.506	0.774	0.484
T _{reactor} /°C	386	385	385	385	386	385

By graphically representing the temperature in the heating jacket against the flow rate, a linear dependence between the two is obvious.

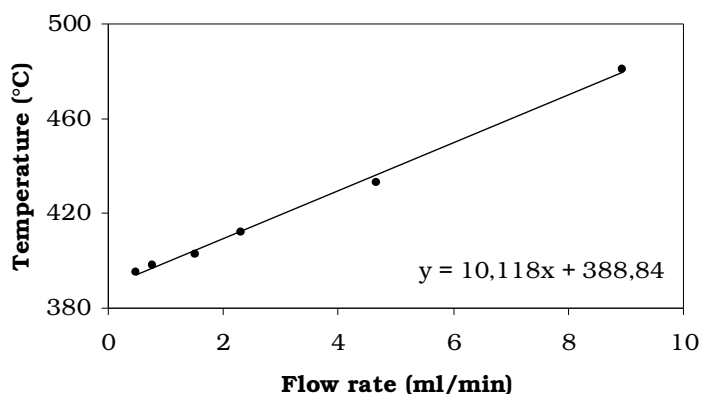


Figure 5-4 Linear dependence of the temperature in the heating jacket with the flow rate for a specified temperature of 385 °C in the reactor.

In this particular case (Figure 5-4) the temperature to be adjusted for a set flow rate can be obtained by the equation:

$$\text{Temperature} = 10.118 \cdot \text{Flow rate} + 388.84 \quad (5-1)$$

the temperature in heating jacket is in °C and the flow rate in ml min⁻¹.

5.3. Operation of the Installation

The feed was pumped from the container through the preheating zone and then through the reactor. The density of the aqueous solutions was always considered to be that of the water at 20 °C and 1 bar (1 g/ml). The term “**residence time**” used further on is equivalent to “**reaction time**” and it refers to the average period of time spent by the reactant in the reactor. The required residence time of the feed in the reactor was set through the flow. The mass flow balance inside and outside the reactor yields the following expression for the residence time:

$$\dot{V} \cdot \rho_{H_2O,STP} = \frac{V_R \cdot \rho_{H_2O,p,T}}{\tau} \quad (5-2)$$

thus,

$$\tau = \frac{V_R \cdot \rho_{H_2O,p,T}}{\dot{V} \cdot \rho_{H_2O,STP}} \quad (5-3)$$

with the following notations:

τ	residence time	/s
V_R	reactor volume	/ml
\dot{V}	pump flow rate	/ml s ⁻¹
$\rho_{H_2O,STP}$	water density at room (standard) temperature and pressure	/g ml ⁻¹
$\rho_{H_2O,p,T}$	water density at reaction temperature and pressure	/g ml ⁻¹

For the aqueous solutions employed as feed, the densities of water at the respective reaction temperatures and pressures were used.

Flushing the installation with the solution resulting from the reactor for a longer time is important for ensuring that the samples collected for the analysis have the correct concentration and that the system reached a steady state. As mentioned earlier, an **UV/VIS spectrometer** is connected to the installation, enabling to monitor the absorption at a chosen wavelength along the time. This enables to collect samples only at constant concentration of the reaction products in the solution. Determining the optimal time for sampling is also important to prevent unnecessary waste of reagents, especially when expensive ones are used. An example of this so-called time drive is given in Figure 5-5.

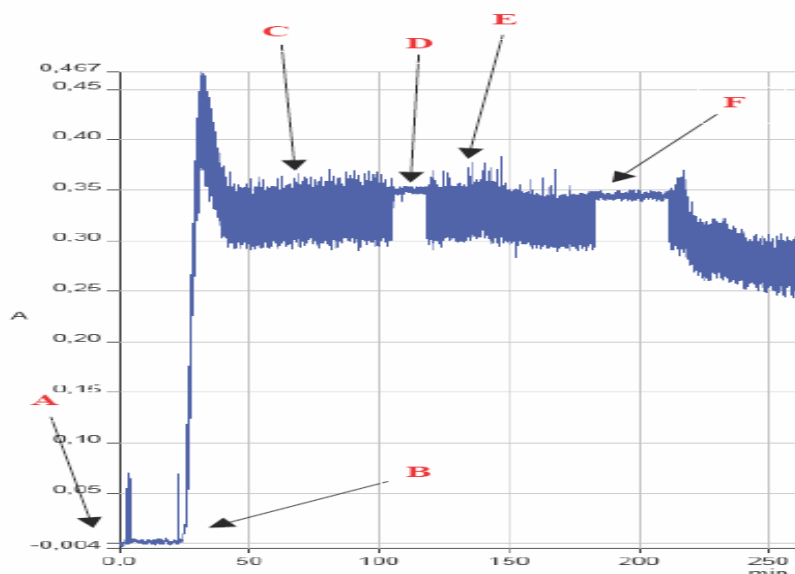


Figure 5-5 Time drive at 240 nm for a reaction using lactic acid feed at 385 °C and various reaction times.

The point **A (0 Min)** corresponds to the moment where the lactic acid feed has been released through the installation at a flow of 0.88 ml min^{-1} . At point **B (24 Min)** the reaction mixture reaches the UV/VIS observation cell. Thus, an approximate volume of the installation of 21 ml ($24 \text{ Min} \cdot 0.88 \text{ ml min}^{-1}$) can be calculated.

At point **C (66 Min)** the composition of the reaction mixture can be considered constant in time. The approximate volume needed for flushing in order to obtain a constant concentration in the reaction mixture is 37 ml ($\sim (66-24) \text{ min} \cdot 0.88 \text{ ml min}^{-1}$).

A sample has been acquired at point **D (104.5 Min)**. At **E (120 Min)** the flow rate has been set to 0.44 ml min^{-1} . The composition of the reaction mixture has been considered constant in **F (179 Min)**. Thus, once the feed has flushed the reactor the waiting time in order to collect accurate samples decreases: $0.44 \text{ ml min}^{-1} \cdot (179-120) \text{ Min} \approx 26 \text{ ml}$.

Temperature in reactor is adjusted through the heating elements mounted in the heating jacket of the reactors. In the case of the pipe reactor, no definite value in the reactor has been measured. Instead, the temperature of the heating jacket has been taken as reaction temperature. For the experiments where well-defined reaction temperature was needed, the continuously stirred tank reactor has been used. The method for the respective temperature control has been described in the previous section.

5.4. Methods of Analysis

Most of the analyses were carried out with the help of a HPLC system. Analysis of the gas phase has been carried out using an FTIR- Spectrometer as seen in section 5.4.3. In the cases where the substance identification by HPLC was unsatisfactory, supplementary ¹H-NMR analyses were carried out.

5.4.1. HPLC Analysis

The HPLC analyses were carried out using a Shimadzu HPLC system equipped with a refractive index detector and a photodiode array UV/VIS detector, as detailed in the Table 5-2.

Table 5-2 Technical specifications for the HPLC used

Instrument designation	Type
Pump	LC-20AD
Autosampler	SIL-20AC
Refractive index detector	RID-10A
Photodiode array detector	SPD-M20A
System controller	CBM-20A
Column oven	Beckman Coulter Jetstream 2

The following conditions were used for the separations:

Table 5-3 System parameters and conditions for the HPLC analyses

Column type	Synergi Hydro 4 μ m 80A 250 x 3 mm
Column oven temperature	17 °C
Mobile phase	H ₂ SO ₄ 10 mM (pH = 2);
Flow rate	0.375 ml/min
Injection volume	20 μ L
RI-Detector temperature	40 °C
PDA-Detector temperature	40 °C
Autosampler/Sample temperature	7 –15 °C

A representative chromatogram where all important substances are present is shown in Figure 5-6.

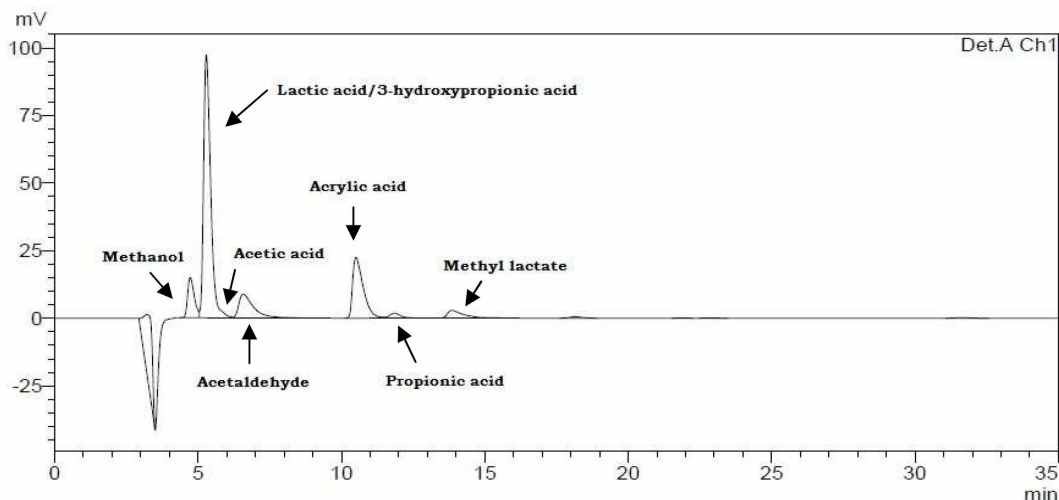


Figure 5-6 Chromatogram of a reaction mixture from an experiment using 0.1 M methyl lactate as feed at a temperature of 385 °C, a pressure of 350 bar and a reaction time of 100 s. Analysis carried out with the refractive index detector.

The detected substances and their retention times at the apex of the peak are given in Table 5-4.

Table 5-4 Identified substances on the chromatograms and their retention times.

Substance	Retention time /Minutes
Methanol	4.8
Lactic acid/ 3-hydroxypropionic acid	5.35
Acetic acid	5.83
Acetaldehyde	6.74
Acrylic acid	10.69
Propionic acid	11.99
Methyl lactate	13.8

As shown in Figure 5-6 this system failed to separate lactic acid from 3-hydroxypropionic acid and although in most of the experiments the latter should be absent, it could account for some measurement errors.

Another important source of errors is the manner in which the chromatogram peaks are graphically integrated. An approach for the estimation of such errors is given in the Appendix.

5.4.2. Quantification of 3-Hydroxypropionic acid

In this section, the results leading to the interpretation of the chromatogram peak of lactic acid/3-hydroxypropionic acid is described in detail. As mentioned in Section 5.4.1, the HPLC

analysis fails to separate lactic acid from its isomer (3-Hpa). However, this inconvenient of the method is negligible for the determinations using lactic acid as feed. As indicated by ¹H-NMR experiments, the lactic acid to 3-Hpa molar ratio is 5 - 10 (See Appendix). The following discussion regards the experiments using acrylic acid as feed where higher amounts of 3-Hpa are formed.

The HPLC analysis yields peaks corresponding to the sum of the concentrations of the two isomers. The area of a peak representing the overlapping of lactic acid and 3-Hpa can be related to the concentrations (Equation 5-4):

$$A_{\text{peak}} = c_{\text{Lac}} \cdot r_{\text{Lac}} + c_{\text{Hpa}} \cdot r_{\text{Hpa}} \quad (5-4)$$

where,

A_{peak}	surface of the peak representing the two substances /mV s
c_{Lac}	concentration of the lactic acid /mol l ⁻¹
c_{Hpa}	concentration of 3-hydroxy-propionic acid /mol l ⁻¹
r_{Lac}	response factor of lactic acid /mV s l mol ⁻¹
r_{Hpa}	response factor of 3-hydroxy-propionic acid /mV s l mol ⁻¹

The response factor is defined as ratio of the area of a peak containing the pure substance to the concentration of that particular substance:

$$r_{\text{Lac}} = \frac{A_{\text{Lac}}}{c_{\text{Lac}}} \quad (5-5)$$

with A_{Lac} the area of a peak of the pure lactic acid.

A linear calibration curve relates the concentration of lactic acid to its peak area through:

$$A_{\text{Lac}} = c_{\text{Lac}} \cdot a + b \quad (5-6)$$

with a, b real numbers. By rewriting (5-6):

$$\frac{A_{\text{Lac}} - b}{c_{\text{Lac}}} = a \quad (5-7)$$

For a fine calibration, which valid for very small concentrations, b is very small and it can be neglected. Thus, by combining (5-5) and (5-7):

$$r_{\text{Lac}} = \frac{A_{\text{Lac}}}{c_{\text{Lac}}} \simeq \frac{A_{\text{Lac}} - b}{c_{\text{Lac}}} = a \quad (5-8)$$

For a linear calibration curve, the **response factor can be considered constant**.

The molar ratio of the two isomers can be defined:

$$B = \frac{c_{\text{Lac}}}{c_{\text{Hpa}}} \quad (5-9)$$

By combining (5-4) with (5-9) (with the assumption that the response factor is a constant) the concentrations can be determined:

$$c_{\text{Hpa}} = \frac{A_{\text{peak}}}{B \cdot r_{\text{Lac}} + r_{\text{Hpa}}} ; c_{\text{Lac}} = \frac{A_{\text{peak}}}{r_{\text{Lac}} + \frac{r_{\text{Lac}}}{B}} \quad (5-10)$$

In conclusion, the concentrations of lactic acid and 3-Hpa can be determined by knowing the area of their common HPLC peak and the ratio of the isomers in the sample (determined by $^1\text{H-NMR}$).

A practical difficulty in pursuing this approach is the determination of the response factor for 3-Hpa. The pure acid has not been obtained. In solution, 3-Hpa is in equilibrium with its water addition product, acrylic acid. Besides, the analysis of 3-Hpa pure substance solutions used for the calibration indicated significant amounts of impurities (other than acrylic acid) which raised serious concerns about the accuracy of the calibration. Given these factors which make the determination of $r_{3\text{-Hpa}}$ difficult, a simplifying assumption, $r_{\text{Lac}} = r_{\text{Hpa}}$ has been made, which for the given experiments lead to a relative error of max. 26% as further explained. Using a single response factor (r_{Lac}) for all substances, the expressions for the concentrations become:

$$c_{\text{Hpa}}^* = \frac{A_{\text{peak}}}{r_{\text{Lac}}(B + 1)} ; c_{\text{Lac}}^* = \frac{A_{\text{peak}}}{r_{\text{Lac}}(1 + \frac{1}{B})} \quad (5-11)$$

The percent errors of calculating concentrations using the response factor of lactic acid for both substances relatively to the concentrations calculated using different ones can be expressed as follows:

$$e_{\text{Hpa}}^{\text{R}} = \left| \frac{c_{\text{Hpa}}^* - c_{\text{Hpa}}}{c_{\text{Hpa}}} \right| \cdot 100 ; e_{\text{Lac}}^{\text{R}} = \left| \frac{c_{\text{Lac}}^* - c_{\text{Lac}}}{c_{\text{Lac}}} \right| \cdot 100 \quad (5-12)$$

By substituting (5-10) and (5-11) in (5-12) the relative errors become:

$$e_{\text{Hpa}}^{\text{R}} = e_{\text{Lac}}^{\text{R}} = \left| \frac{B + \frac{r_{\text{Hpa}}}{r_{\text{Lac}}}}{B + 1} - 1 \right| \cdot 100 \quad (5-13)$$

with the notation:

$$\mathbf{A} = \frac{r_{\text{Hpa}}}{r_{\text{Lac}}} \quad (5-14)$$

the relation above becomes:

$$e_{\text{Hpa}}^{\text{R}} = e_{\text{Lac}}^{\text{R}} = \left| \frac{B + A}{B + 1} - 1 \right| \cdot 100 \quad (5-15)$$

From the HPLC analysis, by integrating the respective peak areas of the chromatograms of the respective pure substances the values of the response factors are obtained (Table 5-5).

Table 5-5 Response factors calculated from the HPLC chromatograms of the pure* substances of lactic acid and 3-hydroxypropionic acid.

Substance	Concentration/ mol l ⁻¹	Peak area /mV s	Response factor /mV s l mol ⁻¹
lactic acid	0.0985	3 743 949	38 009 635
3-hydroxy-propionic acid	0.108	2 779 387	25 735 065

*3-Hpa was calibrated using solutions where other substances were present in significant amounts

The ratio of the response factors is:

$$A = \frac{r_{\text{Hpa}}}{r_{\text{Lac}}} = 0.677 \quad (5-16)$$

The ratio of the two isomers can be obtained from the ¹H-NMR analysis. Thus, knowing the values for A and B, the relative error from (5-15) can be determined. The relative errors for the determination of the isomers at three residence times and 385 °C are given in Table 5-6.

Table 5-6 Molar ratio of lactic acid to 3-hydroxy-propionic acid and the errors in determining the concentration of the two isomers, in a stability test of a 0.05 M acrylic acid solution at different residence times and a temperature of 385 °C.

Residence time /s	$\frac{C_{\text{Lac}}}{C_{\text{Hpa}}}$	$e_{\text{Hpa}}^R = e_{\text{Lac}}^R$
25	0.238	26
80	0.59	20
150	0.741	19

The maximum error is obtained for the highest molar ratio of lactic to 3-hydroxy-propionic acid. This ratio is obviously higher for shorter residence times. Since 25 seconds is the shortest residence time for the measurements at 385 °C, one can conclude that 26 % is the maximum error due to the approximation $r_{\text{Lac}} = r_{\text{Hpa}}$.

For determining the ratio of the isomers various interpolation/extrapolation fits have been used at each temperature, based on ¹H-NMR measurements at three residence time (the ratio is considered to be zero when the residence time equals zero, thus an additional point can be gained). An example of a good fit is given for the measurements at 385 °C in (5-17). The expressions of the other fits used to determine the concentrations of the two isomers are given in the Appendix.

$$B_{385^\circ\text{C}}(\tau) = 0.2833 \cdot \ln(\tau) - 0.668 \quad (5-17)$$

where τ is the residence time in seconds.

Next, the combination of (5-10), (5-11) and (5-17) gives the expressions of the concentrations of the discussed substances.

$$c_{\text{Hpa}} = \frac{A_{\text{peak}}}{(0.2833 \cdot \ln(t) - 0.668) \cdot r_{\text{Lac}} + r_{\text{Hpa}}} \quad (5-18)$$

$$c_{\text{Lac}} = \frac{A_{\text{peak}}}{r_{\text{Lac}} + \frac{r_{\text{Hpa}}}{(0.2833 \cdot \ln(t) - 0.668)}} \quad (5-19)$$

$$c_{\text{Hpa}}^* = \frac{A_{\text{peak}}}{r_{\text{Lac}}(0.2833 \cdot \ln(t) + 0.332)} \quad (5-20)$$

$$c_{\text{Lac}}^* = \frac{A_{\text{peak}}}{r_{\text{Lac}} \left(1 + \frac{1}{0.2833 \cdot \ln(t) - 0.668} \right)} \quad (5-21)$$

Table 5-7 Data from experiments for the stability of acrylic acid (feed 0.05M) at 385 °C and different residence times. The asterisk symbolizes that the respective concentrations were calculated using the response factor of lactic acid for both isomers. "S" is the abbreviation for selectivity.

R.t. /s	0	50	100	150	200	320
$c_{\text{Acr}} / \text{mol l}^{-1}$	0.05015	0.0425	0.04	0.0368	0.0336	0.0307
Conversion /%	0	15	21	27	33	39
$A_{\text{peak}} / \text{mV s}$	0	109897	130740	132874	136717	137848
$c_{\text{Lac}} / \text{mol l}^{-1}$	0	0.0011	0.0017	0.0018	0.0020	0.0021
$c_{\text{Lac}}^* / \text{mol l}^{-1}$	0	0.0009	0.0013	0.0015	0.0016	0.0018
$c_{\text{Hpa}} / \text{mol l}^{-1}$	0	0.0026	0.0026	0.0024	0.0024	0.0022
$c_{\text{Hpa}}^* / \text{mol l}^{-1}$	0	0.0020	0.0021	0.0020	0.0020	0.0018
$S_{\text{Lac}} / \%$	0	15	16	14	12	11
$S_{\text{Hpa}} / \%$	0	34	25	18	14	11

The concentrations of acrylic acid, lactic acid and 3-hydroxypropionic acid are given in Table 5-7, the latter calculated with and without using different response factors.

The two isomers of lactic acid account for max. 50 % of the decomposition products of acrylic acid at 385 °C (50 moles isomers from 100 moles converted acrylic acid). However, these

concentrations are near the lower limit of the calibration range used for quantification and thus, the obtained values are subject to significant errors.

As mentioned, the commercially available 3-hydroxypropionic acid used for the quantification and determination of the response factor contained significant amount of impurities and only an approximate concentration is specified. Thus, the value of the response factor has been considered uncertain and this was the background for its approximation with the response factor of lactic acid which, in contrast, has been accurately determined. The determination of lactic acid and 3-hydroxy-propionic acid is further discussed in Section 6.1.6. and in the Appendix.

5.4.3. FTIR Measurements

The gases resulting from various reactions carried out in near- and supercritical water have been collected using a gas syringe and then identified using an Alpha Spectrometer from Bruker Optics with a DTGS-Detector. A cell for gas measurements has been mounted to the spectrometer. An image of it is presented in Figure 5-7.

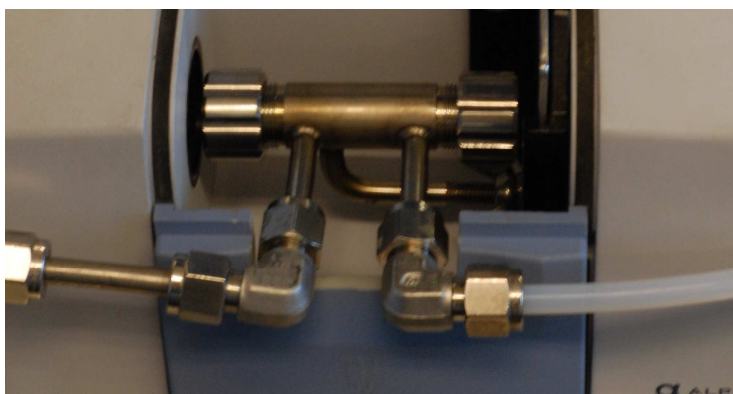


Figure 5-7 An image of the cell used for gas measurements with a FTIR Spectrometer.

Two cylindrical zinc selenite windows of 2 mm thickness and 15 mm in diameter were installed at each end of the cell and the distance between the inner surfaces of the windows is 6 cm.

The single substances were calibrated by filling the cell with a known volume percent of the respective gas. Thus, CO, CO₂ and C₂H₄ were calibrated and their ratio in the gas sample has been measured by integration of the substance specific signal groups from an Extinction/Wave number (Figure 5-8).

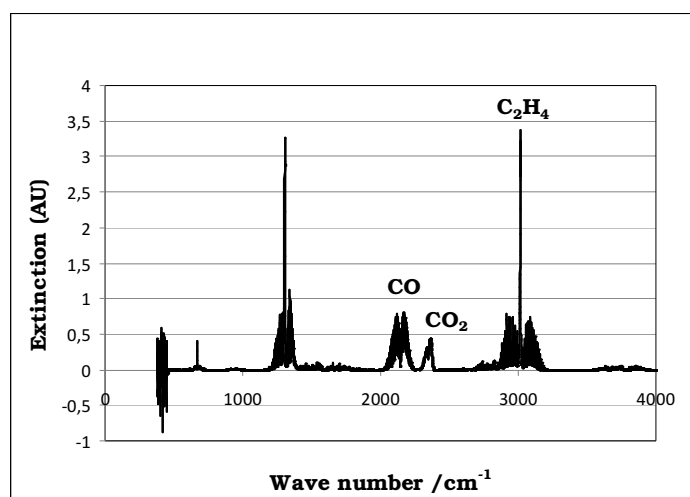


Figure 5-8 Typical spectrum of a gas sample from experiment using 0.1 M lactic acid as feed at a temperature of 420 °C a pressure of 350 bar and a reaction time of 50 s. By integrating the marked peak groups, the CO/CO₂/C₂H₄ ratio has been measured.

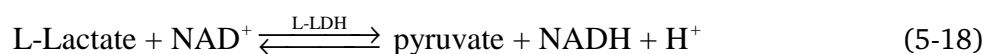
5.4.4. Enzymatic Analysis of L-lactic Acid

A supplementary analysis has been carried out to confirm that the reaction of acrylic acid in supercritical water also yields lactic acid.

The samples required a pH value of 8-10 which has been adjusted with NaOH.

An enzymatic analysis kit for the determination of L-lactic acid from R-Biopharm AG has been used for this purpose.

The analysis is based on a set of enzymatic reactions:



with the abbreviations,

NAD – nicotineamide-adenine dinucleotide

L-LDH – L-lactate dehydrogenase

GPT – glutamate-pyruvate transaminase

In the reaction (5-18) the formed NADH is stoichiometric to the amount of L-lactic acid and is to be determined by its UV-absorbance at 340 nm. Since the first reaction is reversible, reaction (5-19) is used to displace the equilibrium in (5-18) to the right, in the favor of pyruvate formation.

Before analyzing the reaction mixture through this method, a sample consisting of acetaldehyde, 3-hydroxy-propionic acid and acrylic acid has been tested to ensure the specificity of the analysis and the results were negative: no significant difference in the UV

absorption of the sample at 340 nm has been noticed by treating the probe through the method described above.

5.4.5. Preparation of 2-methoxy-propionic Acid

For the experiment in Section 6.3.2 synthesis of 2-methoxypropionic acid was necessary. 38 g sodium methoxide in 160 ml methanol was added slowly to a solution of 2-bromopropionic acid (30 g) in methanol (50 ml) under nitrogen atmosphere and vigorous stirring. The reaction mixture was heated at 50 °C under nitrogen overnight. Afterwards it was concentrated under vacuum. The residue was brought to a low pH by addition of aqueous HCl (1 N) and the solution was then extracted with ethyl acetate or *tert*-Butylmethylether (700 ml, 250 ml, 100 ml) three times. The combined organic layer was dried with Na₂SO₄ and the concentrated under vacuum. The product, a yellowish oil was analyzed via ¹H-NMR and HPLC and used without further purification.

6. Results and Discussion

6.1. Measurements in Pure Water

In this section, the results from experiments carried out in pure water are discussed. The influence of temperature, pressure, initial concentration, reaction time on the dehydration of lactic acid constitutes the core of these experiments. Additionally, the behaviour of acrylic acid in supercritical water has also been studied mainly for gaining an insight in the kinetic of the reaction network.

The approach for studying the influence of the initial concentration is to be briefly explained. At higher concentrations, besides acrylic acid and acetaldehyde an unexpectedly large spectrum of reaction products has been obtained. Since we have encountered difficulties in quantifying them, only acrylic acid have been analyzed.

Unless otherwise specified, the initial concentration of the reactant (lactic acid or similar structures) used in the experiments was 0.1 mol l^{-1} and the reactor used a CSTR.

6.1.1. Influence of the Residence Time

By studying the dependence of the conversion on the residence time of the feed in the reactor one can determine the global kinetic of the dehydration. The conversion vs. residence time curve is shown in Figure 6-1.

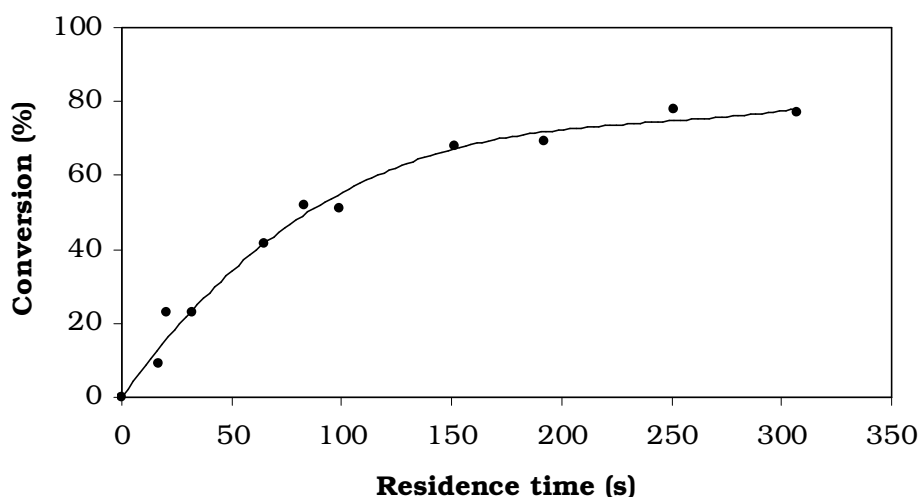


Figure 6-1 Dependence of the conversion of lactic acid (0,1M) on the residence time at 385 °C and 350 bar.

A very simplified model for the reaction consists of a first order irreversible reaction leading to products:

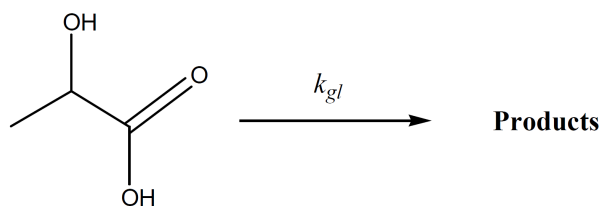


Figure 6-2 Simplified model of the reaction of lactic acid in near- and supercritical water consisting of two first order reactions.

Hence, a global reaction rate constant k_{gl} would be expected together with a $c(t) = c_0 \cdot e^{-k_{gl}t}$ concentration dependence with time, where c_0 is the initial concentration of the lactic acid. In Figure 6-3 a comparison between the experimental data and a first order concentration vs. time function is presented.

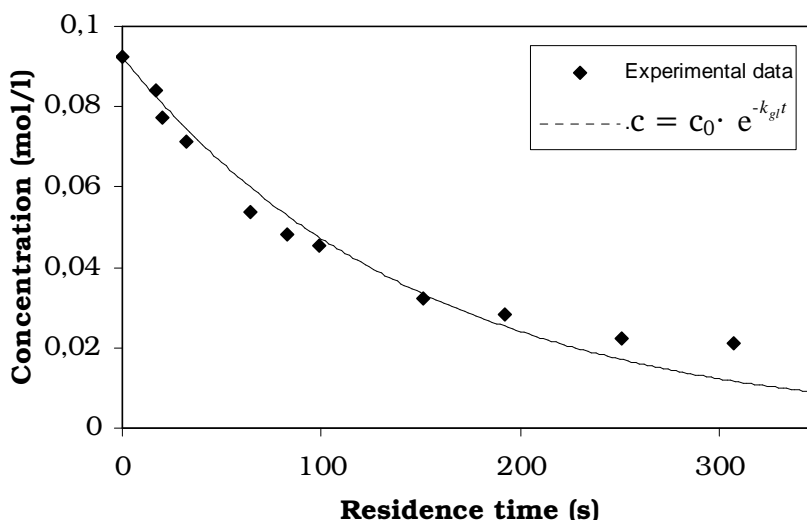


Figure 6-3 Comparison between the experimental data at 385 °C and a theoretical curve for a first order global reaction kinetic for lactic acid.

The result in Figure 6-3 indicates that the deviation from the predicted behaviour is significant at longer residence times where reverse reactions or effects due the reactor itself used in the experiments, seem to play an important role on the reaction of lactic acid. The global reaction rate constant was calculated using the least squares method. At 385 °C the estimated value for the global rate constant was $k_{385^{\circ}\text{C}} \approx 7.67 \cdot 10^{-3} \text{ s}^{-1}$.

The selectivity towards acrylic acid is higher at smaller residence times, indicating a consecutive reaction. Therefore, the stability of acrylic acid has also been studied (Section 6.1.6).

The selectivity as a function of residence time is represented in Figure 6-4. There are difficulties in quantifying the reaction products at residence times that are below 50- 60 seconds. The calibration of the HPLC method is valid for concentrations well below those

corresponding to residence times in the range 10 - 60 seconds. The reason for the errors must be undetected byproducts which interfere with the calibrated substances on the chromatograms. While these interferences can be neglected at higher concentrations of the products, that is, at longer residence times, at short residence times they lead to selectivities which have no “quantitative” relevance. Probably, the acetic acid peak is completely overlapped by that of lactic acid at higher concentrations of the latter and thus, the peaks are integrated together as a lactic acid peak. Nevertheless, even these results can be used to realize a tendency in the variation of the selectivities with the residence times.

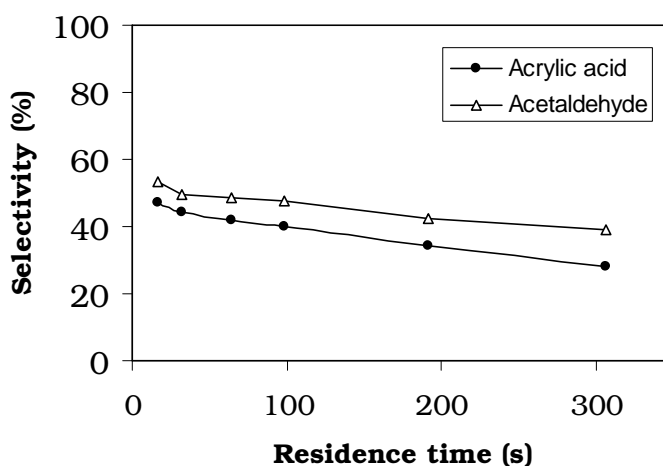


Figure 6-4 Dependence of the selectivity towards acrylic acid and acetaldehyde on the residence time at 385 °C and 350 bar.

6.1.2. Influence of the Pressure

Figure 6-5 and Figure 6-6 show the influence of pressure on the overall conversion and on the acrylic acid yield.

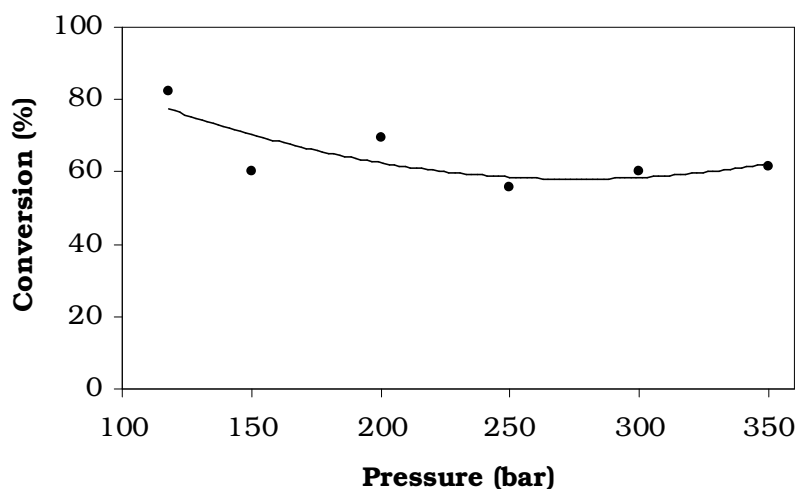


Figure 6-5 Influence of pressure on the conversion of lactic acid at 385 °C and 100 seconds residence time.

In these experiments only the pressure has been modified. In the pressure range 100 - 350 bar, there is an increase in density of more than one order of magnitude. The initial concentration of lactic acid in reactor increases accordingly. In spite of these large variations of the latter, there is no significant effect of pressure on the conversion of lactic acid. Surprisingly, at low pressures lactic acid reacts as much as at high pressures corresponding to near- and supercritical conditions. The acetaldehyde yields are as high as 30 % (at 150 bar). No relevant acrylic acid quantities have been detected at pressures below 150 bar. The rest of the products have not been analysed.

In Figure 6-6, the influence of the pressure on acrylic acid yields is shown.

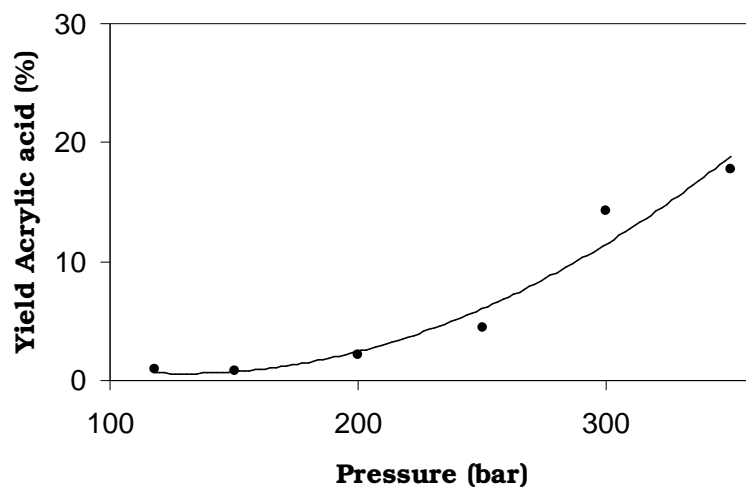


Figure 6-6 Influence of pressure on the acrylic acid yield at 385 °C and 100 seconds reaction time.

Contrary to the results of Mok *et al.* [Mok-1989], these results suggest that pressure plays an important role in the dehydration of lactic acid, at least in matters of acrylic acid yield. There is a steady increase in acrylic acid yield in the region between 250 and 350 bar and the upper limit of this trend is not known. Due to experimental setup limitations 350 bar was the highest pressure employed for these experiments. It can be assumed that increasing pressure above 400 bar brings an increase in the acrylic acid yield.

6.1.3. Influence of the Temperature

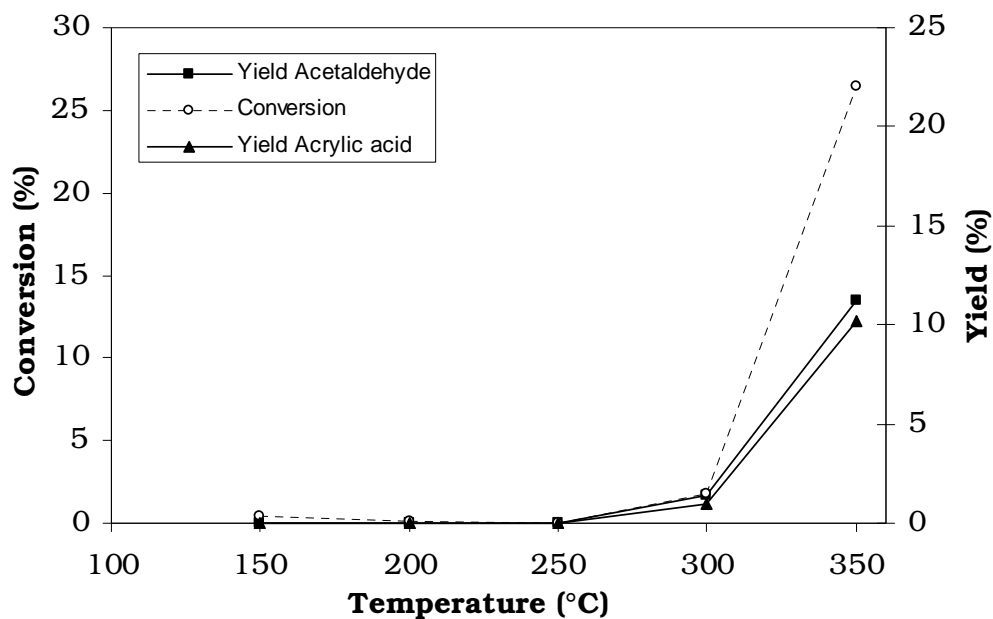


Figure 6-7 Influence of the temperature on the reaction of lactic acid in water at 350 bar and 100 seconds residence time. The yield in acrylic acid and acetaldehyde are to be read from the secondary axis.

In these experiments it has been shown that temperature plays a crucial role for the reaction. In spite of the high pressure, it is only at temperatures near to the critical point of water that significant conversion occurs (Figure 6-7).

Detailed results concerning the influence of temperature on the reaction are presented in Figure 6-8(a and b) as separate isothermal curves. These results show that the highest yield of acrylic acid occur in supercritical water (385 °C and 350 bar). Remarkably, at 350 °C the selectivity towards acrylic acid only slowly decreases with the residence time.

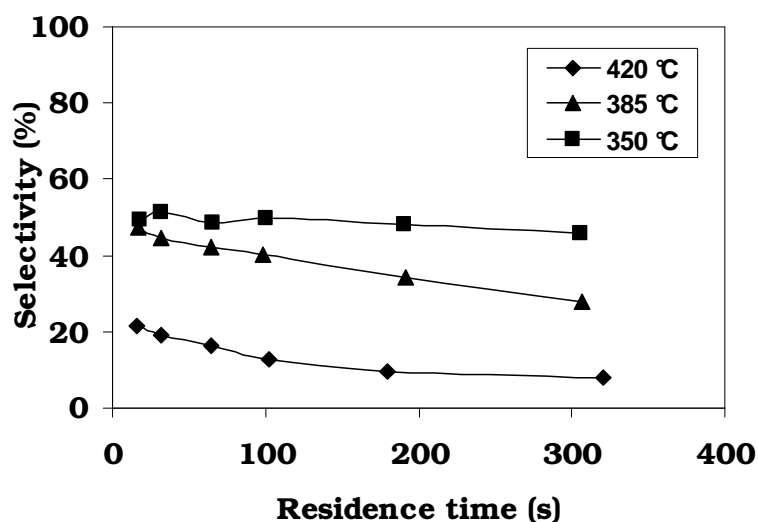
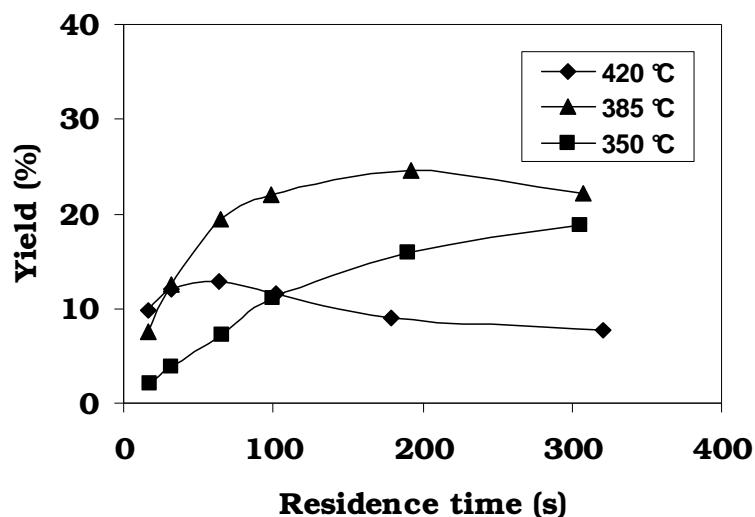


Figure 6-8a Yield and selectivity of acrylic acid as functions of residence time at three temperatures.

It can be seen in Figure 6-8a (above) that since the conversion increases with residence time, with a constant selectivity towards acrylic acid, the respective yield should be the higher at longer residence times. This idea was infirmed by the supplementary experiments carried out up to very long residence times: one of the red points in Figure 6-8b (below) corresponds to a residence time of 507 seconds and to a **maximum** of the yield of acrylic acid (21 %) at 350 °C. The other red point on the curve corresponds to a residence time of 936 seconds and a yield of acrylic acid of 20 %. Thus, at residence times above 500 seconds the yield of acrylic acid begins to decrease slowly. Unfortunately, the highest yield in acrylic acid at 350 °C obtained at approximately 500 seconds (21 %) does not exceed the observed maximum of 27 % obtained at 385 °C, 200 seconds and 69 % conversion.

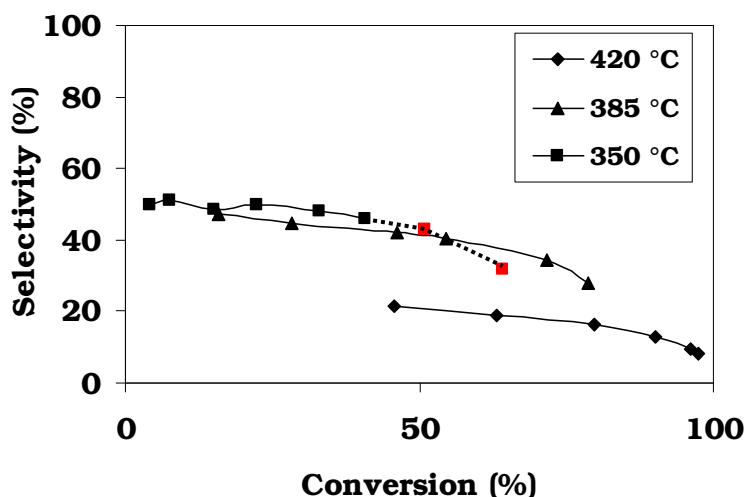
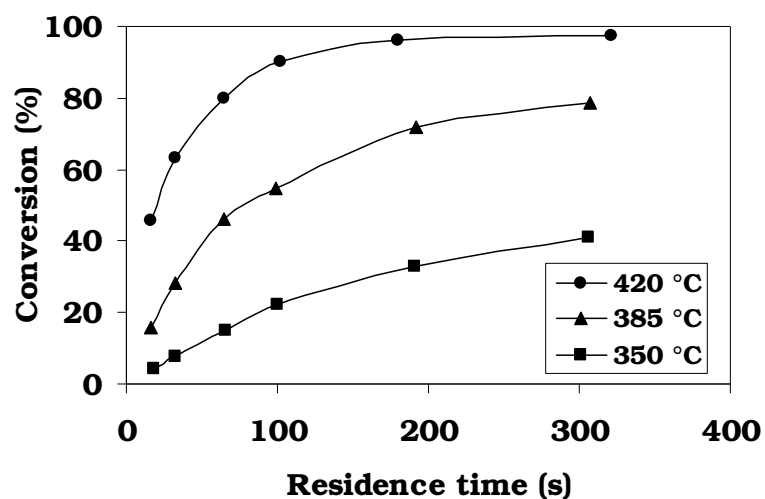


Figure 6-8b The influence of the reaction temperature on the conversion of lactic acid (above). The selectivity towards acrylic acid is represented as a function of conversion at different temperatures (below). The first red point at approx. 50 % conversion corresponds to a maximum yield of 22% in acrylic acid at 350 °C and 507 seconds residence time. The other red point on the 350 °C curve corresponds to a residence time of 936 seconds (and a yield of 20% acrylic acid).

6.1.4. Influence of the Lactic Acid initial Concentration

No clear connection between the initial lactic acid concentration and the outcomes of the dehydration could have been established from our experiments. This is partly due to difficulties in quantification of the reaction products. At smaller initial concentrations, the major reaction products are acetaldehyde, acrylic acid and small amounts of acetic acid and propionic acid. As the initial concentration of lactic acid increases, significant amounts of unidentified byproducts, which were otherwise neglected, interfere with the main peaks on

the chromatograms, making the quantification very problematic. The causes for these disperse results have not been yet identified, but the errors are probably due to sample processing/dilution.

However, a slightly descending trend of the acrylic acid yield by increasing feed concentration can be observed (see Figure 6-9). This is, unfortunately, a disadvantage for the efficiency of the industrial application of the process since higher concentrations are preferred for large scale applications. Further experiments with catalysts should be performed aiming to inhibit the formation of byproducts other than acetaldehyde. Addition of certain salts, such as K_2HPO_4 has been proved to inhibit the formation of acetaldehyde [Lir-1993]. Identification of the byproducts and the influence of salts on the latter remain to be studied.

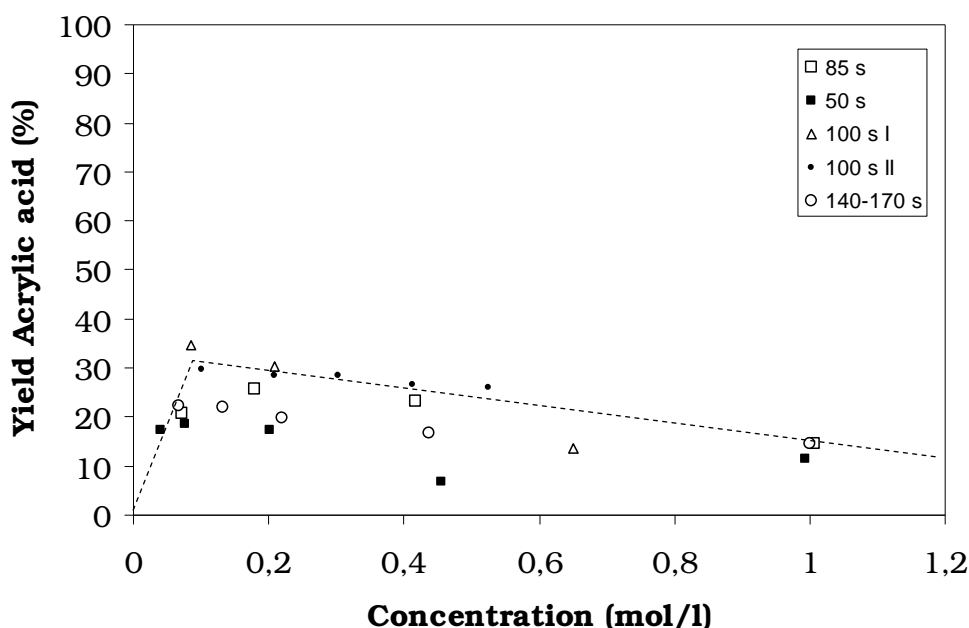


Figure 6-9 Dependence of the conversion on the concentration of the lactic acid feed at 350 bar 385 °C and various residence times.

6.1.5. Influence of the Reactor Aging

The surface of the reactor has been reported to have a significant influence on the composition of the reaction mixture. After about 70 hours, it remains constant, due to reactor passivation [Lir-1993]. The composition of a reaction mixture in contact with a new steel (type 1.4541) pipe reactor has been monitored for 30 hours. The results are shown in Figure 6-10.

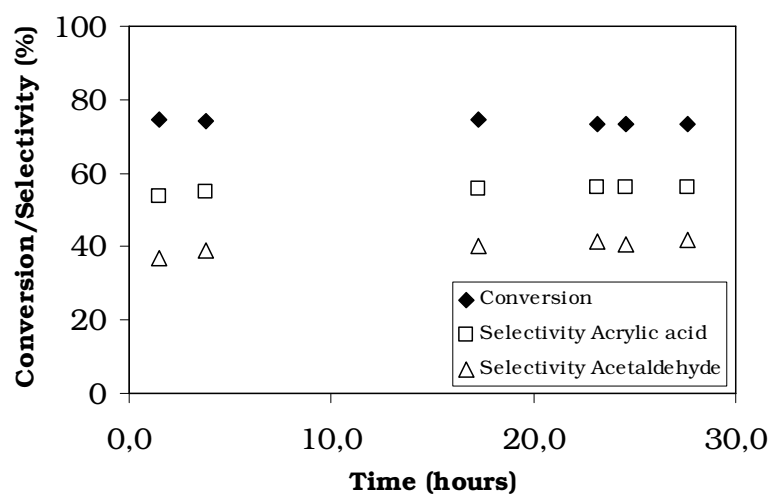


Figure 6-10 Influence of the aging of the reactor on the dehydration of lactic acid at 385 °C, 350 bar and a residence time of 100 s.

It was found that aging of the reactor for 30 hours plays a role neither on the conversion of lactic acid in supercritical water nor on the selectivity towards acetaldehyde or acrylic acid at 385 °C.

6.1.6. Stability of Acrylic Acid

An important factor which characterizes the maximal yields of acrylic acid is its stability in near- and supercritical water. Also, in order to elaborate a kinetic model for the reaction this information is crucial.

Feed solutions of about 0.05 M acrylic acid have been used. The reaction products have been analyzed via HPLC. Experiments have been carried out at three temperatures 350 °C, 385 °C and 420 °C. The results are summarized in Figure 6-11.

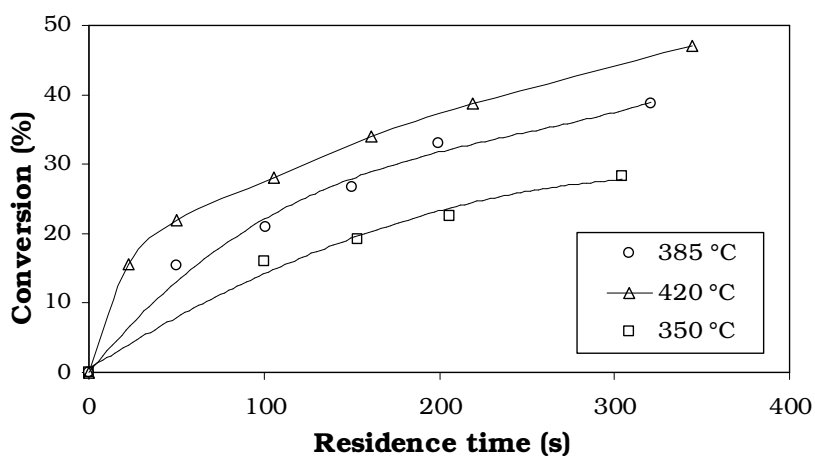


Figure 6-11 Conversion of 0.05 M acrylic acid at different residence times and temperatures.

The following typical HPLC chromatogram characterizes these results (Figure 6-12)

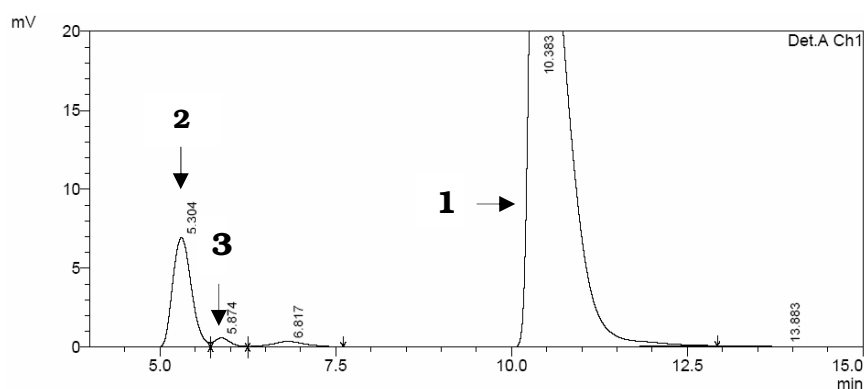


Figure 6-12 A typical chromatogram of a reactor sample from experiments concerning acrylic acid stability. The peak assignment is the following: 1. acrylic acid 2. 3-hydroxypropionic acid/lactic acid 3. acetic acid.

The main product of water addition to acrylic acid is 3-hydroxy-propionic acid and is in accordance with the Markovnikov's rule for addition to the double bonds. However, ¹H-NMR analysis of the reaction mixture revealed the presence of lactic acid. If the response factor of lactic acid is used for the quantification of both acids, the results obtained indicate that the

concentration of lactic acid exceeds that of 3-hydroxypropionic acid at residence times above 100 seconds and a temperature of 385 °C (see Figure 6-15). The concentration of lactic acid does not exceed that of its isomer if different response factors are taken (See Section 5.4.2. for the discussion). The presence of significant amounts of lactic acid has also been confirmed through an enzymatic test for the specific identification of lactic acid (after a method described in Section 5.4.4).

Thus, bearing in mind that acrylic acid also undergoes decarboxylation yielding ethene and hydrogenation yielding propionic acid [Mok-1989], the reaction network of acrylic acid in near- and supercritical water can be outlined in an extended form (Figure 6-13).

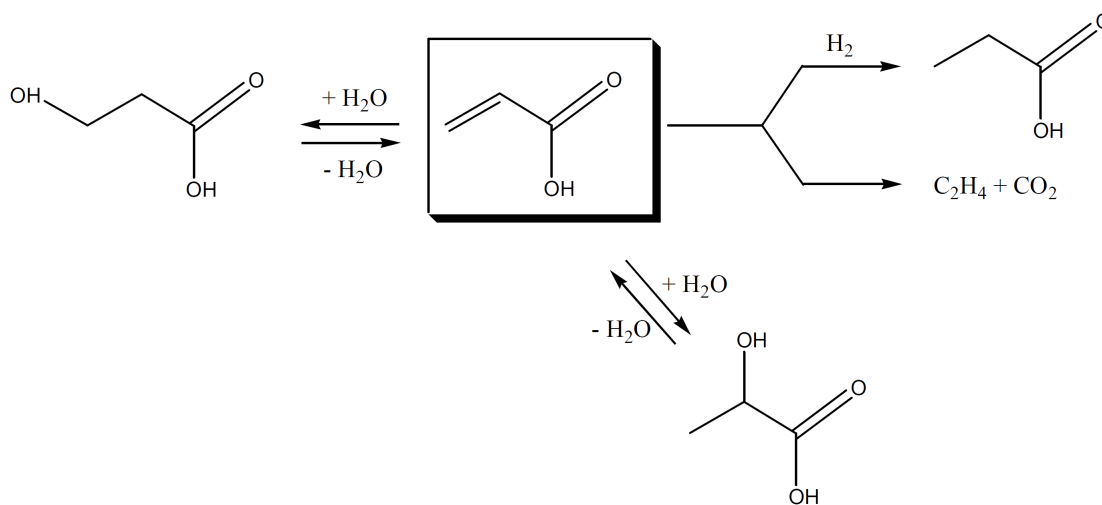


Figure 6-13 Representation of the reaction network of acrylic acid in near and supercritical water.

By these experiments, the reversibility of the dehydration of lactic acid has been shown. The quantification of lactic acid and of 3-hydroxypropionic acid from the HPLC data has been discussed in Section 5.4.2. In Figure 6-14 the data from ¹H-NMR analyses are represented. The red point corresponds to an experiment where the acrylic acid feed was thoroughly degassed to exclude the possibility that lactic acid is formed through radical reactions mediated by the dissolved oxygen.

It is surprising that at 385 °C the 3-hydroxypropionic to lactic acid ratio nears 1. This anti-Markovnikov addition suggests that a hydroxyl radical is implied. In near- and supercritical water, the reaction between nitrobenzene and the hydroxyl radical formed from water increases from 350 to 390 °C[Fen-2002]. This could explain the increase in the lactic acid formation from 350 to 385 °C. The further decrease at 420 °C where significantly less lactic acid is produced might be due to the stability of the latter at these higher temperatures.

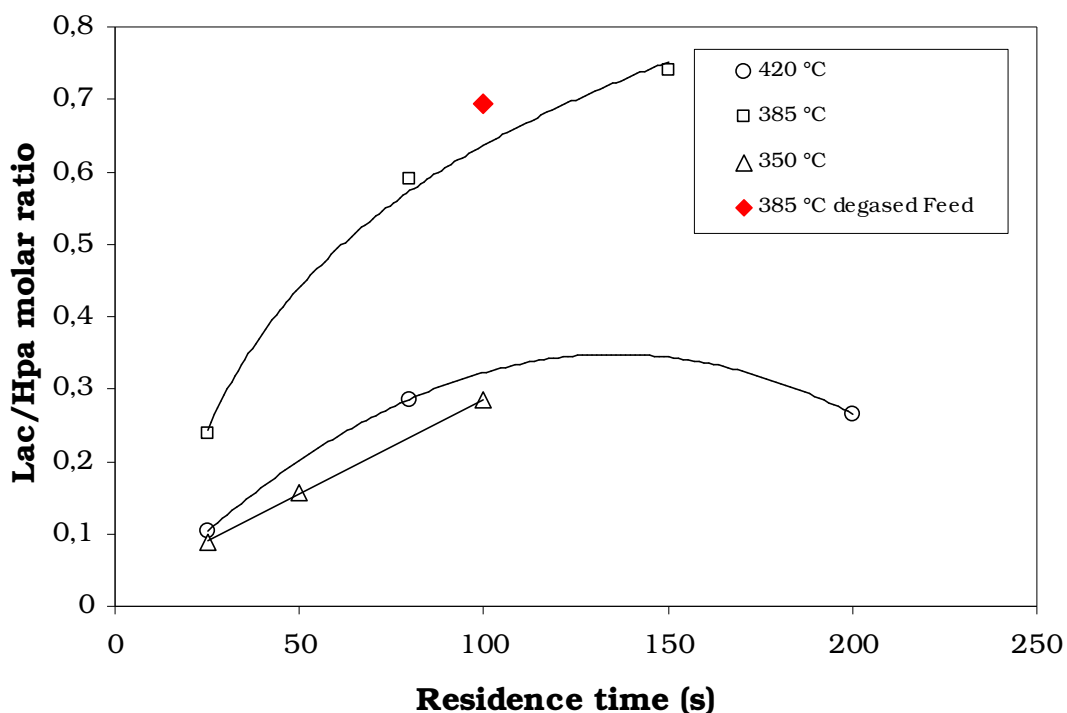


Figure 6-14 Molar ratio between lactic acid and 3-hydroxy-propionic acid, the two hydration products of the reaction of acrylic acid in near- and supercritical water.

The main goal of these experiments is the quantification of lactic acid and 3-hydroxypropionic acid. The results of these efforts detailed in Section 5.4.2 are represented in Figure 6-15.

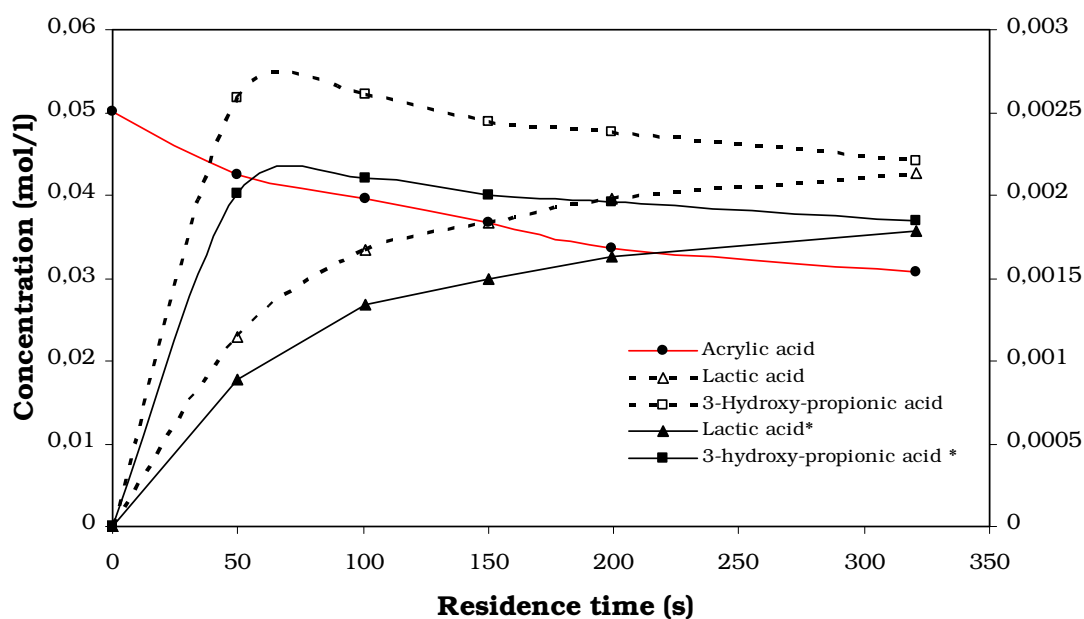


Figure 6-15 Compounds quantified in the experiments for determining the stability of acrylic acid at 385 °C. The asterisk is used for concentrations calculated using only the response factor of lactic acid. The points corresponding to lactic acid and 3-hydroxypropionic acid are to be interpreted using the concentrations from the secondary axis.

The following observations can be made for these experiments. The highest yields of lactic acid are obtained at 385 °C, with a ratio to 3-hydroxypropionic acid in the range 0.44 – 0.97 at this temperature. The three point regression $B_{385^{\circ}\text{C}}(\tau)$ predicts an excess of lactic acid at reaction times above 350 seconds. For the experiments carried out at 350 °C the produced lactic acid has been neglected and the peaks in the respective HPLC chromatograms have been assigned to 3-hydroxypropionic acid.

The formation of lactic acid does not involve radicals generated through the oxygen present in the feed solution, since a thoroughly degassed feed produced under similar conditions an almost identical lactic to 3-hydroxypropionic acid ratio (Figure 6-14).

6.2. Analysis of the gas phase

Analysis of the gas phase brings important information about the unfolding of the reaction of lactic acid in SCW which will be referred to in Section 7.3 concerning the reaction mechanisms. Altogether, in the gaseous phase, decomposition of acrylic acid of SCW yields CO_2 and ethene while acetaldehyde yields predominantly CO with small amounts of CO_2 and traces of ethene. This is however only a qualitative evaluation of these decomposition reactions (See also Appendix).

A systematic investigation has been carried out to establish the CO/CO_2 ratio in the gas phase because the latter should be an excellent indicator for source of the produced acetaldehyde (decarbonylation or decarboxylation [Mok - 1989]). CO is exclusively produced through the decarbonylation path, CO_2 exclusively through decarboxylation of lactic acid and acrylic acid. During the decarboxylation of acrylic acid ethene is formed. Thus, the yield for the decarbonylation and decarboxylation of lactic can be monitored, the latter by subtracting the ethene percent from that of CO_2 (ethene is produced in equal amounts with CO_2 from the decarboxylation of acrylic acid). The composition of the gas phase at 350, 385 and 420 °C is illustrated in Figure 6-16. The ethene yield reaches a maximum at 385 °C.

An excess of CO makes the decarbonylation of lactic acid the principal reaction leading to gaseous products. By correlating the ethene and CO_2 amounts, it can be drawn that a significant quantity of the CO_2 is formed through the decarboxylation of acrylic acid (since ethene is uniquely formed through this reaction). The rest of the CO_2 has been so far assigned to the decarboxylation of lactic acid. The lactic acid decarboxylation product should be ethanol, which is stable in near- and supercritical water, but is absent in the reaction mixture. Thus, without the identification of ethanol, the assignment of significant quantities of CO_2 to the decarboxylation of lactic acid becomes questionable.

Further insight is brought by the variation of the CO/CO_2 ratio with time and temperature (Figure 6-17). At all reaction temperatures this ratio decreases with the residence time. This suggests that a successive reaction is involved in the consumption of CO. These findings are to be further discussed in the section concerning reaction mechanisms (Section 7.3).

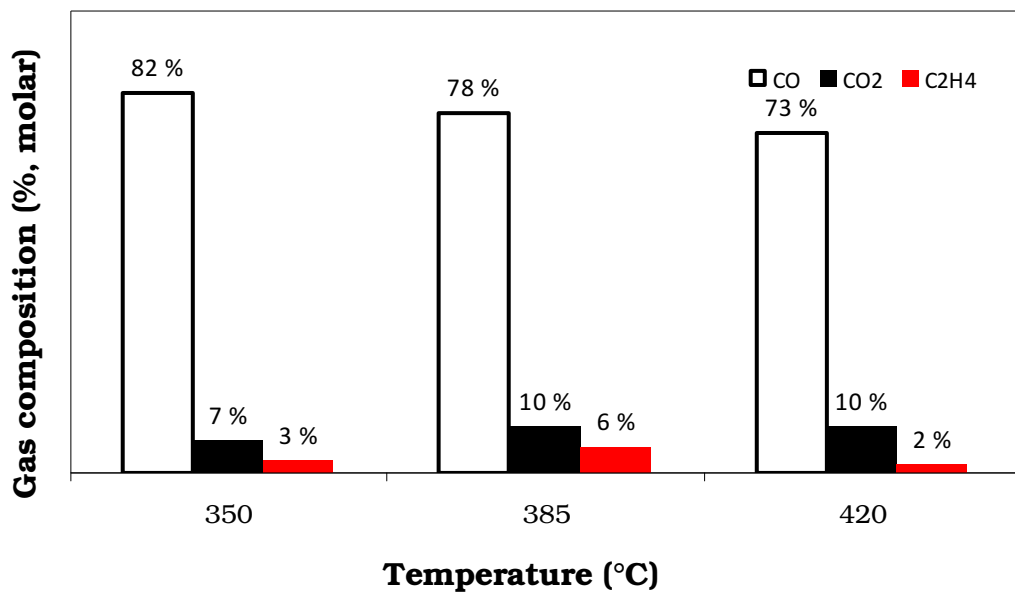


Figure 6-16 Composition of the gas phase from the reaction of lactic acid in SCW at three temperatures and a residence time of 100 seconds.

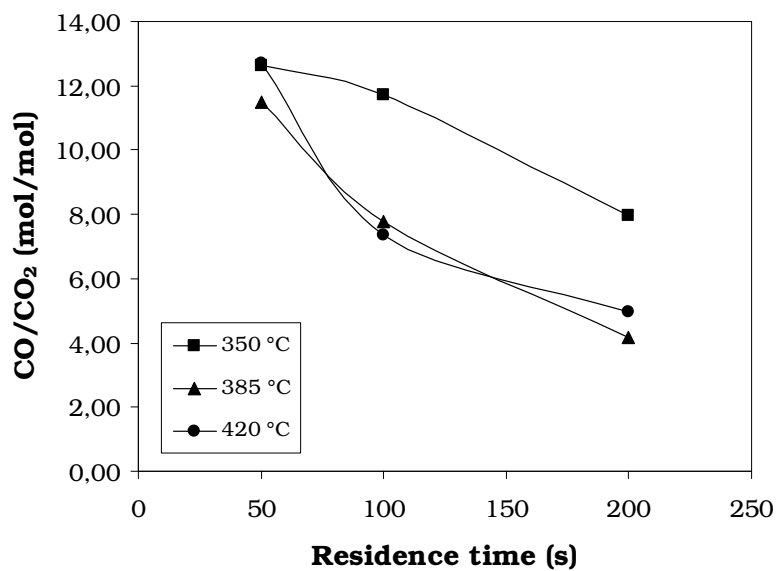


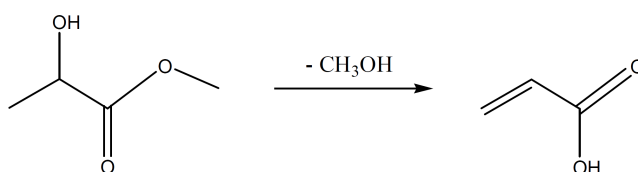
Figure 6-17 The CO/CO₂ molar ratio as a function of temperature and residence time.

6.3. Dehydration of Substances Similar to Lactic Acid

Aiming to better understand the factors that influence the dehydration of lactic acid, substances with related structures have been used for the reaction in SCW. Except for 3-hydroxypropionic acid, these substances are obtained from lactic acid through replacing hydrogen atoms through methyl groups. By this, two main goals were pursued: to block the leaving proton at that specific position or to increase the electron density at the α -carbon where a positive charge is formed by the leaving of the hydroxyl group. All experiments have been carried out at 350 bars and 385 °C.

6.3.1. Lactic Acid Methyl Ester

Using the ester of lactic acid instead of lactic acid should decrease the yield towards acrylic acid by adding a supplementary step to the reaction (hydrolysis of the ester), since according to the reaction mechanisms from *Mok et al.* the dehydration requires the carboxylic proton [Mok-1989].



Experiments have been carried out in a CSTR at two temperatures, 350 and 385 °C at residence times ranging from 25 to 230 seconds. Figure 6-18 shows that the conversions are always higher when the ester is used as feed. The yields of both acrylic acid and acetaldehyde are lower at 385 °C when the ester is used (Figure 6-19). Only 10 % (molar) of the initial methyl lactate is to be found in the reaction mixture at 350 bar, 385 °C and a residence time of 36 seconds (the lower limit of the residence time in the experiments). At the same temperature and pressure but longer residence times, no methyl lactate has been detected. At 350 °C and 31 seconds also 10% of the unhydrolyzed ester is found in the reaction mixture.

Information about the behaviour of the esters in supercritical water can be found in the literature. *Krammer et al.* studied the hydrolysis of ethyl acetate in supercritical water and found that 28 % of the ester is not hydrolyzed at 300 bar, 380 °C and a residence time of 39 seconds [Kra-2000]. Clearly, the hydrolysis of methyl lactate is faster than that of ethyl acetate in supercritical water, but still slow enough to consider the effect of the ester group on the reaction network outlined by *Mok et al.* [Mok-1989].

Through the lower yields in acrylic acid and acetaldehyde, our experiments suggest that the carboxylic proton favours both the dehydration and the decarbonylation pathways with one remarkable exception at 350 °C when the yield of acetaldehyde is higher at all residence times. The lower yields of acetaldehyde obtained from methyl lactate can be attributed to the involvement of the ester group in reactions which are faster than the decarbonylation, thus making the molecule unavailable. The latter is postulated to proceed through a cation formed

by the heterolysis of the C-OH bond (C-OCH₃ for the ester). Since the mechanism proposed by Mok *et al.* (see Figure 2-4) should be valid for the ester as well, it can be concluded that the C-OH bond is split more easily than the C-OCH₃ bond, thus contributing to the observed lower yield of acetaldehyde.

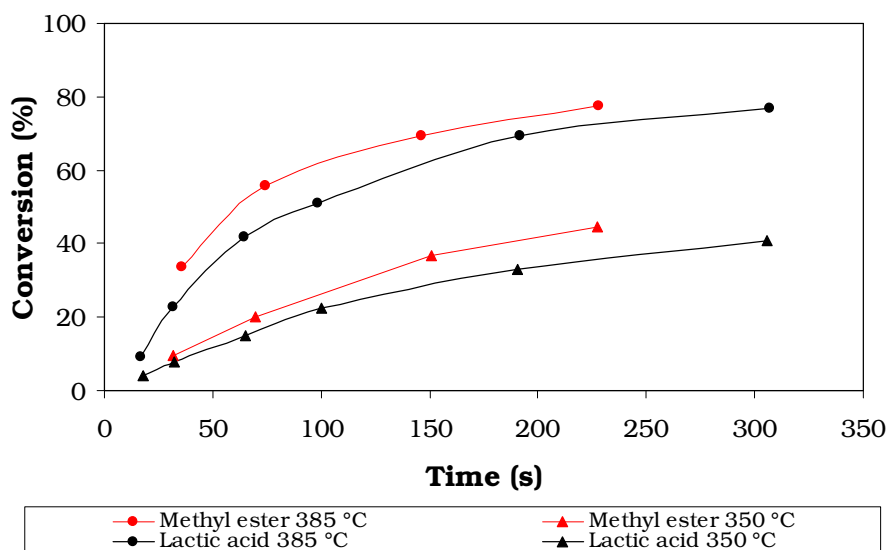


Figure 6-18 Comparison of the conversion of lactic acid and lactic acid methyl ester at different temperatures and residence times.

The higher conversions rates of the methyl lactate (Figure 6-18) can not be calculated by adding up the amounts of acrylic acid and acetaldehyde obtained since their yield is lower as in the case of lactic acid. Probably, the ester is involved in decomposition reactions which have not been yet investigated.

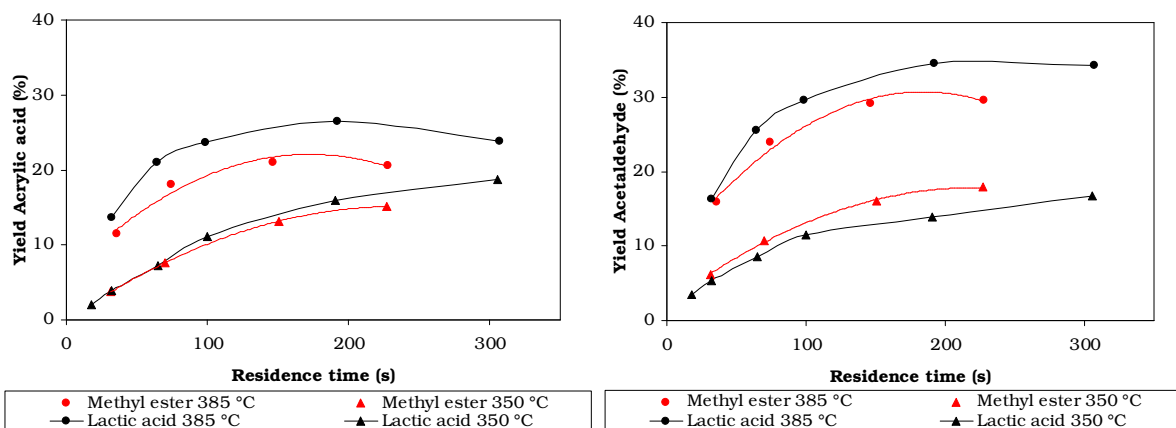
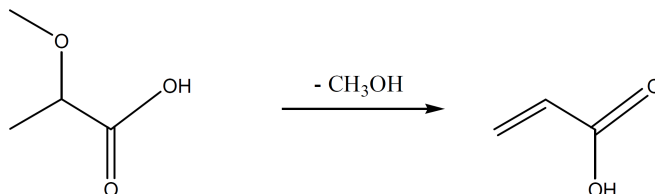


Figure 6-19 Selectivity towards acrylic acid at different temperatures and residence times using lactic acid and the lactic acid methyl ester, respectively as feed (0.1 M).

6.3.2. 2-Methoxy-propionic Acid

The aim of using a methoxy- group instead of the hydroxy- group is to reveal the role of the 2-hydroxy group on the reaction of lactic acid in SCW.



The derivative has been prepared as mentioned in Section 5.4.5. Comparative experiments have been carried out in a pipe reactor at 385 °C, using lactic acid and 2-methoxy-propionic acid as starting material, respectively at 50, 100 and 200 seconds residence time. The HPLC analysis indicates that only lactic acid is present in the reaction mixture. Thus, it is not surprising that the results using the derivative are very similar to those obtained using lactic acid (Figure 6-20). Conversion of 2-methoxy-propionic acid is always 100 % in the observed residence time range. This is probably due to a fast nucleophilic substitution by the attacking hydroxyl groups from the ambient water. The total conversion of the starting material also suggests that the substitution at α -carbon is much faster than the elimination. The yield of acrylic acid is about the same for lactic acid and 2-hydroxy-propionic acid, while the selectivity is slightly higher for the methoxy- derivative (Figure 6-20).

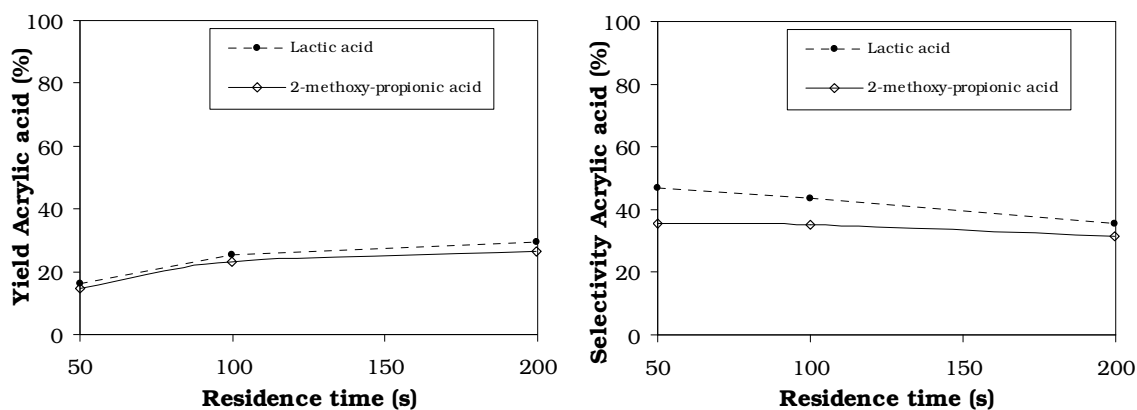


Figure 6-20 Comparison of yield and selectivity towards acrylic acid using lactic acid and 2-methoxy-propionic acid as starting material (the concentration is 0.1 M in each case).

Actually, the selectivities towards both acrylic acid and acetaldehyde are slightly higher for lactic acid than for the 2-methoxy-propionic acid. The proposed mechanism for decarbonylation, leading to the formation of acetaldehyde is presented in Figure 6-21.

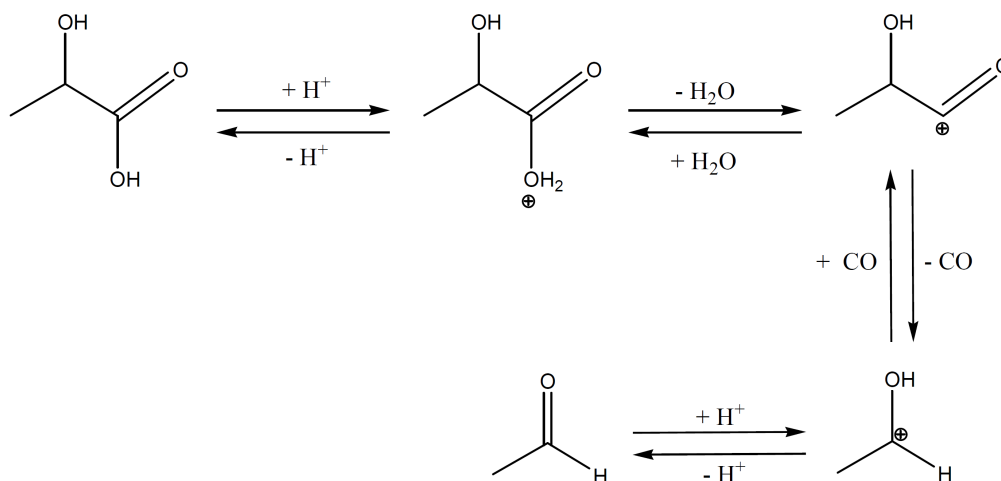
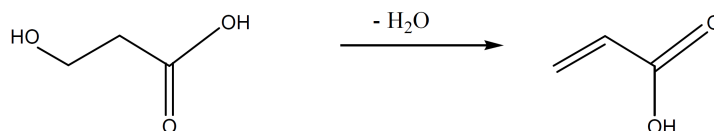


Figure 6-21 Decarbonylation path for the reaction of lactic acid in near- and supercritical water. [Mok-1989].

It can be deduced that acetaldehyde can not be formed from a carbocation where a methoxyl-group is present. This suggests that the conversion of 2-methoxy-propionic acid to lactic acid has to occur before dehydration or decarbonylation takes place. Thus, if the $\text{CH}_3\text{O}/\text{OH}$ -substitution were not spontaneous, the dehydration of the lactic acid derivative would be favoured by short residence times. Since the investigation of such short residence time has not been carried out yet, this remains an important issue for future research activities.

6.3.3. 3-Hydroxypropionic Acid

One of the mechanisms proposed by *Mok et al.* for the dehydration of lactic acid in supercritical water involves an unstable α -lactone [Mok-1989]. In a similar manner, the 3-hydroxy isomer of lactic acid should undergo dehydration through a β -lactone intermediate which is much more stable. Thus the yield of the dehydration should be higher. It is to mention that this isomer of lactic acid can also be obtained from renewable feedstock thus making it an alternative to lactic acid [Gok-2007].



Experiments in a pipe reactor at $385\text{ }^\circ\text{C}$ and residence times ranging from 50 to 200 seconds have been carried out to confirm the ideas of a more stable lactone intermediate. $^1\text{H-NMR}$ analysis of the reaction mixture indicates the existence of ethylene glycol. In the same analysis the peaks specific for acetaldehyde are absent. The experimental results illustrating the higher selectivity and yields towards acrylic acid using 3-hydroxypropionic acid as starting material are presented in Figure 6-23.

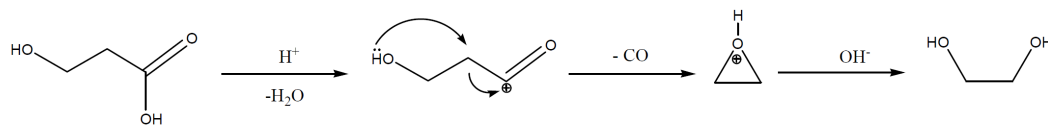


Figure 6-22 Proposed mechanism for the decarbonylation of 3-hydroxypropionic acid in supercritical water.

In conformity with the expectations, 3-hydroxypropionic acid yields more acrylic acid as lactic acid under the same conditions. In fact, the reaction occurs even at room temperature so that in an aqueous solution of 3-hydroxy-propionic acid small amounts of acrylic acid can be found. Decarbonylation leading to ethylene glycol possibly proceeds through successive eliminations (Figure 6-22).

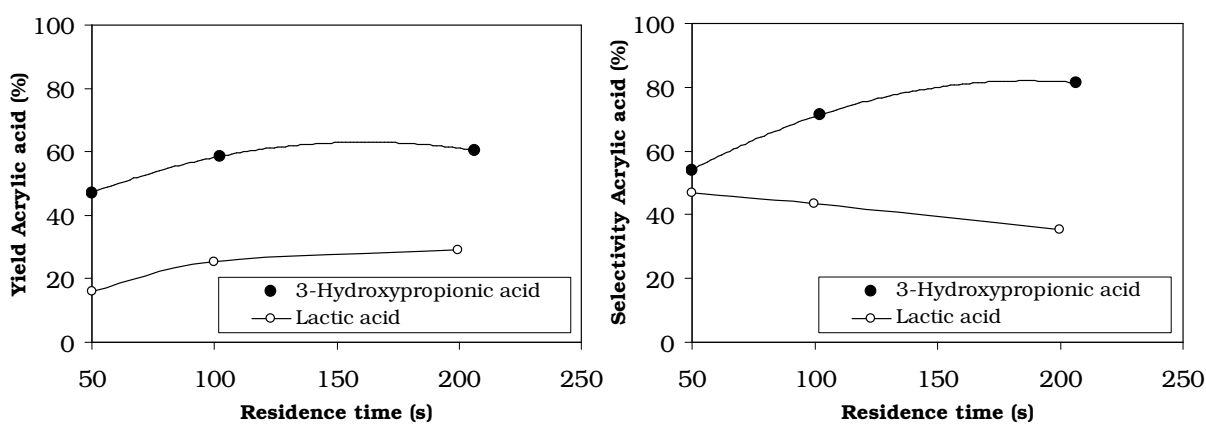
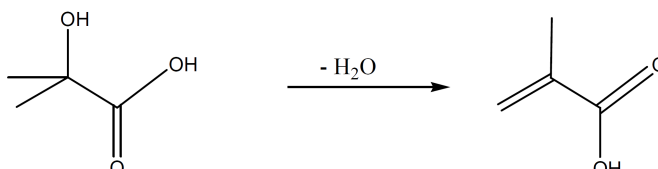


Figure 6-23 Yield and selectivity towards acrylic acid at 385 °C using a 0.1 M solution of 3-hydroxypropionic acid.

Nevertheless, from both proposed, unlikely to occur mechanisms, given the successive unstable stages through which they proceed, it can be concluded that decarbonylation is less probable than in the case of lactic acid giving a good explanation for the comparatively high yields of acrylic acid.

6.3.4. 2-Hydroxy-isobutyric Acid

If a lactone is an intermediate in the dehydration of lactic acid, the same should be valid for 2-hydroxy-isobutyric acid which has the structure of lactic acid where the hydrogen atom at the α -carbon has been replaced by a methyl group. In both cases, the formation of the unstable strained α -lactone should be the rate determining step, so that the yield of the two dehydration products should be similar.



Besides, 2-Hydroxyisobutyric can also be obtained from renewable feedstock and its dehydration product, methacrylic acid is an important intermediate in the chemical industry [Roh-2010]. Experiments to investigate the behaviour of 2-hydroxyisobutyric acid in supercritical water have been carried out in a pipe reactor. These results represent a comparison between the behaviour of 2-hydroxy-isobutyric acid and lactic acid at 350 bars and 385 °C as shown in Figure 6-24. Surprisingly, the former has up to 90 % selectivity towards methacrylic acid and a much higher conversion rate than lactic acid.

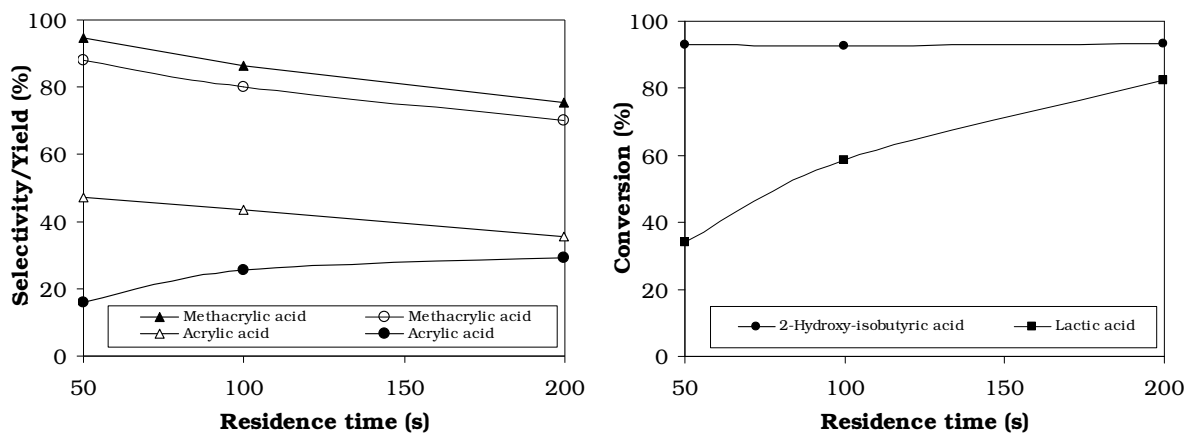


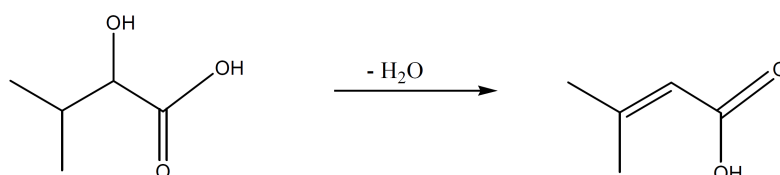
Figure 6-24 On the left: selectivity (triangles) and yield (circles) toward acrylic and methacrylic acid using lactic acid and 2-hydroxy-isobutyric acid respectively, as starting materials. On the right: conversion of lactic acid and 2-hydroxy-isobutyric acid. Measurements at 385 °C and 300 bar.

This result implies that the supplementary methyl group has a stabilizing role during the reaction. It could be hypothesised that the dehydration proceeds rather through an E1 elimination where a more stable tertiary carbocation is formed in the case of 2-hydroxy-isobutyric acid. It has been shown in Section 6.3.3 that 3-hydroxypropionic acid gives high yields in acrylic acid comparatively to lactic acid. This has been explained through the existence of a more stable lactone intermediate. This is not the case with the two acids discussed in this section where the stability of the intermediates should be equally reduced. This observation confirms the idea of *Mok et al.* that dehydration can proceed through two independent pathways: one involving a lactone, and the other through direct elimination of

the OH- group [Mok-1989]. Furthermore, if the hydroxyl group is attached to the α -carbon the second mechanism is more likely to account for the formation of the dehydration product. The elimination of the hydroxyl group can be assisted by the carboxyl group but a simple E1 mechanism could also explain this reaction.

6.3.5. 2-Hydroxy-3-methylbutyric acid

The idea for using 2-hydroxy-3-methylbutyric acid as starting material was to reduce the availability of the hydrogen atoms involved in the formation of the water molecule during dehydration. An easier method to investigate the influence of the number of C-H bonds and their strength on the dehydration is replacing one or more hydrogen atoms at the β -carbon with deuterium. For economic reasons, 2-hydroxy-3-methylbutyric acid has been used instead.



The experiments have been carried out in a pipe reactor at 350 bar, 385 °C and residence times ranging from 50 to 200 seconds. Two series of experiments have been carried out, one using solutions of 2-hydroxy-3-methylbutyric acid (0.1 M) as starting material and the other using 3-methyl-2-butenoic acid (0.05 M) as starting material. In both cases the conversion was around 90 % for all residence times considered. In the experiments where 3-methyl-2-butenoic acid was used as starting material, the hydration product, 2-hydroxy-3-methylbutyric acid yielded up to 23 %. All analyses have been carried out using HPLC.

Contrary to the expectations, the reaction of 2-hydroxy-3-methylbutyric acid yields no or very low yield in 3-methyl-2-butenoic acid (Figure 6-25). The high conversions can be explained by decomposition reactions yielding unidentified products.

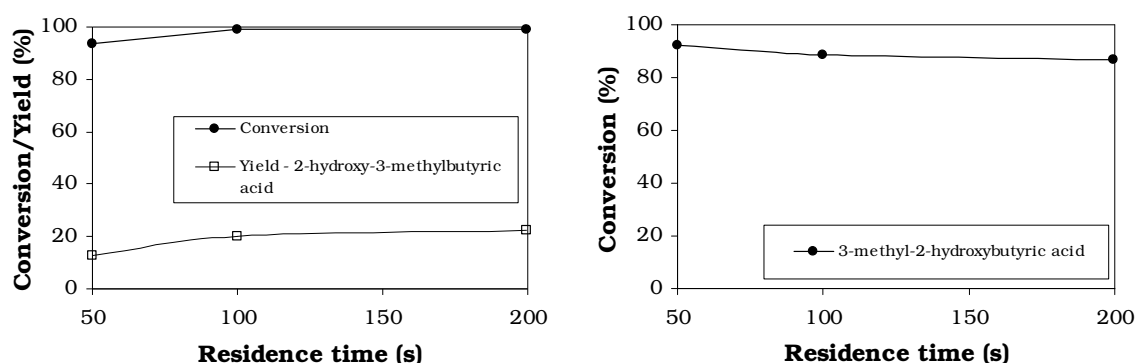


Figure 6-25 On the left: Conversion of 3-methyl-2-butenoic acid in SCW and the yield of 2-hydroxy-3-methylbutyric acid. On the right: Conversion of 2-hydroxy-3-methylbutyric in SCW (no dehydration product detected). The concentrations of the feeds were, respectively 0.05 M and 0.1 M. Experiments were carried out at 350 bar and 385 °C.

Besides, it can be presumed that 3-hydroxy-3-methylbutyric acid is also formed in these reactions, that the chromatographic column used can not separate the two isomers and that the corresponding peak on the chromatograms overlaps with that of the 2-hydroxy-3-methylbutyric acid. Assuming that 3-methyl-2-butenic acid is very unstable and 3-hydroxy-3-methylbutyric acid is relatively stable, part of the reaction network in SCW would that from Figure 6-26.

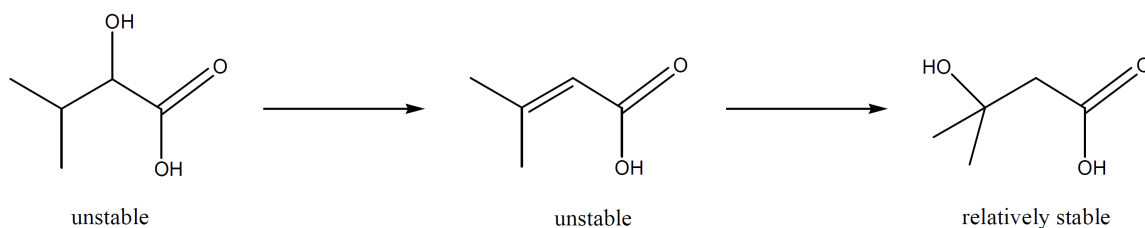


Figure 6-26 Proposed reaction scheme for explaining the results of the reactions of 2-hydroxy-3-methylbutyric acid and 3-methyl-2-butenic acid in SCW.

Thus, when using 2-hydroxy-3-methylbutyric acid as starting material, apart from decomposition which explains the high conversions, the absence of 3-methyl-2-butenic acid is due to its fast conversion to 3-hydroxy-3-methylbutyric acid. The same explanation can be given for the experiments where 3-methyl-2-butenic acid was the starting material.

Due to this unexpected behaviour of the used substances, no conclusion concerning the dehydration reaction could be drawn from these experiments.

From all the results presented in Section 6.3 some important information has been obtained. Depending on the position of the hydroxyl group, the dehydration reaction in SCW of the studied substances can take place through a simple E1 mechanism, if the OH- is bound to the α -carbon or through a lactone intermediate, if the OH- is bound to the β -carbon. It is also possible, however, that the two mechanism work simultaneously.

The hydrolysis of the methoxy groups in near- and supercritical water is relatively fast. At 385 °C and 36 seconds residence time, only 10% of the ester is found unhydrolyzed. At similar conditions the 2-methoxy derivative of the lactic acid converts completely to lactic acid.

Nevertheless, it has been shown that the dehydration rate of the ester is slower than that of the free acid probably due to the involvement of the carboxylic proton in the reaction.

As for the stability of a secondary carbocation that should influence an E1 dehydration a deuterated methyl group should be used to avoid steric effects in a study which only concerns inductive effects of the methyl group and the strength of the C-H or respectively C-D bonds.

6.4. Influence of Phosphates

Apart from the results presented in Chapter 6.1, numerous ionic species have been tested for their catalytic activity. This screening for catalyst is presented in Chapter 6.4.1. An important enhancement of the reaction towards acrylic acid is provided by phosphate species [Lir-1993]. As a next step, various phosphate species and their effect on the conversion, selectivity and yield toward acrylic acid at different concentrations temperatures and residence times have been investigated.

6.4.1. Preliminary Experiments for Catalyst Screening

Apart from the reactions in pure water or with phosphate additives, experiments where ionic species were dissolved in water have been carried out in search for a catalytic effect. These results are presented hereinafter. As mentioned in the introduction of this work (Chapter 4), the solutions of ionic species in near- and supercritical water differ from room temperature solutions through two main effects: a change in the dissociation constant of the solutes and an enhancement in density inhomogeneities within the solvent structure. A summary of some screening experiments using salts as additives is presented in Figure 6-27 and Figure 6-28. From these figures, some conclusions can be drawn. ZnSO_4 is an inhibitor for the formation of acrylic acid and the higher the concentration, the lower the yield and selectivity towards acrylic acid. KHCO_3 has also been excluded from further experiments as a strong inhibitor of acrylic acid formation.

MgSO_4 , K_2HPO_4 and Na_2SO_4 were found to increase the selectivity towards acrylic acid. A straightforward explanation for the influence of MgSO_4 is difficult since at small concentrations it inhibits the formation of acrylic acid but at higher concentrations it has little or no effect on the reaction. The experiments with salts mentioned so far were carried out in a pipe reactor. Some further experiments have been made in a CSTR (See Figure 6-29). Unlike reactions taking place in the pipe reactor, from these experiments it can be concluded that the addition of 200 ppm MgSO_4 has a beneficial influence on the formation of acrylic acid while Na_2SO_4 , apart from the high selectivity at 50 seconds residence time (which again could be an artefact), has no significant effect neither on the selectivity nor on the yield of acrylic acid.

The differences in the experimental results depending on the type of reactor used for the reactions have determined the exclusion of these species from further investigations of their catalytic effect.

From the salts used for our study of the homogeneous catalysis of the lactic acid dehydration, phosphates have been most thoroughly studied. In the forthcoming experiments (Section 6.4.2 to 6.4.5) the influence of various phosphates (and of phosphoric acid) on the reaction of lactic acid has been investigated. As a general procedure for the experiments, these salts have been prepared as a mixture of an alkaline metal hydroxide and phosphoric acid. Two major influences on the dehydration of lactic acid have been studied: that of the ratio of base to acid as well as that of using different (alkaline) metal hydroxides.

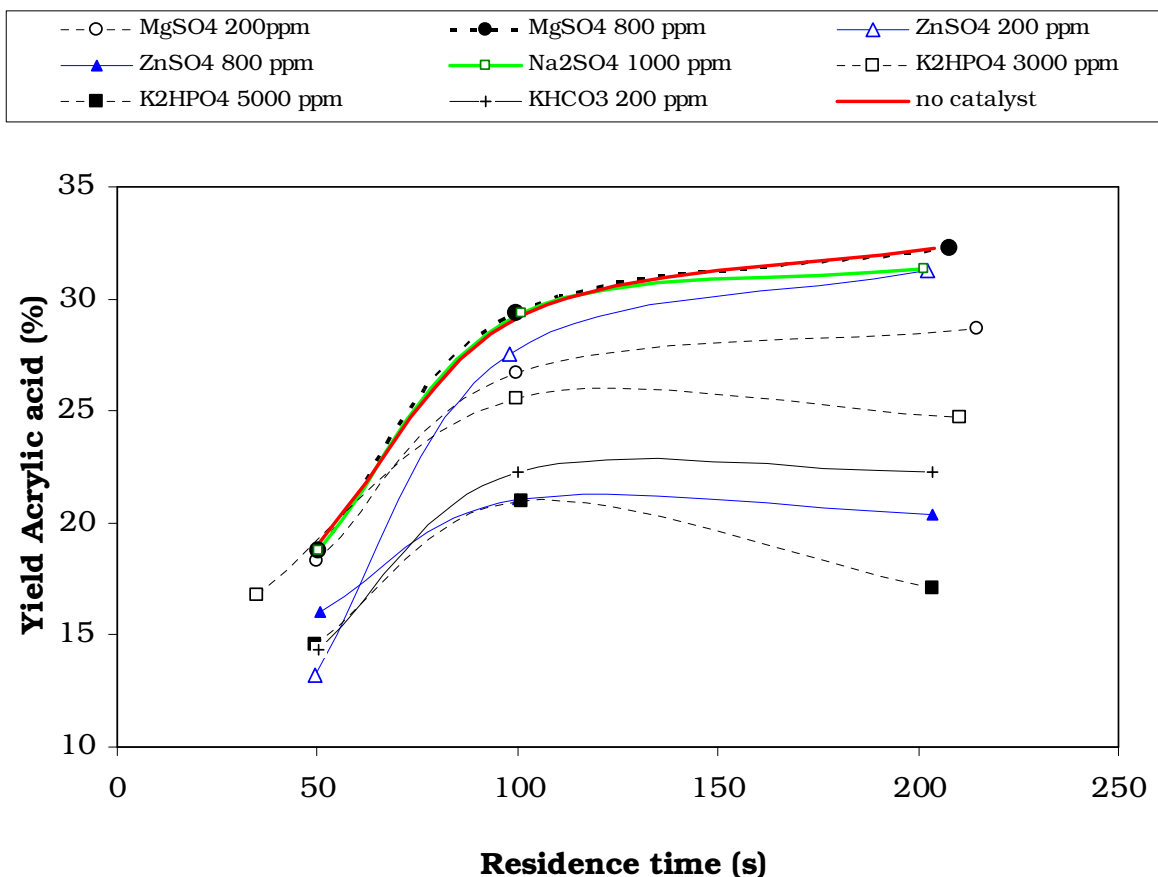


Figure 6-27 Summary of a screening for homogeneous catalysts. Yield of acrylic acid vs. residence time at 385 °C and 350 bar in a pipe reactor with 0.1 M lactic acid feed. (Salt concentrations in g g^{-1}).

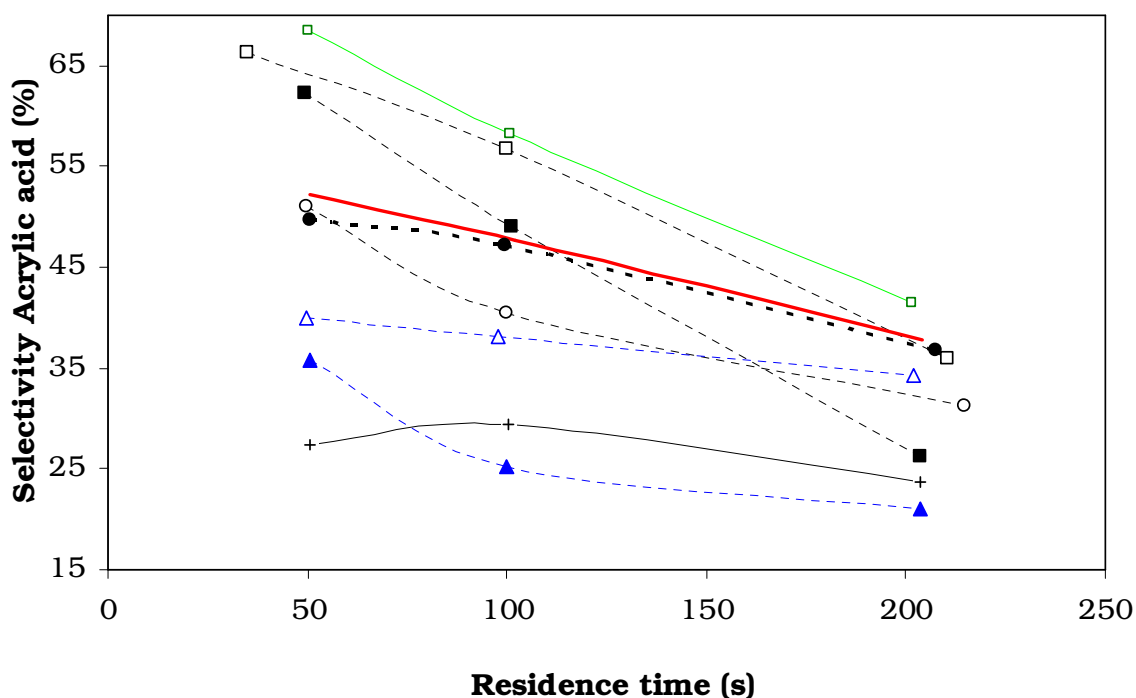
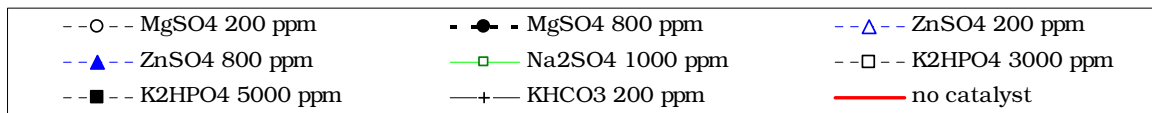


Figure 6-28 Selectivity towards acrylic acid vs residence time at 385 °C and 350 bar in a pipe reactor with 0.1 M lactic acid feed. (Salt concentrations in g g⁻¹)

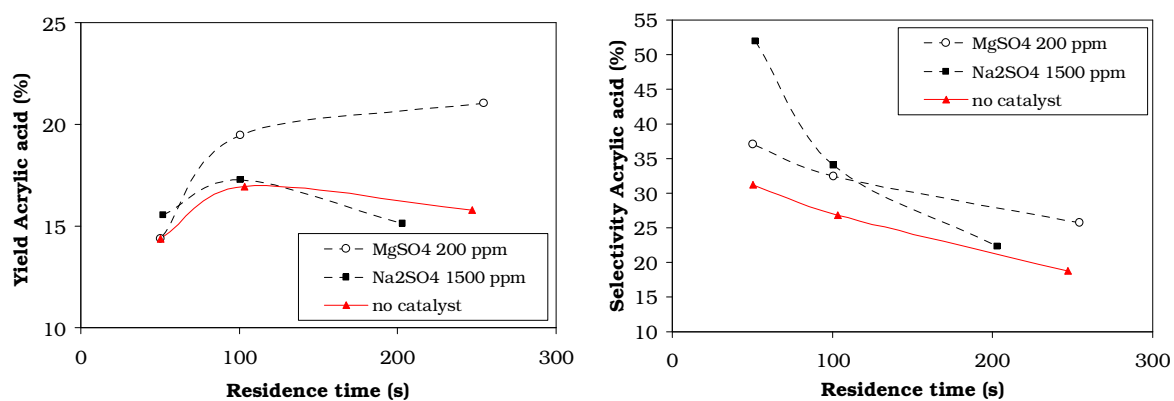


Figure 6-29 Selectivity and yield in acrylic acid at 385 °C and 350 bar using a CSTR.

Except for the search for homogeneous catalysts, some preliminary experiments to find heterogeneous catalyst for the dehydration have been carried out in CSTR to find species which are stable in SCW. Steatite and Al₂O₃ pellets from CeramTec GmbH have been used. These were found to be stable in SCW at 350 bar and 385 °C for several hours, i.e. as long as the experiments lasted. The pellets were supported within the CSTR using two round-formed stainless steel grids which had the same diameter as the reactor.

Apart from the stability of the two mentioned materials, which makes them suitable as catalyst supports in SCW, no improvement in the formation of acrylic acid has been observed when using an initial concentration of 0.1 M lactic acid, a residence time of 100 seconds, 350 bar and 385 °C.

6.4.2. Influence of Acetic and Phosphoric Acid

Theoretically, acids should favor the formation of acetaldehyde via decarbonylation [Mok-1989]. The effect of acetic and phosphoric acid on the reaction of lactic acid in SCW has been investigated. Sulfuric and other acids have not been used due to corrosion problems. As illustrated in Figure 6-30 and reported in the literature [Mok -1989], acidifying the feed has a negative effect on the formation of acrylic acid at least when using phosphoric acid. Surprisingly, acetic acid has no effect on the reaction.

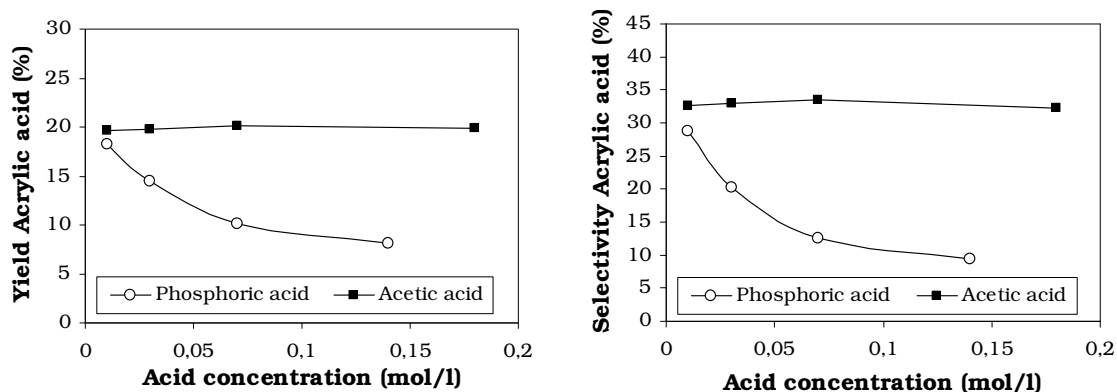


Figure 6-30 Influence of the addition of acetic and phosphoric acid on the formation of acrylic acid at 385 °C and 350 bar.

A reasonable explanation for this behaviour lies in the different dissociation degree of the two acids. A comparison at 350 bar and 385 °C is not possible because the data found in the literature only characterizes dissociation until 300 °C in the case of phosphoric acid. Nevertheless, the dissociation constants of the two acids at 300 °C and saturated vapour pressure (87.5 bar) have been calculated.

The data available for H_3PO_4 is derived from the equilibrium reaction:



At 300 °C and 87.5 bar (saturated vapour pressure) the calculated equilibrium constant for (6-1) is given by [Tre-2004]:

$$\lg K_{I,H_3PO_4,OH} = 6.901 \quad (6-2)$$

since

$$K_{I,H_3PO_4,OH} = \frac{a_{H_2PO_4} a_{H_2O}}{a_{H_3PO_4} a_{OH^-}} \quad (6-3)$$

where a denotes the activities of the respective species, one can write

$$K_{I,H_3PO_4,OH} = \frac{a_{H_2PO_4} a_{H^+}}{a_{H_3PO_4}} \cdot \frac{a_{H_2O}}{a_{H^+} a_{OH^-}} \quad (6-4)$$

or in logarithmic form:

$$\lg K_{I,H_3PO_4,OH} = \lg K_{I,a,H_3PO_4} - \lg K_w \quad (6-5)$$

with K_w the dissociation constant of water.

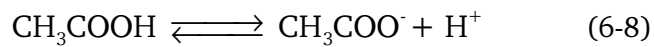
At 300 °C and 87.5 bar (saturated vapour pressure) [Mar-1981]:

$$\lg K_w = -11.406 \quad (6-6)$$

By inserting (6-2) and (6-6) in (6-5):

$$\lg K_{I,a,H_3PO_4} = -4.505 \quad (6-7)$$

For acetic acid, at 300 °C and saturated vapor pressure, extending an empirical equation from the work of Sue *et al.* [Sue-2003] to lower values of the water density, the dissociation constant of acetic acid corresponding to the equilibrium:



can be approximated:

$$\lg K_{a,CH_3COOH} = -6.59 \quad (6-9)$$

Comparing (6-7) and (6-9) it can be concluded that *at least* at 300 °C and saturated vapor pressure, the dissociation constant of phosphoric acid is two orders of magnitude higher than that of acetic acid, thus making the latter a much weaker acid than H_3PO_4 . By presuming that the ratio between the dissociation constants of the two acids changes insignificantly at 385 °C and 350 bar, that is, phosphoric acid remains much stronger than acetic acid, the insensitivity of the dehydration towards the latter can be explained.

6.4.3. Phosphates: The H₃PO₄/KOH Ratio

In the previous section it has been shown that phosphoric acid has a strong activity upon the reaction, unlike the relatively “inert” acetic acid.

On the other hand, the addition of sodium hydroxide to the lactic acid feed has been reported to inhibit the formation of acrylic acid [Mok-1989]. Nevertheless, adding the minutest amounts of phosphoric acid to the lactic acid feed where KOH or NaOH is present brings significant changes in the formation of acrylic acid, as shown further on.

With the notation:

$$A = \frac{n_{\text{H}_3\text{PO}_4}}{n_{\text{KOH}}} \quad (6-10)$$

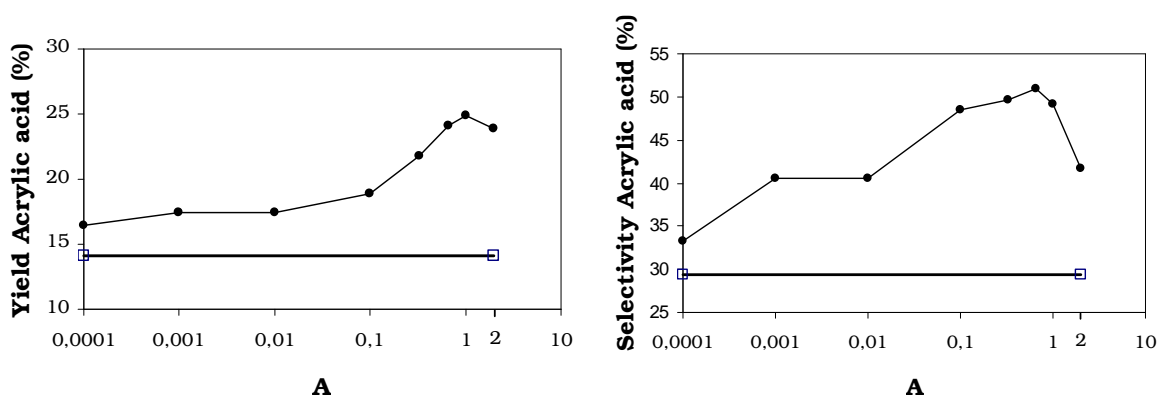


Figure 6-31 Yield and selectivity towards acrylic acid at 385 °C and 350 bar with a 0.1 M lactic acid feed and a starting concentration of 1500 ppm KOH. H₃PO₄ has been gradually added. The bold straight line indicates the yield and selectivity for acrylic acid without addition of acid.

The best results with a yield of acrylic acid of max. 25 % are obtained for **A** in the range between 0.1 and 1 as seen in Figure 6-31. A ratio of 1:1, which is the most suitable for the formation of acrylic acid is equivalent to the addition of KH₂PO₄ to the feed solution. A set of experiments where the effect of K₂HPO₄ and KH₂PO₄ are compared in CSTR confirm this result (Figure 6-32).

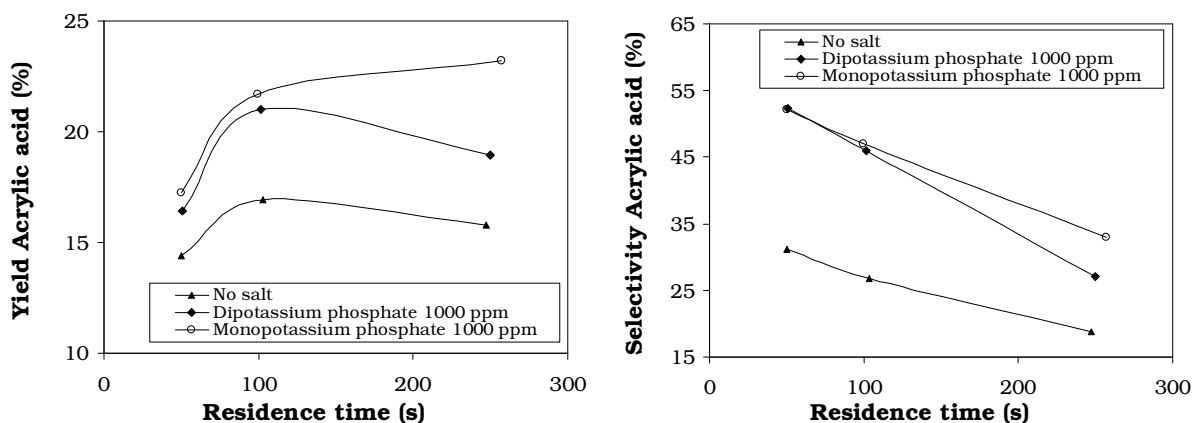


Figure 6-32 Influence of different phosphates on the dehydration at 385 °C and 350 bar in a CSTR (Salt concentrations in g g⁻¹).

6.4.4. Phosphates: Effect of Different Concentrations

Different concentrations of KH_2PO_4 have been studied in order to determine an optimum in its catalytic activity. Once this optimum is determined for a fixed residence time, temperature and pressure, all subsequent experiments are to be carried out using that particular concentration of catalyst.

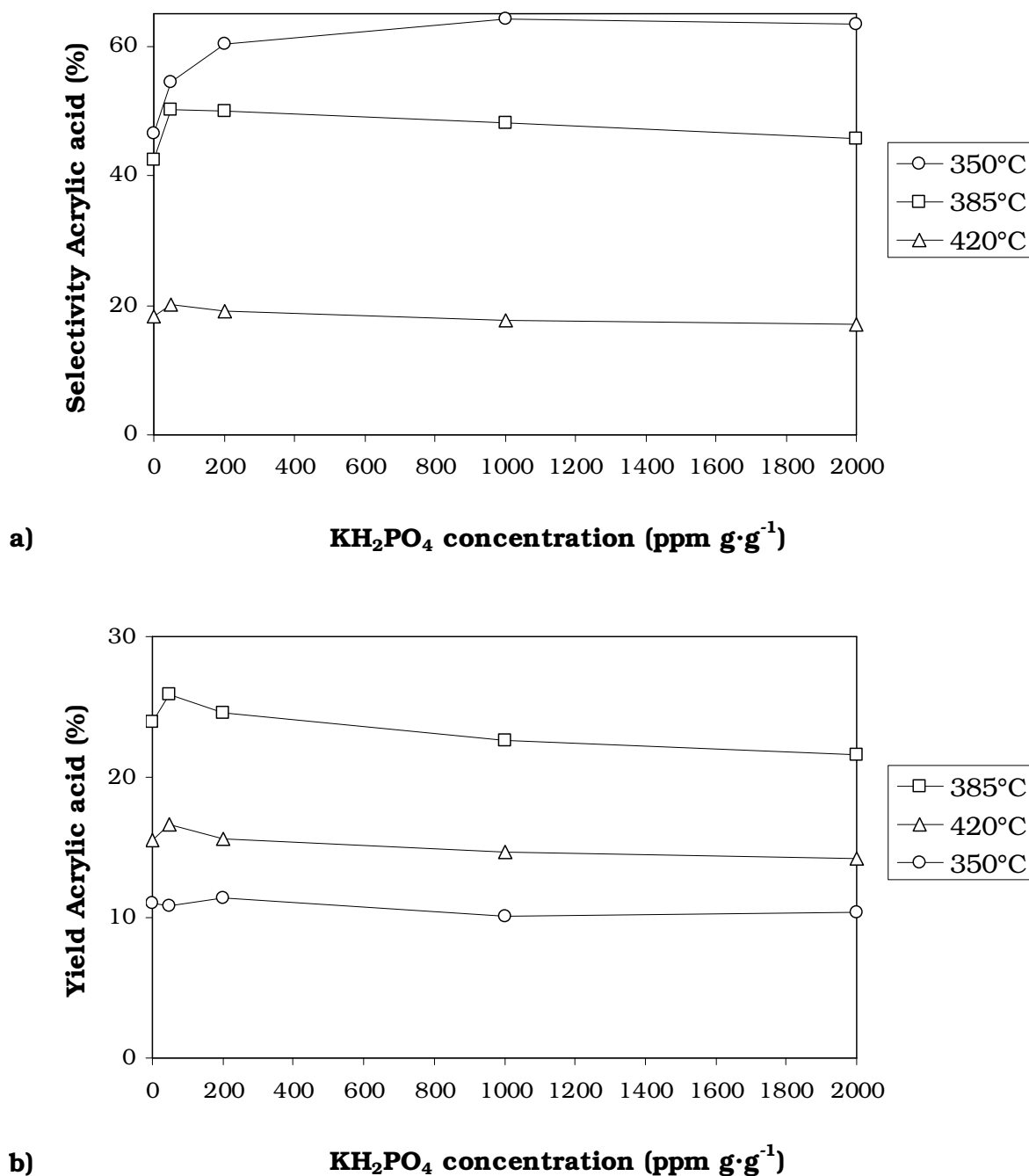


Figure 6-33 Effect of KH_2PO_4 concentration on the dehydration of lactic acid in near- and supercritical water at 350 bar 385 °C and 100 seconds residence time. a) Influence on the selectivity of acrylic acid; b) influence on the yield of acrylic acid.

The optimal catalytic activity of KH_2PO_4 is between 50 and 200 ppm (g g^{-1}) with a yield of acrylic acid of max. 26 %. In this range a maximal selectivity of 60 % has been obtained. Further increase in the concentration results in a slow steady decrease of both the selectivity and yield of acrylic acid.

6.4.5. Phosphates: Effect of Different Cations

The solubility of electrolytes in supercritical water is very different from that in water at standard temperature and pressure. Even between metals belonging to the same group of the periodic table, their hydroxides can differ in solubility under high pressure and high temperature [Wei-2005].

Given such anomalies the idea of studying the influence of different cations on the dehydration of lactic acid emerged. This has been investigated first by adding NaOH, KOH and CsOH to the feed. Since hydroxides inhibit the formation of acrylic acid, as known from the literature [Mok-1989], the less inhibiting activity of these bases has been investigated. The experiments were carried out using the same amounts of hydroxydes **in grams** and this resulted in different molarities in the hydroxyde solutions. However, the effect of different cations on the formation of acrylic acid seems to be similar for all hydroxydes considered in these experiments, as seen from the trends in the curves illustrated in Figure 6-34. It could be concluded that a pH effect is likely. The small differences in the values of the association constants of LiOH, NaOH and KOH in aqueous solutions at 663 K and 28-29 MPa [Ho-2000] also speak for a pure pH effect for the observed effect of the addition of different hydroxydes on the yield of acrylic acid.

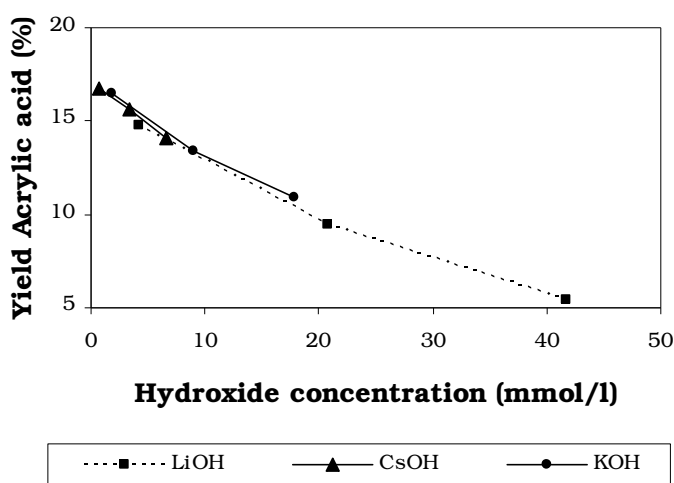


Figure 6-34 A representation of the hydroxide influence of LiOH, KOH and CsOH on the yield of acrylic acid at 385 °C, 350 bar and 100 seconds residence time.

Further experiments have been carried out to compare the differences in using caesium and potassium phosphate species. As seen in Figure 6-35 the use of potassium species results in slightly superior yields of acrylic acid at $A = 1$ (a 1:1 molar ratio of KOH to H_3PO_4 corresponding to the KH_2PO_4 salt).

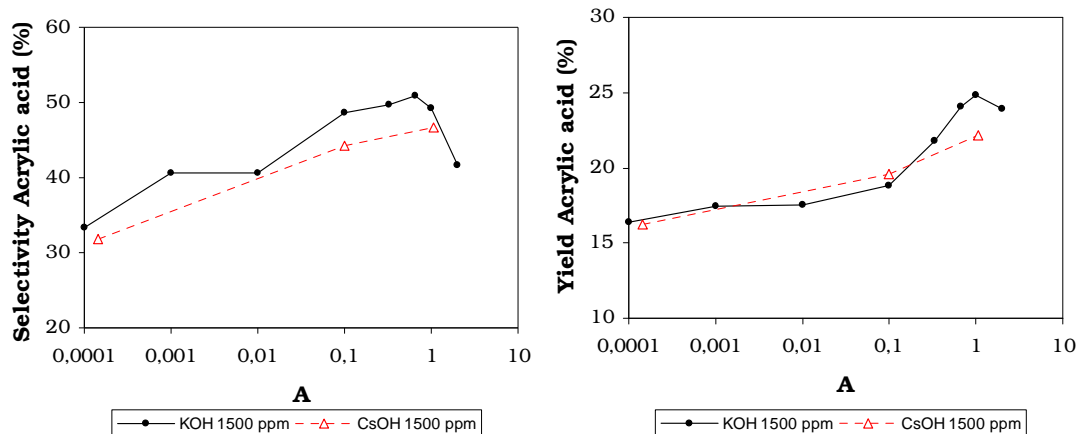


Figure 6-35 Comparison between the catalytic effect of CsOH and KOH with gradual neutralization with H_3PO_4 . The data for KOH is the same as in Figure 6-31. (Concentrations in $g\ g^{-1}$).

Nevertheless, the influence of increasing phosphate concentration has been tested only until a higher limit of $A = 1$. From Figure 6-35 it is, however, likely that a significantly better activity for caesium can not be obtained.

The differences in acrylic acid yields are small by the addition of moderate quantities of catalyst (0-2000 ppm ($g\ g^{-1}$)). The major difference lays in the inhibition of acetaldehyde. Figure 6-36 summarizes some of these results with a confirmation of the optimal catalytic activity at 200 ppm ($g\ g^{-1}$) KH_2PO_4 which will be used in further experiments such as the data necessary for elaborating a kinetic model and comparing the reaction rate constants with and without catalyst.

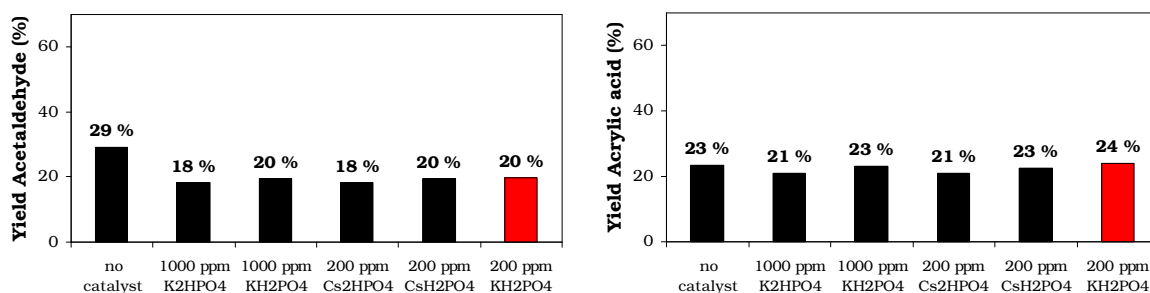


Figure 6-36 Comparison between the use of potassium and caesium species as catalyst. The reaction conditions were : 0.1M Lactic acid feed, 350 bar 385 °C and 100 seconds residence time. (Concentrations in $g\ g^{-1}$).

6.4.6. Phosphates: Effect on the Stability of Acrylic Acid

A limitation of the applicability of phosphates for enhancing the reaction towards acrylic acid is the effect that they have on acrylic acid itself. A first insight can be gained from Figure 6-37.

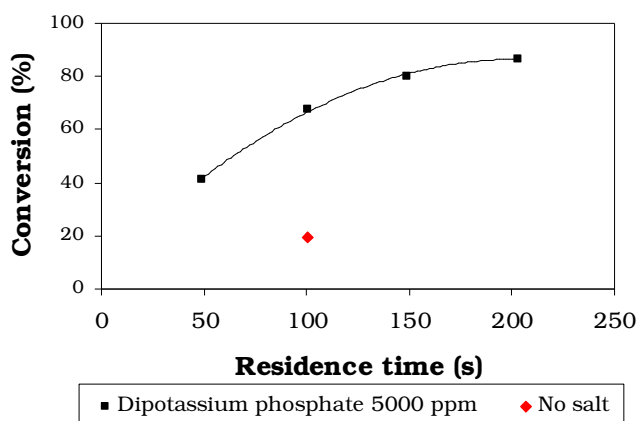


Figure 6-37 Stability of acrylic acid (0.1 M feed) at 385 °C and 350 bar with and without addition of salt. (Concentrations in g g^{-1}).

Clearly, high concentrations of phosphate dramatically destabilize acrylic acid in supercritical water: at 350 bar, 385 °C and a residence time of 100 seconds, the addition of 5000 ppm (g g^{-1}) dipotassium phosphate increases the conversion of acrylic acid from 20 % obtained without any phosphate to about 70 % as illustrated in Figure 6-37.

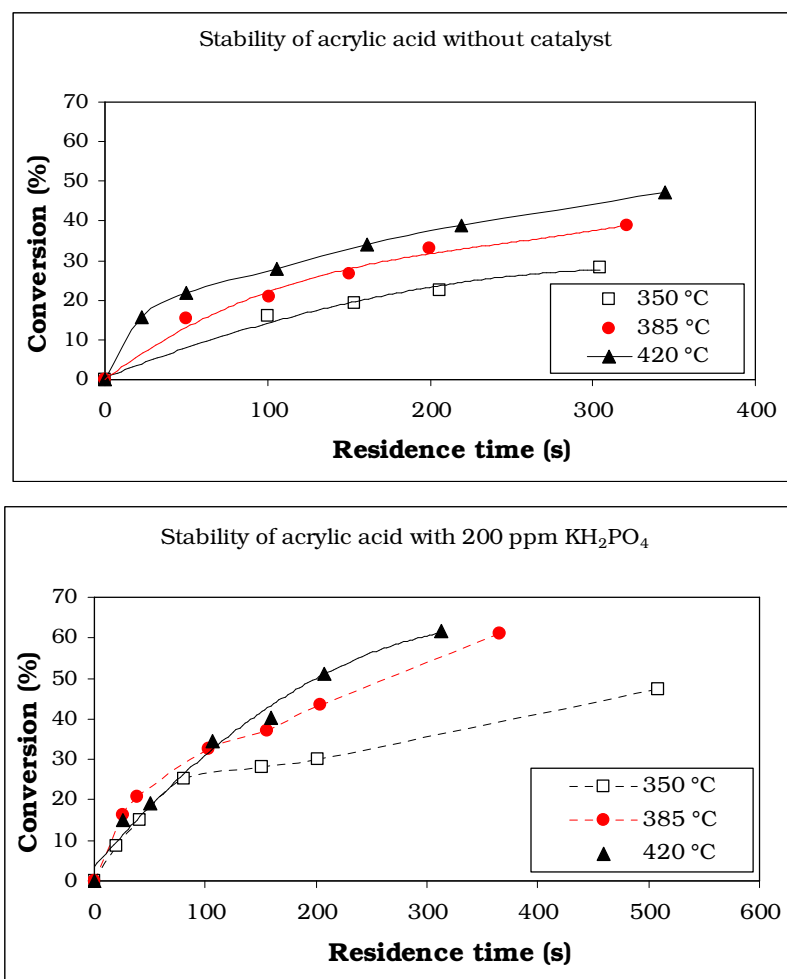


Figure 6-38 Comparison of the stability of acrylic acid in the presence and absence of 200 ppm (g g^{-1}) KH_2PO_4 (feed 0.05M) in near- and supercritical water at different residence times.

A systematic investigation of phosphate concentration on the stability of acrylic acid has not been carried out. The effect of adding 200 ppm (g g^{-1}) KH_2PO_4 has been studied at various temperatures and pressures. As it can be seen in Figure 6-38, the phosphate has a negative effect on the stability of acrylic acid at all temperatures. Two main features characterize the differences in the behaviour of acrylic acid in the presence and in the absence of KH_2PO_4 . First, the slope of the conversion-time curve is larger in presence of phosphate, thus the global reaction rate is higher. The carbon balance in the experiments where phosphates were present is lower than in those without phosphates, probably indicating that the decarboxylation reaction is faster in the first case.

A second feature is that the stability of acrylic acid is relatively insensitive to temperature in the range 350 – 420 °C at residence times lower than 100 seconds. The latter effect could be a result of a step in the unfolding of the reaction which is kinetically controlled. A quantification of these effects can be gained using the kinetic model of the reaction which will be presented in Chapter 7.

7. Reaction Kinetics and Mechanisms

Based on the results described important ideas concerning the reaction network, kinetics and reaction mechanisms of the dehydration of lactic acid in supercritical water could be drawn. In this chapter, they are to be discussed in detail.

7.1. Description of the Kinetic Model

The reaction network has been already indicated in the literature [Mok-1989]. The experiments concerning the stability of acrylic acid in SCW indicate the formation of 3-hydroxypropionic acid and lactic acid by the hydrolysis of acrylic acid. This result has been confirmed by $^1\text{H-NMR}$ analysis. Thus, an extended reaction network has been developed (see Section 6.1.6. and Figure 7-1).

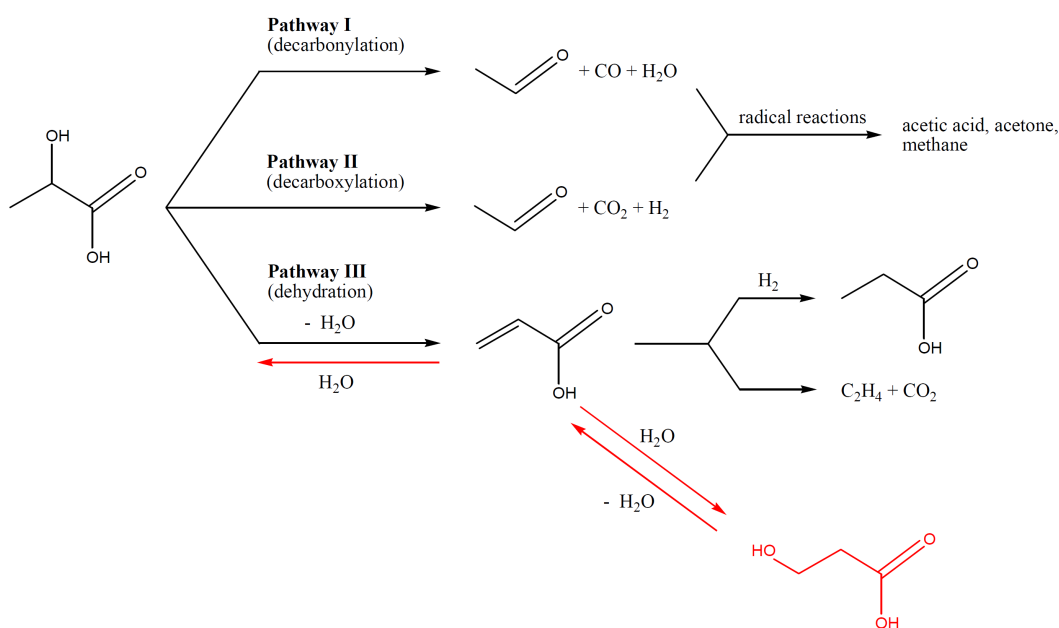


Figure 7-1 Extended reaction network pointing out the hydrolysis of acrylic acid in SCW.

By some simplifications, the actual network for a kinetic model has been developed (Figure 7-2) and is explained hereinafter.

Propionic acid, which has only been detected in traces in some of the reactions, has been excluded from the network. Also 3-hydroxy-propionic acid has been excluded from most of the reactions using lactic acid as feed since these produced only traces of it.

Pathway I and II have been unified and only one reaction of lactic acid producing acetaldehyde has been used.

As mentioned earlier (Section 6.3.3), it has been hypothesized that the decarboxylation of 3-hydroxy-propionic acid would produce ethylene glycol or acetaldehyde. The latter has not been detected in the respective experiments. Therefore no link between 3-hydroxypropionic acid to acetaldehyde has been considered. On the other hand, the reaction of 3-hydroxypropionic acid to ethylene glycol has been considered a minor side reaction and has been excluded from the model.

A fictive product, labelled **D**, has been used to generically designate side (Decomposition) reactions. It has been quantified from the carbon balance and has been used to justify the gaps in it. That is, any gap in the carbon balance has been postulated to occur through first order reactions yielding **D**. However, lactic acid has not been linked directly to **D**. As a simplifying assumption, only two reactions involving lactic acid have been considered in the model: one leading to acrylic acid and the other leading to acetaldehyde.

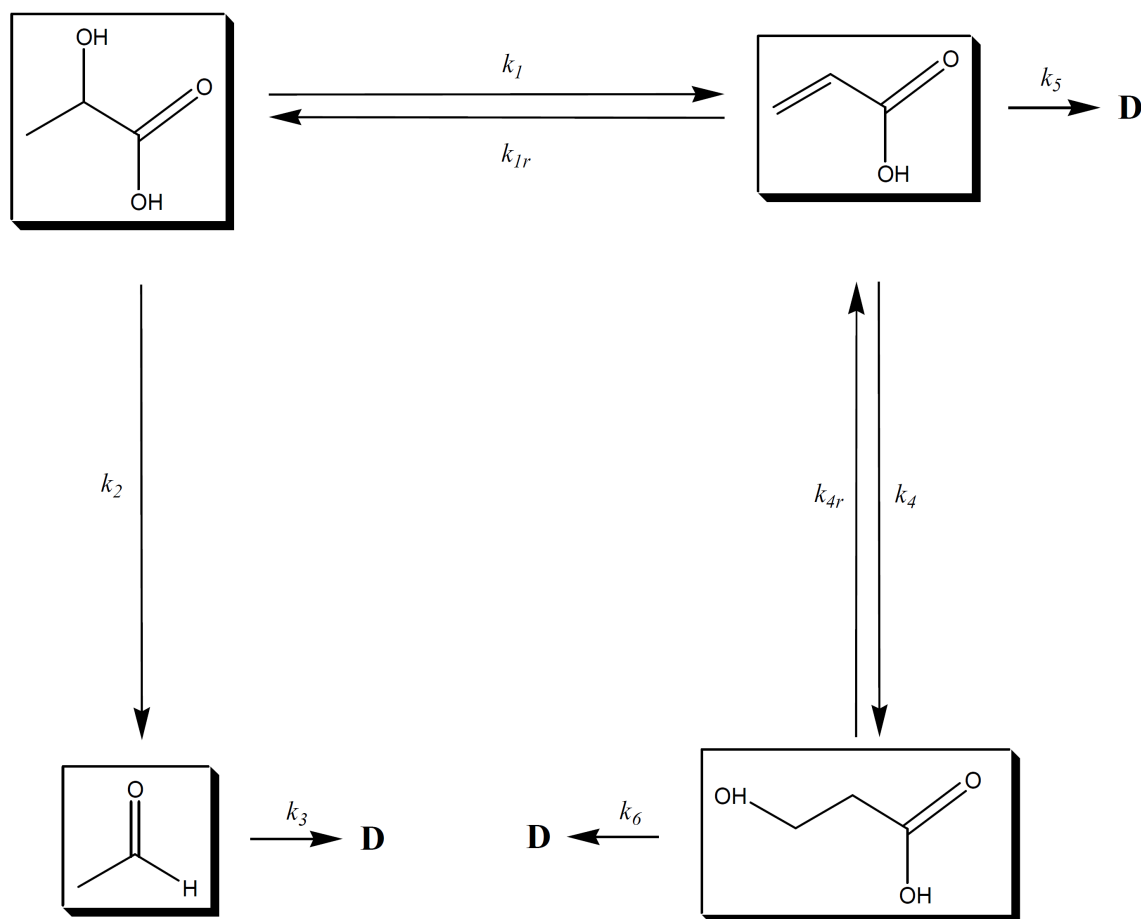
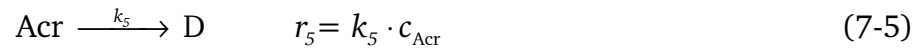
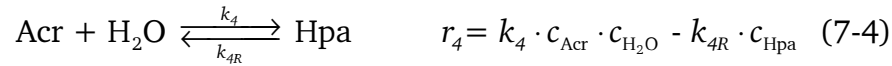
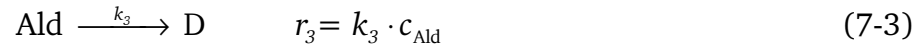
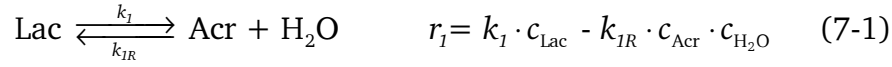


Figure 7-2 The kinetic model used for estimation of the reaction rate constants.

The detailed reactions from the model and the corresponding rate equations are the following (concentrations in mol l⁻¹):



Reactions (7-1) and (7-4) which are theoretically of second order are practically reduced to first order reactions since the solvent concentration $c_{\text{H}_2\text{O}}$ can be considered constant.

Therefore the two reactions are considered pseudo first order reactions.

The concentrations are calculated at the conditions in the reactor. As density for all feed solutions, the density of pure water has been considered:

$$c_{i,\text{Reactor}} = c_{i,\text{STP}} \cdot \frac{\rho_{\text{H}_2\text{O},\text{Reactor}}}{\rho_{\text{H}_2\text{O},\text{STP}}} \quad (7-7)$$

with

$c_{i,\text{Reactor}}$ concentration of the substance i at the reaction conditions /mol l⁻¹

$c_{i,\text{STP}}$ concentration of the substance i at 25 °C and 1 atm /mol l⁻¹

$\rho_{\text{H}_2\text{O},\text{Reactor}}$ density of water at the reaction conditions /g l⁻¹

$\rho_{\text{H}_2\text{O},\text{STP}}$ density of pure water at 25 °C and 1 atm /g l⁻¹

7.2. Estimation of the Reaction Rate Constants with Presto Kinetics® Software

The simulation was carried out at three different temperatures, 350, 385 and 420 °C, using the respective experimental data with and without addition of 200 ppm KH_2PO_4 . One key idea in setting up the initial conditions for the model was that the reaction rate constants should be the same, regardless of the starting material in the reaction. Thus, at a given temperature and pressure the rate constants would be the same regardless of the starting material, be it lactic acid or acrylic acid (Figure 7-3). The software has been “forced” to estimate simultaneously the rate constant for the data where lactic acid has been used as starting material and for the data where acrylic acid has been used as starting material (at the same temperature and pressure).

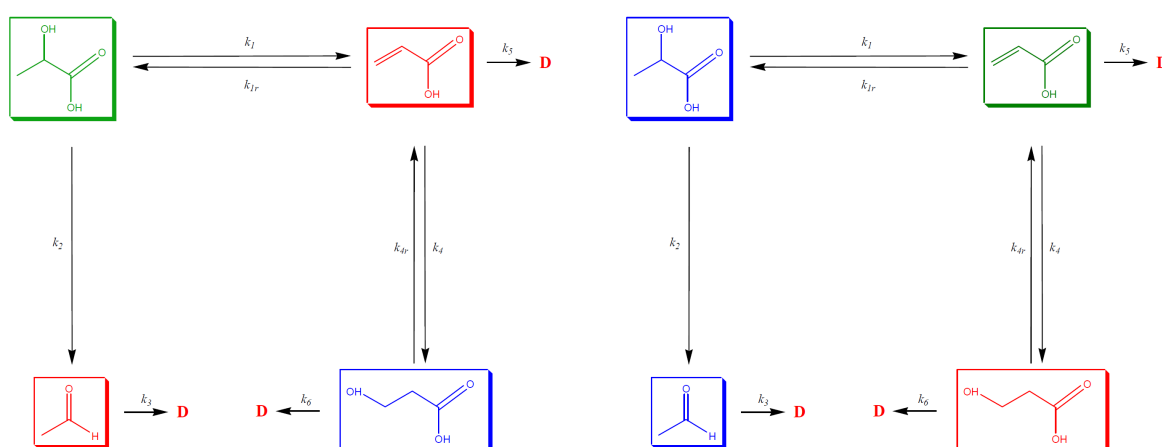
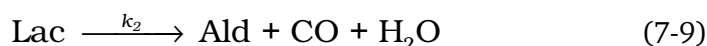


Figure 7-3 The reaction network used for the kinetic model with emphasis on the two different starting materials, marked with green. The main products are marked with red and those products where just traces were present with blue.

A first important estimation of the reaction rate has been made by calculating a “global” reaction rate. For this the reaction network has been reduced to two irreversible reactions:



For this system the global reaction rate is given by:

$$-\frac{dc_{\text{Lac}}}{dt} = k_{\text{global}} \cdot c_{\text{Lac}} = (k_1 + k_2) \cdot c_{\text{Lac}} \quad (7-10)$$

with c_{Lac} the concentration of the lactic acid (mol l^{-1}) and t the residence time (seconds).

By integrating and putting $c_{\text{Lac}} = c_{\text{Lac},0}$ at $t = 0$ the solution for the equation above is

$$c_{\text{Lac}} = c_{\text{Lac},0} \cdot e^{-(k_1+k_2) \cdot t} \quad (7-11)$$

or

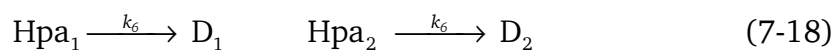
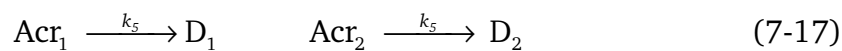
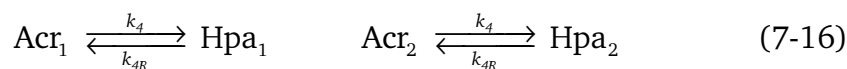
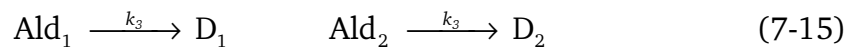
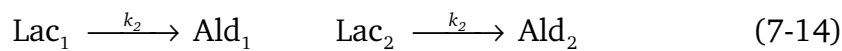
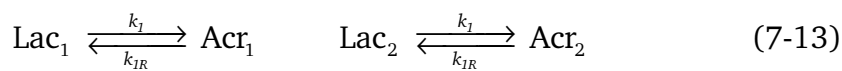
$$\ln(c_{\text{Lac}}) = -(k_1+k_2) \cdot t + \ln(c_{\text{Lac},0}) \quad (7-12)$$

By plotting the logarithm of the experimental concentrations against the residence time and using a linear regression, an estimation of k_{global} can be obtained. The rate constants k_1 and k_2 obtained from the simulation should have the same order of magnitude. The values of the global rate constant are presented in Table 7-1.

Table 7-1 Global rate constants for reaction of lactic acid at three temperatures with and without catalyst

	no additive			200 ppm (g g ⁻¹) KH ₂ PO ₄		
Temperature /°C	350	385	420	350	385	420
$k_{\text{global}} / 10^{-3} \text{ s}^{-1}$	1.8	5	10.4	1.5	5.1	9.5

Inserting the supplementary condition that the variation of concentration with residence time be that of a CSTR resulted in a simulation failure. Therefore, the simplest, **Batch reactor model** has been taken in the software as a base for the simulations. The rate constants have been *simultaneously* estimated for experimental data originating from the starting substances, lactic acid and acrylic acid. In each case the reactions were separately considered. In this manner, twelve reactions were used in the simulation. They are presented below as used in the simulation.



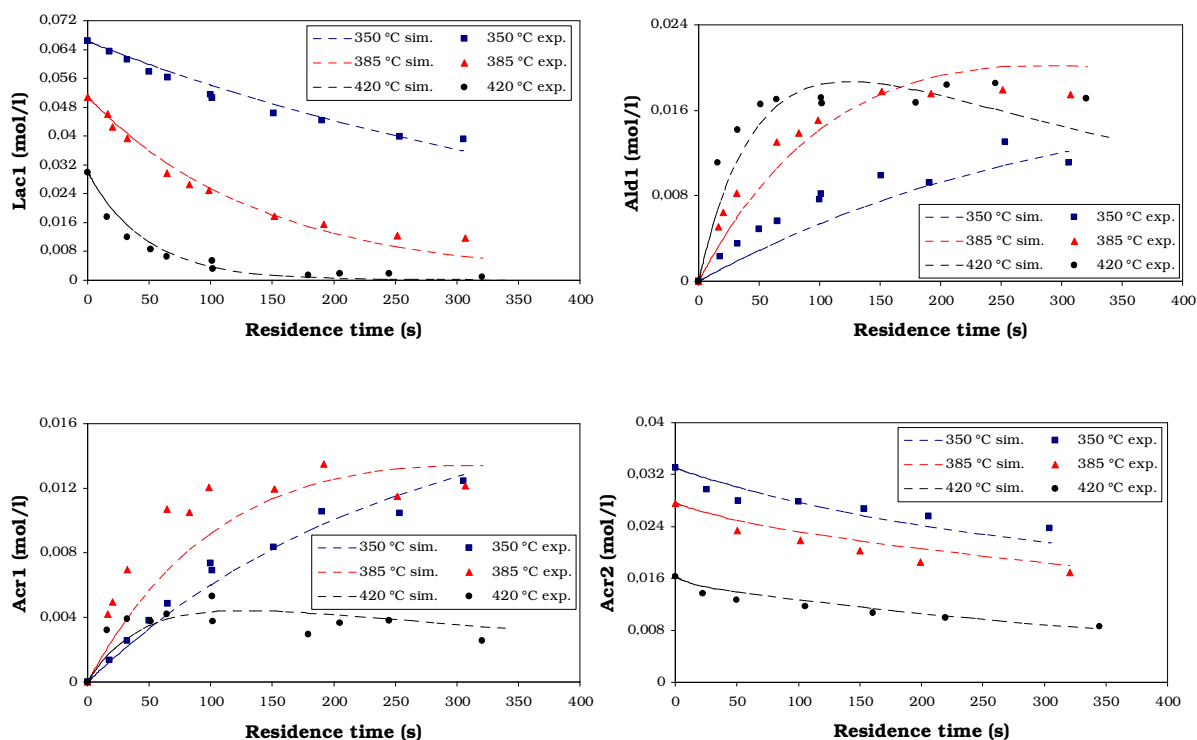


Figure 7-4 Experimental data from reactions at different temperatures and no additives and the respective simulation-based fit curves.

The main results from the simulation at 350, 385 and 420 °C are presented in Figure 7-4 and Figure 7-5 . The reaction rate constants are given in Table 7-2.

Table 7-2 Results of the simulation using Presto®. Two series of reaction rate constants corresponding to experiments with and without homogeneous catalysis through KH_2PO_4 (columns with "-" and "+cat.") .

Rate constant	Temperature /°C					
	350		385		420	
	-	cat.	-	cat.	-	cat.
$k_1/10^{-3} \text{ s}^{-1}$	1.10	1.08	2.79	3.83	4.17	4.64
$k_{1R}/10^{-4} \text{ s}^{-1}$	2.00	2.00	3.76	4.78	3.95	4.24
$k_2/10^{-4} \text{ s}^{-1}$	9.40	9.38	42.18	27.02	167.54	175.73
$k_3/10^{-4} \text{ s}^{-1}$	9.40	33.00	15.55	15.55	20.66	17.39
$k_4/10^{-4} \text{ s}^{-1}$	9.80	9.76	11.76	15.99	47.79	43.86
$k_{4R}/10^{-3} \text{ s}^{-1}$	5.00	5.00	1.83	17.62	72.63	75.69
$k_5/10^{-4} \text{ s}^{-1}$	7.99	7.99	8.98	26.65	15.94	25.89
$k_6/10^{-3} \text{ s}^{-1}$	2.43	2.43	1.40	0.67	0.093	0.04

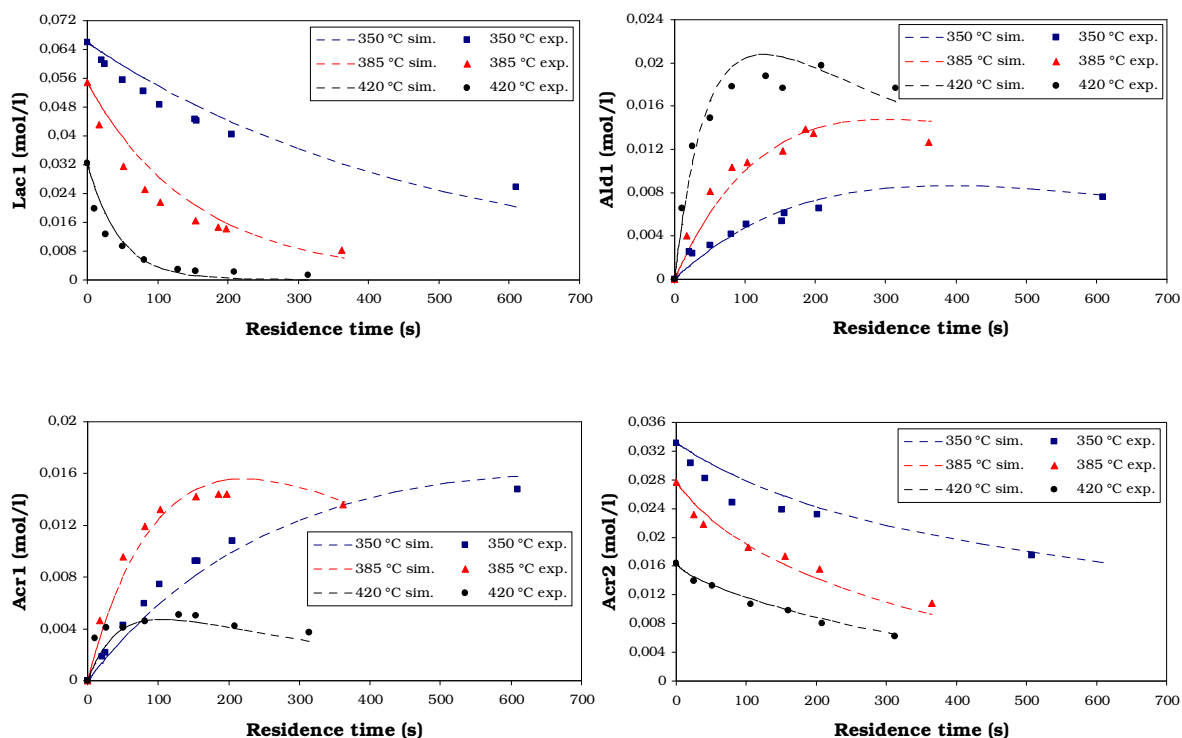


Figure 7-5 Experimental data from reactions at different temperatures and 200 ppm K_2HPO_4 and the respective simulation-based fit curves.

It was considered useful to represent the rate constants graphically to facilitate the discussion about the simulated results (Figure 7-6). The following observations have been made:

The reaction rates tend to increase with temperature with the notable exception of k_5 and of k_3 in the presence of the catalyst.

The rate constant for dehydration (k_7) is higher with phosphates at all temperatures, while the formation of acetaldehyde (k_2) is only effectively inhibited by the catalyst at 385 °C.

The higher value of k_5 in the presence of KH_2PO_4 confirms the finding that phosphate also catalyzes the decomposition of acrylic acid.

With an exception for r_4 at 420 °C, phosphate increases the reaction rates r_1 , r_{1R} , r_4 , r_{4R} and k_5 . Since all these reaction involve acrylic acid, this suggests that the catalyst has an “activating” effect specifically on the latter. Together with the finding that small concentrations of phosphoric acid, unlike HNO_3 or H_2SO_4 enhance the formation of acrylic acid and inhibits that of acetaldehyde [Lir-1993], it could be hypothesized that phosphates play an active catalytic role, probably through a phosphorus containing reaction intermediate, rather than through an indirect influence on the pH of the medium or on its ionic strength.

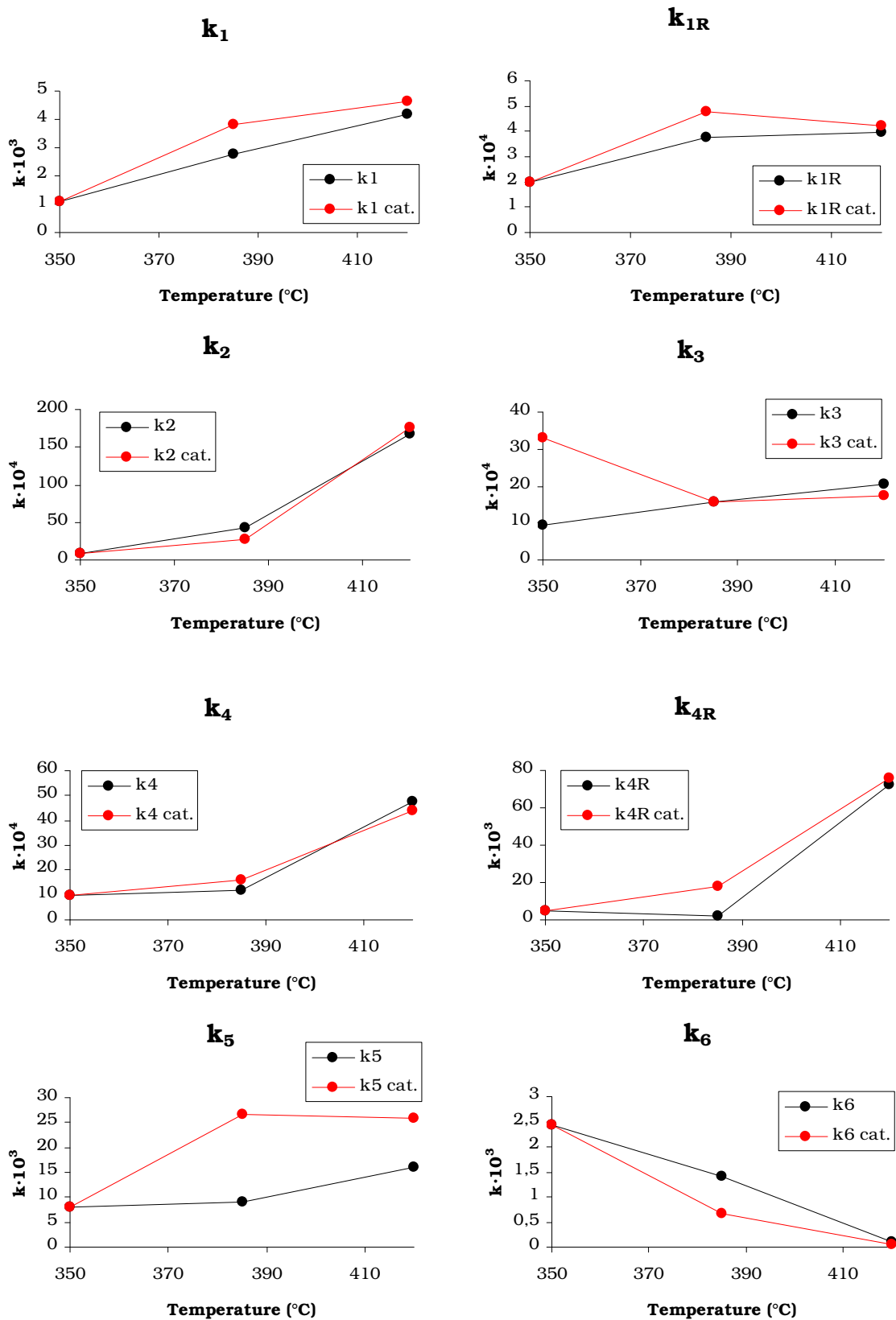


Figure 7-6 Graphical representation of the reaction rates (s^{-1}) obtained from the simulation as a function of temperature and of different reaction conditions (presence or absence of the catalyst).

7.3. The mechanism of the acetaldehyde formation

It has been emphasized that acetaldehyde is formed through two independent pathways: a decarbonylation and a decarboxylation pathway [Mok-1989]. In experiments using ^{13}C -labelled lactic acid ($\text{CH}_3\text{-CH}(\text{OH})\text{-}^{13}\text{COOH}$) both ^{13}CO and $^{13}\text{CO}_2$ have been detected. There is an elegant mechanistic explanation for the decarbonylation (See Chapter 2) involving an attack of the proton on the carboxylic group followed by successive elimination of water and CO. There is, however, no straightforward explanation for the decarboxylation. *Mok et al.* hypothesized that a radical mechanism is responsible for the decarboxylation and that pressure effectively suppresses this pathway via the cage effect [Mok-1989]. There is an important puzzle surrounding this reaction. A simple decarboxylation of lactic acid should produce ethanol and CO_2 . On the other hand no ethanol has been detected among the reaction products [Mok-1989] and, besides, ethanol has been proved to be stable at temperatures well above the critical point of water [Ram-1987]. Reaction parameters like the residence time in reactor and acidity of the feed have an influence on the CO and CO_2 formation (Figure 7-7).

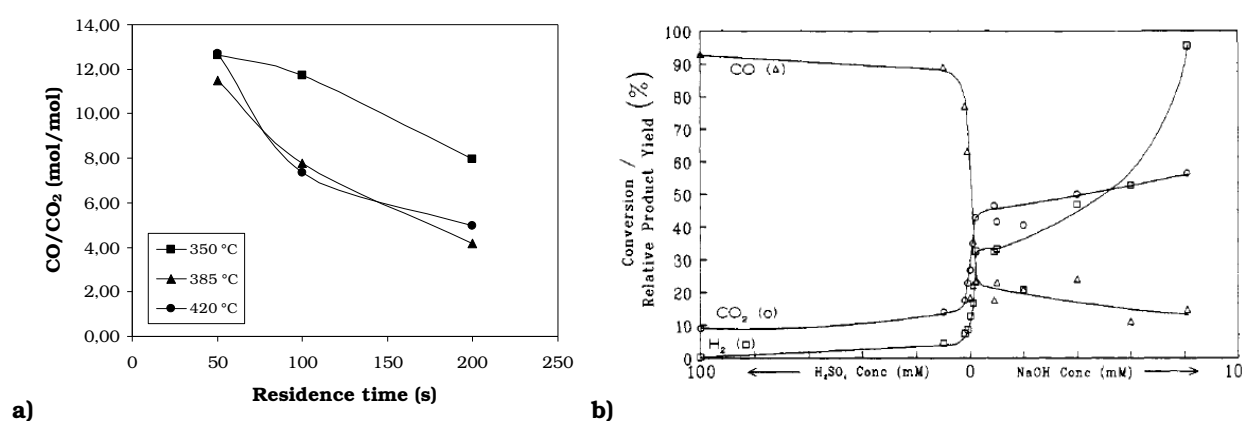
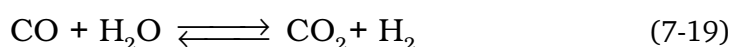


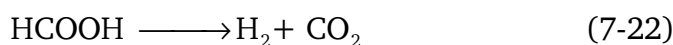
Figure 7-7 a) Influence of the residence time on the CO/CO₂ ratio (Section). b) Influence of the addition of NaOH and H₂SO₄ on the gaseous products of the reaction of lactic acid in water at 385 °C, 345 bar and a residence time of 30 seconds [Mok-1989].

Longer residence times decrease the proportion of CO among the gaseous products suggesting that a consecutive reaction involving the latter might take place. Altogether, at 30 seconds of residence time, increasing the acidity of the feed with H₂SO₄ results in higher amounts of CO while increasing the basicity of the feed with NaOH increases the amounts of *both* CO₂ and H₂.

These important findings suggest that CO₂ might not arise directly from the decarboxylation of lactic acid but indirectly via the **water gas shift reaction**:



Helling *et al.* [Hel-1987] support not only this idea but also the influence of H⁺ and OH⁻ on the reaction by the following mechanism:



Thus, the higher OH^- concentration would shift the equilibrium towards the formation of CO_2 while the higher H^+ concentration would bring an increase in the CO proportion among the gaseous products. These findings make the hypothesis of CO_2 production via decarboxylation very improbable. It could be argued that the carbon dioxide is formed mainly through decarboxylation of acrylic acid rather than through the water gas shift reaction. If it were so, the ethene, which is uniquely identified with the acrylic acid decarboxylation, should have about the same concentration as CO_2 in the gas phase. The analysis of the gaseous products indicates a higher molar concentration of CO_2 than that of ethene (See Section 6.2). This idea can be, therefore, ruled out. Rather, CO_2 is formed, as mentioned above, through a consecutive reaction from CO . If an ionic mechanism (7-20 to 7-22) can explain this reaction, the formation of CO_2 is favored by a higher OH^- concentration, a fact that has also been observed experimentally.

From these results it can be concluded that acetaldehyde is formed solely by decarbonylation of lactic acid in near- and supercritical water.

7.4. The reaction network and proposed elementary reactions

Summarizing all findings concerning the reaction mechanisms and the different pathways which occur during the reaction of lactic acid in near- and supercritical water, an extended reaction network can be outlined (Figure 7-8). The steps concerning the reaction of 3-hydroxy-propionic acid to acetaldehyde for which the analyses indicated no evidence (Section 6.3.3), has been marked with red on the scheme.

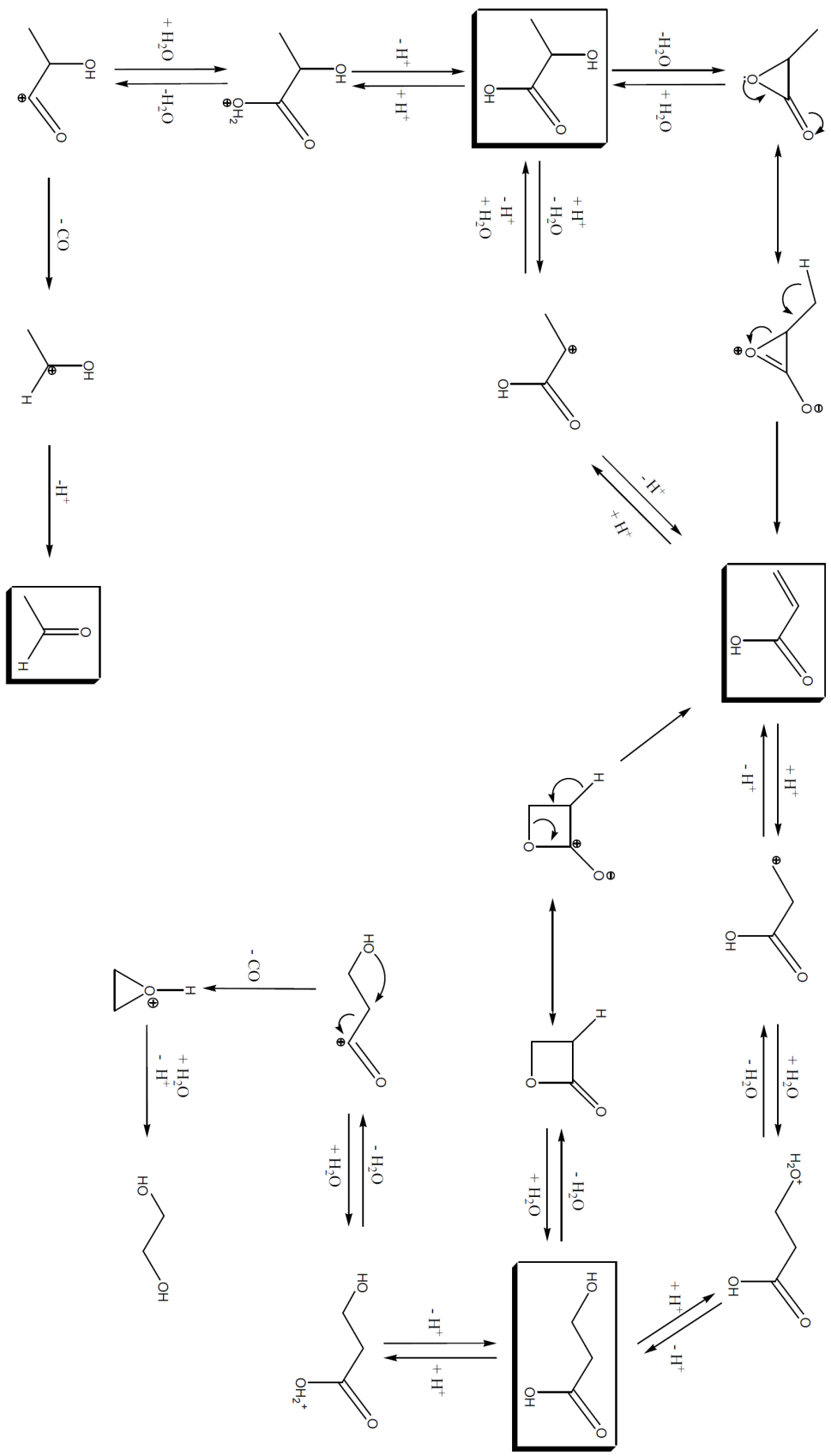


Figure 7-8 Extended network and proposed mechanisms for the reaction of lactic acid in near- and supercritical water.

8. Summary and Outlook

The predicted depletion of fossil raw materials, especially oil and natural gases is reflected in an increase of their market price. This compels the chemical industry to search for alternative production processes. The renewable raw materials derived from the biomass which is available in large amounts in nature and scarcely exploited for industrial uses, emerge as a promising alternative to avoid a feedstock crisis.

Acrylic acid is an important intermediate produced nowadays entirely from fossil raw materials. An alternative route starts from lactic acid which is a relatively inexpensive substance derived from biomass. Since an efficient catalyst for the dehydration of lactic acid which leads to acrylic acid is not known, a key concept could be to use near- and supercritical water as a clean, versatile reaction medium.

Thorough research on this promising route has been carried out by Mok *et al.* [Mok-1989] and Lira *et al.* [Lir-1993]. Significant quantities of acrylic acid are obtained when the reaction parameters pressure, temperature, reaction time are in the following ranges, respectively: 300 - 340 bar, 350 - 400 °C, 40 -120 s. In the presence of disodium phosphate the yield of acrylic acid increases [Lir-1993]. A reaction network has been outlined, partly with suggestions about the respective reaction mechanisms. In near- or supercritical water lactic acid undergoes transformations through three pathways [Mok-1989]:

Decarbonylation leading to acetaldehyde, carbon monoxide and water.

Decarboxylation also leading to acetaldehyde, carbon dioxide and hydrogen.

Dehydration leads to acrylic acid, water and decomposition products of the former (it has been found that acrylic acid decarboxylates to ethene and carbon dioxide and the presence of propionic acid has been assigned to a hydrogenation reaction). The proposed mechanisms for acetaldehyde and acrylic acid formation are represented in Figure 8-1 to 8-3.

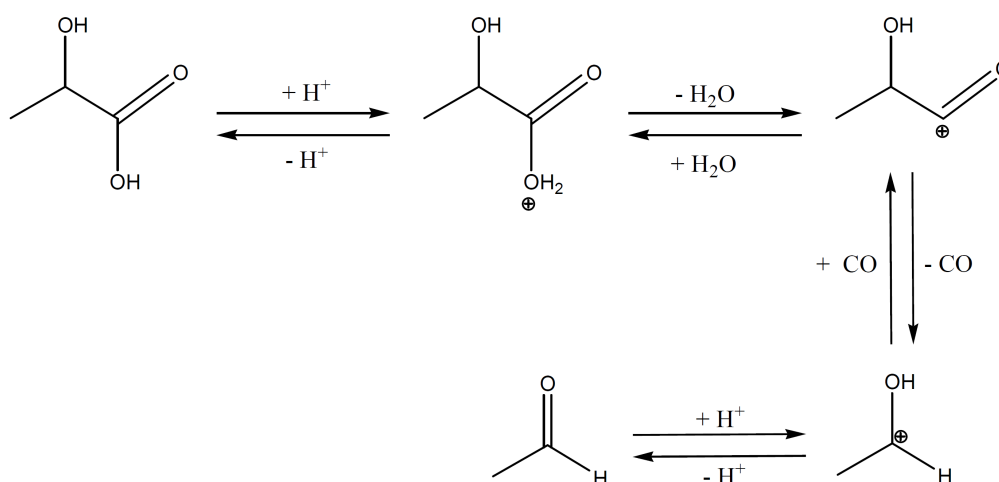


Figure 8-1 Mechanism for the acetaldehyde formation through decarbonylation of lactic acid in near- and supercritical water [Mok-1989].

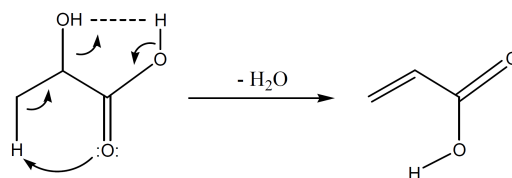


Figure 8-2 Proposed concerted mechanism for acrylic acid formation in near- and supercritical water [Mok-1989].

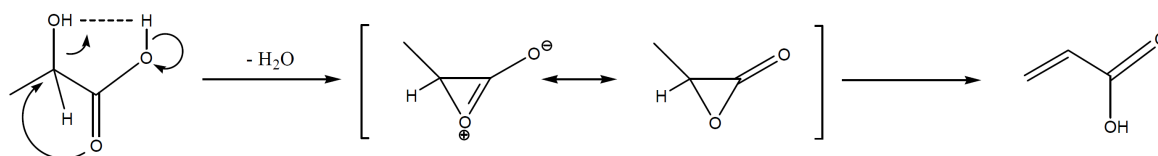


Figure 8-3 Proposed mechanism for acrylic acid formation in near- and supercritical water through an α -lactone intermediate [Mok-1989].

The presence of acids such as sulphuric acid or nitric acid in the reaction feed lowers the acrylic acid yields. The same is valid for bases such as sodium hydroxide. High concentration of added acids (110 mM sulphuric acid) lead to up to 90 % yield of acetaldehyde. This effect is in good agreement with the proposed mechanism for decarbonylation (Figure 8-1) which indicates that acids favour this pathway. High concentrations of added bases (81 mM of sodium hydroxide) significantly increase the concentration of hydrogen, apparently through the decarboxylation of lactic acid. Phosphoric acid favours the formation of acrylic acid if small concentrations are used (0.02 M). Further increases in the concentration of the latter bring no improvement in acrylic acid yields. While a shift in the pH of the feed is generally unfavourable for the dehydration of lactic acid, increasing the ionic strength favours all pathways (decarbonylation, decarboxylation and dehydration).

The main objective of this thesis was to find conditions which improve the yields of acrylic acid. A secondary goal was to extend the knowledge about the pathways by which lactic acid reacts in near- and supercritical water and to estimate the reaction rate constants for each important pathway.

The influence of temperature, pressure, reaction time and initial concentration has been investigated as a first step, in order to confirm validity of the data found in the literature, with a focus on increasing the yield of acrylic acid. By this, reaction conditions have been found, with higher acrylic acid yields, which were not previously reported.

The information found in the literature regarding the influence of additives, especially of salts has been considered insufficient. Therefore, I have carried out a screening for salt catalysts with emphasis on phosphates which have been reported to increase the yield in acrylic acid [Lir-1993]. Since small concentrations of phosphoric acid were reported to have a positive influence, part of the phosphate catalyst screening has been carried out by mixing potassium hydroxide or caesium hydroxide with phosphoric acid, in various proportions in the lactic acid feed and monitoring the effect on the acrylic acid yield.

As far as the reaction mechanisms are concerned, Mok *et al.* explained that part of the formed carbon dioxide is a product of the lactic acid decarboxylation together with hydrogen and acetaldehyde. Ethanol, the expected decarboxylation product has not been detected in the reaction mixture [Mok-1989]. To understand this abnormal behaviour of lactic acid during decarboxylation I have carried out an investigation. Altogether, experiments using as feed substances derived from the structure lactic acid by substituting a hydrogen atom with a methyl group and with 3-hydroxy-propionic acid have been carried out in an effort to evaluate the dehydration mechanisms outlined in the literature (Figure 8-2 and 8-3).

To conduct the necessary experiments in near- and supercritical water I have constructed an appropriate experimental installation. A stainless steel continuously stirred tank reactor was the core of this installation, operational up to 420 °C and 400 bar. An analytical HPLC system has been developed allowing the separation of all identified substances except for 3-hydroxy-propionic acid which could not be separated from its isomer, lactic acid. This inconvenient has been overcome by supplementary ¹H-NMR analyses. Altogether, these experiments proved that the dehydration of lactic acid *per se* in near- and supercritical water led to negligible amounts of 3-hydroxy-propionic acid, regardless of the experimental conditions used.

Without any catalyst, the yield of acrylic acid reaches a maximum at 385 °C, 350 bars and 200 seconds reaction time with a yield of acrylic acid (23-26 %) above the respective maximum reported in the literature (18 % [Mok-1989]). At 350 °C, 350 bars and a reaction time of 930 seconds the yield is still relatively high (20 %) since the selectivity remains between 30 and 45 % for a wide range of reaction times (50-930 seconds), while the conversion increases with longer reaction times. Under all studied reaction conditions, acetaldehyde has been found to be the main by-product which impedes higher acrylic acid yields.

Among the homogeneous catalysts investigated, zinc sulfate and potassium hydrogen carbonate inhibit the formation of acrylic acid while magnesium sulfate, sodium sulfate and the phosphates of alkaline metals have been found to increase the yield of acrylic acid. A maximal yield of acrylic acid has been obtained during a phosphate catalyst screening 200 ppm (g g⁻¹) potassium diphosphate, reducing the acetaldehyde yield from 29 % without catalyst to 20 % under the mentioned conditions while the acrylic acid yields remain almost unaffected. The selectivities for both products, however, increase. The respective results are represented in Figure 8-4.

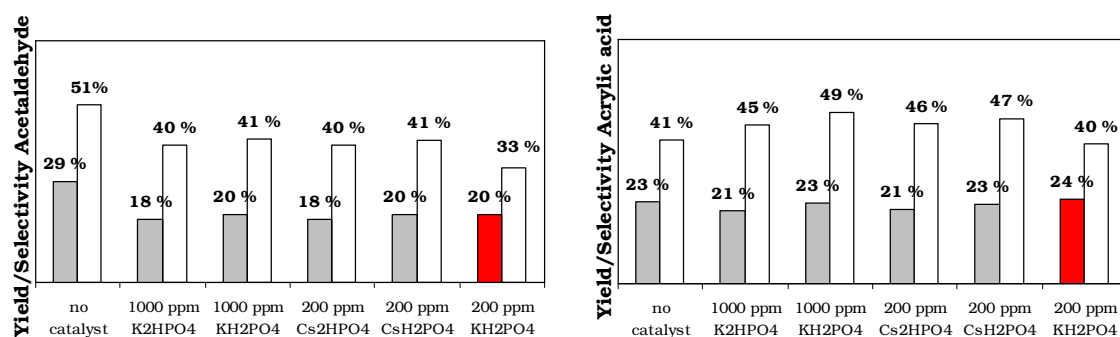


Figure 8-4 Effect of use of potassium and caesium species as catalyst on the dehydration of lactic acid in supercritical water. The reaction conditions were: 0.1M Lactic acid feed, 350 bar 385 °C and 100 seconds reaction time. (Concentrations in g g⁻¹). The filled columns represent yields while empty columns represent selectivities, respectively. The red columns correspond to the conditions where the best acrylic acid yield was obtained.

As a general rule, phosphates have been found to inhibit the formation of acetaldehyde but they have a negative effect on the stability of acrylic acid. The optimum between the two antagonist effects has been obtained by the addition of 50 to 200 ppm sodium or potassium diphosphate. These phosphates are slight inhibitors for acetaldehyde formation, hence the slight increase observed in the selectivity of acrylic acid. Nevertheless, the yield of the latter is not significantly affected by the addition of the catalyst.

Based on the data gained through the experiments which have been carried out, a model for the reaction network including all important detected substances has been developed and component reaction rates were estimated using a simulation software at 350, 385 and 420 °C in the presence and in the absence of potassium diphosphate. These results indicate that the addition of the latter enhances all reaction rates where acrylic acid is involved. This suggests that, rather than a pure pH effect or an influence of the ionic strength, a phosphate intermediate of acrylic acid might be formed, lowering the activation energy for the respective reactions.

An important finding concerning the reaction mechanisms is related to the decarboxylation of lactic acid. Strong evidence has been found that the carbon dioxide apparently formed through decarboxylation of lactic acid is a product of the reaction of carbon monoxide with water (water-gas shift reaction). From the analysis of the gas phase, the ratio of carbon monoxide to carbon dioxide decreases with longer reaction times, which also suggests a consecutive reaction in which both carbon monoxide and carbon dioxide are involved. As reported in the literature [Mok-1989], an increase in pH in the lactic acid feed favours the formation of carbon dioxide and hydrogen over carbon monoxide (and water). This behaviour is in accordance with the hypothesis of a successive reaction leading to carbon dioxide because the water gas shift reaction involved is also an equilibrium reaction shifted toward carbon dioxide at increased pH [Hel-1987].

Another finding reported in my thesis leading to the reshaping of the reaction network is that the reaction of acrylic acid in near- or supercritical water yields to both 3-hydroxy-propionic acid and lactic acid, probably through parallel reactions. This result prompted me to quantify both isomers. This has been accomplished with the help of supplementary ¹H-NMR analyses. The quantities of 3-hydroxy-propionic acid found in the reaction mixture in the dehydration of lactic acid are negligible comparing to the reaction where acrylic acid was used as starting material, leading to 3-hydroxy-propionic acid as a major reaction product.

A reaction network involving all important reactions and taking into account the experimental results reported in this thesis and which describe the behaviour of lactic and acrylic acid in near- and supercritical water is illustrated in Figure 8-5.

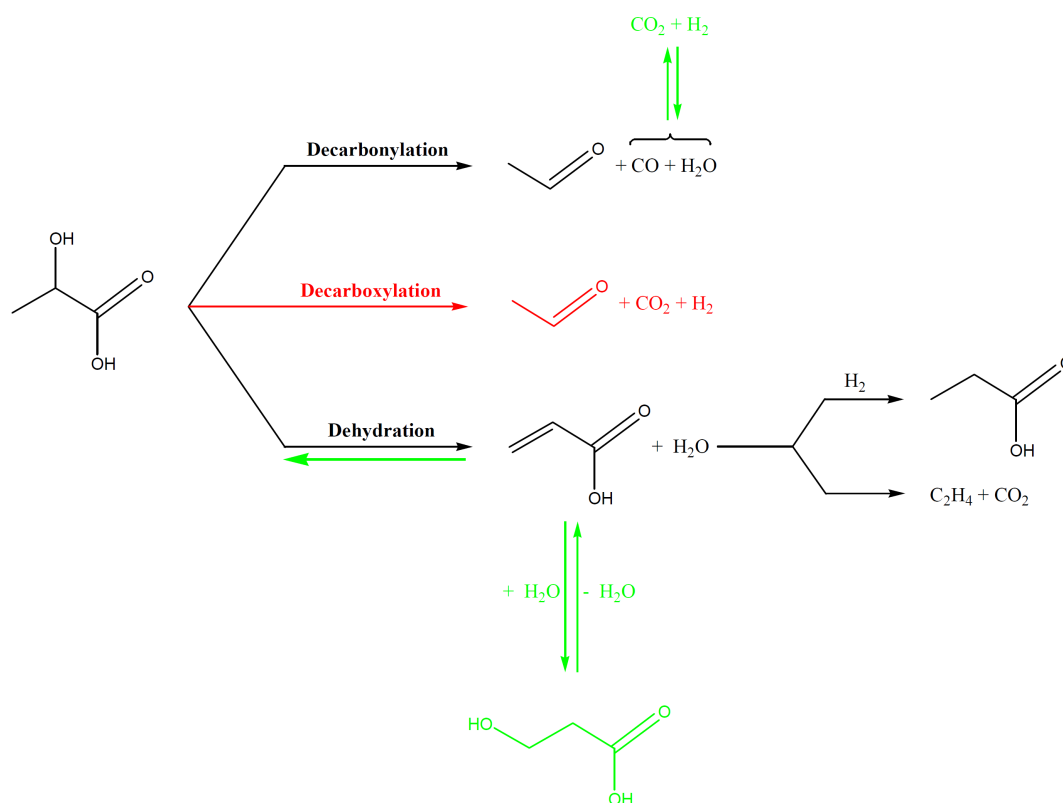


Figure 8-5 Reaction network for the dehydration of lactic acid in near- and supercritical water with emphasis on the results of the present work: with red - the excluded decarboxylation pathway; with green - the reported reactions involving acrylic acid and the formation of carbon dioxide through the water gas shift reaction.

The hydrogenation of acrylic acid has not been studied in this thesis. Decarboxylation of the latter is a side reaction with a low conversion rate and therefore it can not account for the entire quantity of carbon dioxide formed in the reaction. Thus, instead of three pathways governing the decomposition of lactic acid as mentioned in the literature, only two pathways are in fact plausible because of the formation of carbon dioxide from carbon monoxide, as mentioned above.

I have also investigated substances that have similar structure to lactic acid (2-methoxy-propionic acid, methyl lactate, 2-hydroxy-isobutyric acid, 3-hydroxy-propionic acid and 2-hydroxy-3-methylbutyric acid). It has been found that two different mechanisms, a lactonization and E1 elimination are probably responsible for the dehydration of hydroxy-carboxylic acids in supercritical water. E1 should have prevalence in the dehydration of α -hydroxy-carboxylic acids because of the relative stability of the secondary carbocations formed, while lactonization in that of β -hydroxy-carboxylic acids due to a smaller ring strain.

Part of the work to identify the reaction network and develop a kinetic model has been already done. Further work should aim to determine the rate constants within a larger range and smaller increments of the respective parameters which are necessary for an accurate determination of the activation energy and of the activation volume (300 to 420 °C, $\Delta T = 10$ °C, 200 to 500 bar, $\Delta p = 50$ bar and 10 to 500 seconds, $\Delta t = 40$ s). The longer reaction times should be used in future experiments for a more clear view on the equilibrium reactions. Deviations from the model should be ascribed to the neglected reactions which,

therefore, should also be investigated and included in a model describing the experimental data more accurately.

Methacrylic acid which also is an important intermediate in the chemical industry can be produced with high yields from a renewable raw material, 2-hydroxyisobutyric acid in supercritical water. The “renewable”, 3-hydroxypropionic acid can also be used instead of lactic acid as starting material leading to high yields of acrylic acid. The high yields in the dehydration reaction of these hydroxy acids can be well explained by the occurrence of the two different reaction mechanisms mentioned earlier.

For further quantitative and qualitative analyses it would be advisable using simultaneously two tools for the analyses, HPLC-MS and $^1\text{H-NMR}$, especially where overlapping substances impedes an accurate quantification. In this respect, although very difficult and costly, shifting the attention towards online analysis (FTIR or Raman Spectroscopy) would certainly unlock many options for both qualitative and quantitative analysis.

A still promising line is the screening for homogeneous catalysis to improve the productivity of acrylic acid.

A last aspect is heterogeneous catalysis. Two materials, steatite and $\alpha\text{-Al}_2\text{O}_3$ have been studied for their heterogeneous catalytic effect, but no catalytic action thereof has been noticed and it has been found that they are stable in supercritical water for at least several hours. Therefore, materials which can be used as catalyst supports in supercritical water for a longer period of time are available. There is an interesting challenge in searching for materials with catalytic effect in supercritical water. Altogether, since the catalyst has the role of reducing the activation energy, bringing the system to milder reaction conditions where the investigated heterogeneous catalysts are stable are promising ways of efficiently producing acrylic acid by the dehydration of lactic acid or one of its derivatives which could lead to the desired industrial scale application of the reaction in the near future.

9. Bibliography

- And-1993 A. Anderko, K. Pitzer, *Geochim. Cosmochim. Acta.*, **1993**, 57, 1657.
- Arm-1993 F. J. Armellini, J. W. Tester, *Fl. Phase. Equil.*, **1993**, 84, 123.
- Bal-1996 P. B. Balbuena, K. P. Johnston, P. J. Rossky, *J. Phys. Chem.*, **1996**, 100, 2706.
- Bau-1988 H. Baumann, M. Bühler, H. Fochem, F. Hirsinger, H. Zobelein, J. Falbe, *Angew. Chem.* **1988**, 27, 41.
- Bri-1990 D. J. O'Brien, C. C. Panzer, W. P. Eisele, *Biotechnol. Progr.*, **1990**, 6, 237.
- Brö-1999 D. Bröll, C. Kaul, A. Krämer, P. Krammer, T. Richter, M. Jung, H. Vogel, P. Zehner, *Angew. Chem. Int. Ed.*, **1999**, 38, 2998.
- Chi-1999 A. A. Chialvo, P. T. Cummings, J. M. Simonson, R. E. Mesmer, *J. Chem. Phys.*, **1999**, 110, 1064.
- Chi-2000 A. A. Chialvo, P. T. Cummings, J. M. Simonson, *J. Chem. Phys.*, **2000**, 113, 8093.
- Cla-2006 J. H. Clark, V. Budarin, F. E. I. Deswarte, J. J. E. Hardy, F. M. Kerton, A. J. Hunt, R. Luque, D. J. Macquarrie, K. Milkowski, A. Rodriguez, O. Samuel, S. J. Tavener, R. J. White, A. J. Wilson, *Green Chem.*, **2006**, 8, 853.
- Cla-2008 J.H. Clark, F. E. I. Deswarte in *Introduction to Chemicals from Biomass*; John Wiley & Sons, **2008**.
- Cor-2007 A. Corma, S. Iborra, A. Velty, *Chem. Rev.*, **2007**, 107, 2411.
- Cui-1995 S. T. Cui, J. G. Harris, *J. Phys. Chem.*, **1995**, 99, 2900.
- Deb-1989 P. G. Debenedetti, R. S. Mohamed, *J. Chem. Phys.*, **1989**, 90, 4528.
- Dja-2010 E. Djamali, J. W. Cobble, *J. Phys. Chem. B*, **2010**, 114, 3887.
- Fen-2002 J. Feng, S. N. Aki, J. E. Chateaufneuf, J. F. Brennecke, *J. Am. Chem. Soc.*, **2002**, 124, 6304.
- Fla-1989 W. M. Flarsheim, A. J. Bard, K. P. Johnston, *J. Phys. Chem.*, **1989**, 93, 4324.
- Fla-1997 L. W. Flanagan, P. B. Balbuena, K. P. Johnston, P. J. Rossky, *J. Phys. Chem. B*, **1997**, 101, 7998.
- Gal-2007 P. Gallezot, *Green Chem.*, **2007**, 9, 295.
- Gok-2007 R. R. Gokarn, O. V. Selifonova, H. J. Jessen, S. J. Gort, T. Selmer, W. Buckel, **2007**, US. Pat. 7186541.

-
- Gun-1995 G.C. Gunter, R.H. Langford, J.E. Jackson, D.J. Miller, *Ind.Eng.Chem.Res.*, **1995**, 34, 974.
- Har-2004 A. H. Harvey, D. G. Friend in *Aqueous systems at elevated temperatures and pressures*, Elsevier Academic Press **2004**.
- Hel-1987 R. K. Helling, J. W. Tester, *Energy & Fuels*, **1987**, 1, 417.
- Ho-2000 P. C. Ho, D. A. Palmer, R. H. Wood, *J. Phys. Chem. B*, **2000**, 104, 12084.
- Hod-2004 M. Hodes, P. A. Marrone, G. T. Hong, K. A. Smith, J. W. Tester, *J. Supercrit. Fl.*, **2004**, 29, 265.
- Hol-1958 R. E. Holmen, **1958**, US Pat. 2859240.
- Joh-1996 K. P. Johnston, G. E. Bennett, P. B. Balbuena, P. J. Rossky, *J. Am. Chem. Soc.*, **1996**, 118, 6746.
- Joh-2001 R. E. Westacott, K. P. Johnston, P. J. Rossky, *J. Am. Chem. Soc.*, **2001**, 123, 1006.
- Kam-2004 B. Kamm, M. Kamm, *Appl.Microbiol.Biotechnol.* **2004**, 64, 137.
- Kon-2001 S. Koneshan, J.C. Rasaiah, *J.Chem.Phys.* **2001**, 114, 7544.
- Kra-2000 P. Krammer, H. Vogel, *J. Supercrit. Fl.*, **2000**, 16, 189.
- Kri-2004 P. Kritzer, *J. Supercrit. Fl.*, **2004**, 29, 1.
- Laa-2007 D. Laage, J.T. Hynes, *Proc. Natl. Acad. Sci.*, **2007**, 104, 11167.
- Leh-2008 V. Lehr, Ph. D. Thesis, TU Darmstadt **2008**.
- Leu-2010 I. Leusbrock, S. J. Metz, G. Rexwinkel, G. F. Versteeg, *J. Supercrit. Fl.*, **2010**, 54, 1.
- Lic-2010 F. W. Lichtenthaler in *Ullmann's Encyclopedia of industrial chemistry*, Wiley-VCH **2010**
- Lir-1993 C. T. Lira, P. J. McCrackin, *Ind. Eng. Chem. Res.*, **1993**, 322608.
- Lil-2004 M. A. Lilga, T. A. Werpy, J. E. Holladay, 2004,
US Pat. Appl. (2004)00110974
- Luz-1996 A. Luzar, D. Chandler, *Phys. Rev. Lett.*, **1996**, 76, 928.
- Mar-1981 W. L. Marshall, E. U. Franck, *J. Phys. Chem. Ref. Data.*, **1981**, 10, 295.
- Mar-1985 W. L. Marshall, *Pure. Appl. Chem.*, **1985**, 57, 283.
- Mar-2006 Y. Marcus, G. Hefter, *Chem. Rev.*, **2006**, 106, 4585.
- Mat-1997 N. Matubayasi, C. Wakai, M. Nakahara, *J. Chem. Phys.*, **1997**, 107, 9133.

-
- Mes-1974 R. E. Mesmer, C. F. Baes, *J. Sol. Chem.*, **1974**, 3, 307.
- Mes-1988 R.E. Mesmer, W. L. Marshall, D. A. Palmer, J. M. Simonson, H. F. Holmes, *J. Sol. Chem.*, **1988**, 17, 699.
- Mok-1989 W. S. L. Mok, M. J. Antal, M. Jones, *J. Org. Chem.*, **1989**, 54, 4596.
- Ode-1985 B. Odell, G. Earlam, D.J. Cole-Hamilton, *J. Organomet. Chem.*, **1985**, 290, 241.
- Pap-1985 C. Papparizos, W. G. Shaw, S. R. Dolhyj, **1985**, EP 181718.
- Pen-1976 D. Y. Peng, D. B. Robinson, *Ind. Eng. Chem. Fund*, **1976**, 15, 59.
- Pen-2000 J. M. L. Penninger, R. J. A. Kersten, H. C. L. Baur, *J. Supercrit. Fl.*, **2000**, 17, 215.
- Pfu-1994 D. M. Pfund, J. G. Darab, J. L. Fulton, Y. Ma, *J. Phys. Chem.*, **1994**, 98, 13102.
- Ram-1987 S. Ramayya, A. Brittain, C. DeAlmeida, W. S. L. Mok, M. J. Antal, *Fuel*, **1987**, 66, 1364.
- Rat-1945 W. P. Ratchford, C. H. Fisher, *Ind. Eng. Chem.*, **1945**, 37, 382.
- Roh-2010 T. Rohwerder, R. H. Müller, *Microbial Cell Factories*, **2010**, 9:13.
- San-2011 K. Sanderson, *Nature* **2011**, 469, 18.
- Saw-1988 R. A. Sawicki, **1988**, US Pat. 4729972.
- Sco-1970 R. L. Scott, P. H. van Konynenburg, *Disc. Faraday. Soc.*, **1970**, 49, 87.
- Sig-1996 H. Sigman, *Journal of environmental economics management* **1996**, 30, 199.
- Smi-1942 L. T. Smith, C. H. Fisher, W. P. Ratchford, M. L. Fein, *Ind. Eng. Chem.*, **1942**, 34, 473.
- Sou-1962 S. Sourirajan, G. C. Kennedy, *Am. J. Sci.*, **1962**, 260, 115.
- Sue-2003 K. Sue, T. Usami, K. Arai, *J. Chem. Eng. Data*, **2003**, 48, 1081.
- Sue-2004 K. Sue, F. Ouchi, K. Minami, K. Arai, *J. Chem. Eng. Data*, **2004**, 49, 1359.
- Str-2005 A. J. J. Straathof, S. Sie, T. T. Franco, L. A. M. van der Wielen, *Appl. Microbiol. Biotechnol.*, **2005**, 67, 727.
- Tam-1997 M. S. Tam, G. C. Gunter, R. Craciun, D. J. Miller, J. E. Jackson, *Ind. Eng. Chem. Res.*, **1997**, 36, 3505.
- Tre-2004 P. Tremaine, K. Zhang, P. Bénézech, C. Xiao in *Aqueous systems at elevated temperatures and pressures*, Elsevier Academic Press **2004**.

-
- Tuc-1998 S. C. Tucker, M. W. Maddox, *J. Phys. Chem. B*, **1998**, 102, 2437.
- Val-2004 V. M. Valyashko in *Aqueous systems at elevated temperatures and pressures*, Elsevier Academic Press **2004**.
- Wad-1997 D. C. Wadley, M. S. Tam, P. B. Kokitkar, J. E. Jackson, D. J. Miller, *Journal of catalysis*, **1997**, 165, 162.
- Wag-2000 W. Wagner, A. Pruß, *J. Phys. Chem. Ref. Data*, **2000**, 31, 387.
- Wal-1991 P. C. Walkup, C. A. Rohrmann, R. T. Hallen, D. E. Eakin, **1991**, US Pat. 5071754.
- Was-2004 K. L. Wasewar, A. A. Yawalkar, J. A. Moulijn, V. G. Pangarkar, *Ind. Eng. Chem. Res.*, **2004**, 43, 5969.
- Wei-2005 H. Weingärtner, E. U. Franck, *Angew. Chem. Int. Ed.*, **2005**, 44, 2672.
- Wes-2001 R. E. Westacott, K. P. Johnston, P. J. Rossky, *J. Phys. Chem. B*, **2001**, 105, 6611.
- Xia-1997 T. Xiang, K. P. Johnston, *J. Sol. Chem.*, **1997**, 26, 13.
- Xu -1990 X. Xu, C.P. DeAlmeida, M.J. Antal, *J. Supercrit. Fluids* 3(4) (**1990**) 228-232
- Yag-2005 T. Yagasaki, K. Iwahashi, S. Saito, I. Ohmine, *J. Chem. Phys.*, 2005, 122, 144504.

10. Appendix

Commonly used abbreviations

Notation	Meaning	Units
AcOH	acetic acid	
Acr	acrylic acid	
Ald	acetaldehyde	
c_i	concentration of compound i	mol l^{-1}
Conc.	concentration	%
Conv.	conversion	%
CSTR	continuously stirred tank reactor	
Mba	3-methyl-2-butenoic acid	
$^1\text{H-NMR}$	proton nuclear magnetic resonance	
FTIR	Fourier Transform Infrared	
Hba	2-hydroxy-isobutyric acid	
Hmb	2-hydroxy-3-methylbutyric acid	
Hpa	3-hydroxypropionic acid	
HPLC	high performance liquid chromatography	
Lac	lactic acid	
LacMe	methyl lactate	
M	molar concentration	mol l^{-1}
Maa	methacrylic acid	
m.v.	mean value	
n_i	number of moles of i	mol
ppm	parts per million	g g^{-1}
p	pressure	
R.t.	residence/reaction time	
Sel.	selectivity	%
SCW	supercritical water	
t	reaction time/residence time	s, h
T	temperature	K
UV/VIS	ultra-violet/ visible	
Y.	yield	

Estimation of the errors from the HPLC analyses

Overlapping of the peaks in the chromatograms is a source of errors in the calculation of the concentration of the analyzed substances. The use of different graphical integration methods for calculating peak areas lead to different results for the concentrations of the substances. The basic methods used are represented in Figure 10-1.

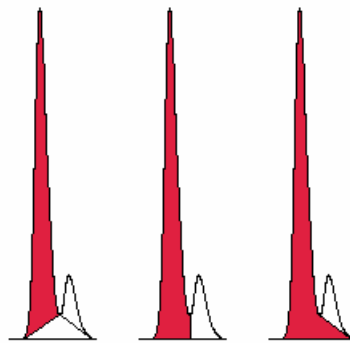


Figure 10-1 Different methods used for the graphical integration of overlapping peaks for the calculation of the concentration of the respective substances.

The overlapping in analyses always had a similar configuration to that seen in Figure 10-1 and involved a large peak preceded by a relatively small one. The area corresponding to the real concentration at least in the case of the larger peak should be in a range limited by the smallest and largest areas marked with red on Figure 10-1.

The results of the graphical integration using the methods mentioned in Figure 10-1 from experiments carried out at 385 °C are given in Table 10-1. The variance for samples (s^2) is calculated using (10-1). At 0 seconds residence time the concentration of lactic acid is that of the feed. It was set at 0.1 mol l⁻¹ and was considered free of graphical integration errors since no overlapping was present in the analysis of the pure lactic acid solution.

$$s^2 = \frac{1}{n-1} \sum_{i=1}^n (x_i - \bar{x})^2 \quad (10-1)$$

with the mean value $\bar{x} = \frac{\sum_{i=1}^n x_i}{n}$. The methods represented in Figure 10-1 yield area intervals that include the value corresponding to the real concentration, at least in the case of the first peak which in all encountered overlapping cases is the larger.

Table 10-1 Graphical integration of data at 385 °C and residence times between 0 and 300 s.

Feed: Lactic acid 0.1 mol l ⁻¹ ; Pressure: 350 bar; Temperature: 385 °C									
R.t.	Conc. Lac	Conc. Acr	Conc. Ald	Conc. Lac	Conc. Acr	Conc. Ald	S ² _{Lac}	S ² _{Acr}	S ² _{Ald}
/s	/mol l ⁻¹	/mol l ⁻¹	/mol l ⁻¹	m.v.	m.v.	m.v.			
0	0	0	0.1	0.1	0	0	0	0	0
16	0.08398	0.00755	0.00922	0.083988	0.007533	0.008483	1.32E-07	1.083E-08	6.231E-07
	0.08359	0.00739	0.0078						
	0.08447	0.00764	0.0078						
	0.08391	0.00755	0.00911						
32	0.07149	0.01259	0.01507	0.0715925	0.012328	0.013958	1.38E-07	5.063E-08	5.504E-07
	0.07113	0.01234	0.01356						
	0.072	0.01234	0.0136						
	0.07175	0.01204	0.0136						
65	0.05391	0.01929	0.0237	0.05371	0.019263	0.022383	4.35E-08	8.502E-08	1.298E-06
	0.05387	0.01929	0.02297						
	0.05353	0.01888	0.02143						
	0.05353	0.01959	0.02143						
100	0.04535	0.02192	0.02739	0.04542	0.021895	0.026038	1.89E-07	1.075E-07	1.167E-06
	0.0453	0.02192	0.02637						
	0.045	0.02147	0.02493						
	0.04603	0.02227	0.02546						
200	0.02829	0.02453	0.03191	0.028168	0.024503	0.030468	4.5E-08	1.71E-07	4.814E-06
	0.02826	0.02453	0.03273						
	0.02785	0.02397	0.02905						
	0.02827	0.02498	0.02818						
300	0.02129	0.02207	0.03174	0.021205	0.022153	0.030843	3.75E-08	2.225E-07	7.936E-07
	0.02092	0.02152	0.02961						
	0.02135	0.02256	0.03101						
	0.02126	0.02246	0.03101						

The errors from quantifying the concentrations also influence indirect quantities such as selectivities. For estimating the indirect errors arising from this propagation of errors, a deviation of 2 s (two times the standard deviation of the mean) from the mean will be considered. A confidence interval of ± 2 s gives a level of certainty of 95 % for a normal distribution for the errors.

The mean selectivities towards products determined from the graphical integration can be written as:

$$\overline{\text{Sel}}_{\text{Acr}} = \frac{\overline{C}_{\text{Acr}}}{C_{0,\text{Lac}} - C_{\text{Lac}}} \cdot 100 \quad (10-2)$$

$$\overline{\text{Sel}}_{\text{Ald}} = \frac{\overline{C}_{\text{Ald}}}{C_{0,\text{Lac}} - C_{\text{Lac}}} \cdot 100 \quad (10-3)$$

\bar{C}_{Acr}	mean concentration of acetaldehyde /mol l ⁻¹
\bar{C}_{Ald}	mean concentration of acetaldehyde /mol l ⁻¹
\bar{C}_{Lac}	mean concentration of lactic acid /mol l ⁻¹
$C_{0,Lac}$	initial concentration of lactic acid /mol l ⁻¹

The mean values of the concentrations of lactic acid, acrylic acid and acetaldehyde are subject to errors from graphical integration. For the initial concentration of lactic acid, these errors are negligible. Thus, the two selectivities can be written as functions of \bar{C}_{Acr} , \bar{C}_{Ald} and \bar{C}_{Lac} :

$$\bar{Sel}_{Acr} = f_1(\bar{C}_{Acr}, \bar{C}_{Lac}) \quad (10-4)$$

$$\bar{Sel}_{Ald} = f_2(\bar{C}_{Ald}, \bar{C}_{Lac}) \quad (10-5)$$

For each substance an error is set in accordance with the 95 % level of certainty:

$$\varepsilon_{Acr} = 2s_{Acr} \quad (10-6)$$

$$\varepsilon_{Ald} = 2s_{Ald} \quad (10-7)$$

$$\varepsilon_{Lac} = 2s_{Lac} \quad (10-8)$$

with s_{Acr} , s_{Ald} , s_{Lac} the standard deviations from the mean of the respective substances.

The functions defined in (10-4) and (10-5) can be expanded through Talyor series around the points $(\bar{C}_{Acr}, \bar{C}_{Lac})$ and $(\bar{C}_{Ald}, \bar{C}_{Lac})$ using (10-6) to (10-8) in the following manner:

$$f_1(\bar{C}_{Acr} + \varepsilon_{Acr}, \bar{C}_{Lac} + \varepsilon_{Lac}) = f_1(\bar{C}_{Acr}, \bar{C}_{Lac}) + \sum_{p=0}^{\infty} \sum_{q=0}^{\infty} \frac{\varepsilon_{Acr}^p \varepsilon_{Lac}^q}{p!q!} \cdot \frac{\partial^{p+q}}{\partial \bar{C}_{Acr}^p \partial \bar{C}_{Lac}^q} f_1(\bar{C}_{Acr}, \bar{C}_{Lac}) \quad (10-9)$$

$$f_2(\bar{C}_{Ald} + \varepsilon_{Ald}, \bar{C}_{Lac} + \varepsilon_{Lac}) = f_2(\bar{C}_{Ald}, \bar{C}_{Lac}) + \sum_{p=0}^{\infty} \sum_{q=0}^{\infty} \frac{\varepsilon_{Ald}^p \varepsilon_{Lac}^q}{p!q!} \cdot \frac{\partial^{p+q}}{\partial \bar{C}_{Ald}^p \partial \bar{C}_{Lac}^q} f_2(\bar{C}_{Ald}, \bar{C}_{Lac}) \quad (10-10)$$

For the purposes concerning the errors, the expansions can be limited to first order derivatives and first degree terms for the errors (provided that the errors are sufficiently small):

$$f_1(\bar{C}_{Acr} + \varepsilon_{Acr}, \bar{C}_{Lac} + \varepsilon_{Lac}) = f_1(\bar{C}_{Acr}, \bar{C}_{Lac}) + \varepsilon_{Acr} \frac{\partial f_1}{\partial \bar{C}_{Acr}} + \varepsilon_{Lac} \frac{\partial f_1}{\partial \bar{C}_{Lac}} \quad (10-11)$$

$$f_2(\bar{C}_{Ald} + \varepsilon_{Ald}, \bar{C}_{Lac} + \varepsilon_{Lac}) = f_2(\bar{C}_{Ald}, \bar{C}_{Lac}) + \varepsilon_{Ald} \frac{\partial f_2}{\partial \bar{C}_{Ald}} + \varepsilon_{Lac} \frac{\partial f_2}{\partial \bar{C}_{Lac}} \quad (10-12)$$

By derivating using (10-2) and (10-3) and regrouping:

$$f_1(\bar{C}_{Acr} + \varepsilon_{Acr}, \bar{C}_{Lac} + \varepsilon_{Lac}) - f_1(\bar{C}_{Acr}, \bar{C}_{Lac}) = \frac{\varepsilon_{Acr}}{C_{0,Lac} - C_{Lac}} + \frac{\bar{C}_{Acr} \cdot \varepsilon_{Lac}}{(C_{0,Lac} - C_{Lac})^2} \quad (10-13)$$

$$f_2(\bar{C}_{Ald} + \varepsilon_{Ald}, \bar{C}_{Lac} + \varepsilon_{Lac}) - f_2(\bar{C}_{Ald}, \bar{C}_{Lac}) = \frac{\varepsilon_{Ald}}{C_{0,Lac} - C_{Lac}} + \frac{\bar{C}_{Ald} \cdot \varepsilon_{Lac}}{(C_{0,Lac} - C_{Lac})^2} \quad (10-14)$$

One can define $\varepsilon_{\overline{Sel}_{Acr}}$ and $\varepsilon_{\overline{Sel}_{Ald}}$ as:

$$\varepsilon_{\overline{Sel}_{Acr}} = f_1(\bar{C}_{Acr} + \varepsilon_{Acr}, \bar{C}_{Lac} + \varepsilon_{Lac}) - f_1(\bar{C}_{Acr}, \bar{C}_{Lac}) = \frac{\varepsilon_{Acr}}{C_{0,Lac} - C_{Lac}} + \frac{\bar{C}_{Acr} \cdot \varepsilon_{Lac}}{(C_{0,Lac} - C_{Lac})^2} \quad (10-15)$$

$$\varepsilon_{\overline{Sel}_{Ald}} = f_2(\bar{C}_{Ald} + \varepsilon_{Ald}, \bar{C}_{Lac} + \varepsilon_{Lac}) - f_2(\bar{C}_{Ald}, \bar{C}_{Lac}) = \frac{\varepsilon_{Ald}}{C_{0,Lac} - C_{Lac}} + \frac{\bar{C}_{Ald} \cdot \varepsilon_{Lac}}{(C_{0,Lac} - C_{Lac})^2} \quad (10-16)$$

By replacing the errors from (10-6) to (10-8) one obtains:

$$\varepsilon_{\overline{Sel}_{Acr}} = \frac{2s_{Acr}}{C_{0,Lac} - C_{Lac}} + \frac{\bar{C}_{Acr} \cdot 2s_{Lac}}{(C_{0,Lac} - C_{Lac})^2} \quad (10-17)$$

$$\varepsilon_{\overline{Sel}_{Ald}} = \frac{2s_{Ald}}{C_{0,Lac} - C_{Lac}} + \frac{\bar{C}_{Ald} \cdot 2s_{Lac}}{(C_{0,Lac} - C_{Lac})^2} \quad (10-18)$$

Thus, an estimate for the errors of selectivities has been obtained based on the mean concentrations and errors of lactic acid, acrylic acid and acetaldehyde. The respective results are to be found in Table 10-2.

Table 10-2 Estimation of errors for selectivities at 385 °C, 350 bars, residence times from 16 to 300 seconds and 0.1 M lactic acid feed.

R.t. / s	ε_{Acr} /%	ε_{Ald} /%	ε_{Lac} /%	\overline{Sel}_{Acr} /%	\overline{Sel}_{Ald} /%	$\varepsilon_{\overline{Sel}_{Acr}}$ /%	$\varepsilon_{\overline{Sel}_{Ald}}$ /%
16	2.76	18.61	0.87	47 ±7	53 ±23	7.31	23.15
32	3.65	10.63	1.04	43 ±6	49 ±13	6.27	13.25
65	3.03	10.18	0.78	42 ±4	48 ±11	3.93	11.08
100	2.99	8.30	1.92	40 ±5	48 ±10	4.59	9.89
200	3.38	14.40	1.51	34 ±4	42 ±15	3.97	14.99
300	4.26	5.78	1.83	28 ±5	39 ±6	4.75	6.27

Results

Influence of the residence time (reaction time)

Feed: Lactic acid 0.1 mol l ⁻¹ ; Pressure: 350 bar										
T /°C	R.t. /s	Conv. /%	Conc. Lac /mol l ⁻¹	Conc. Ald /mol l ⁻¹	Sel. Ald /%	Y. Ald /%	Conc. Acr /mol l ⁻¹	Sel. Acr /%	Y. Acr /%	
350	18.0	4.17	0.0964	0.0025	59.19	2.47	0.0021	49.58	2.07	
	32.2	7.53	0.0930	0.0042	55.05	4.15	0.0039	51.21	3.86	
	50.0	12.64	0.0879	0.0074	58.40	7.38	0.0058	45.27	5.72	
	65.3	15.00	0.0855	0.0086	56.92	8.54	0.0073	48.59	7.29	
	100.1	22.35	0.0781	0.0116	51.55	11.52	0.0112	49.76	11.12	
	101.2	23.76	0.0767	0.0124	51.85	12.32	0.0105	43.87	10.42	
	150.8	30.00	0.0704	0.0150	49.85	14.95	0.0126	41.86	12.56	
	190.5	33.11	0.0673	0.0140	42.09	13.93	0.0160	48.17	15.95	
	253.5	40.02	0.0603	0.0198	49.24	19.71	0.0158	39.30	15.73	
	305.7	40.90	0.0595	0.0168	40.85	16.71	0.0189	45.87	18.76	
	506.9	50.99	0.0459	0.0204	42.86	21.85	0.0205	42.96	21.91	
	936.5	64.25	0.0358	0.0186	28.95	18.60	0.0204	31.66	20.34	
385	16.6	15.92	0.0840	0.0085	53.33	8.49	0.0075	47.36	7.54	
	20.2	23.06	0.0775	0.0118	50.65	11.68	0.0090	38.92	8.98	
	31.9	28.33	0.0716	0.0140	49.32	13.97	0.0126	44.51	12.61	
	64.6	46.23	0.0537	0.0224	48.46	22.41	0.0194	42.09	19.46	
	83.0	52.12	0.0482	0.0252	47.97	25.01	0.0191	36.37	18.96	
	98.7	54.61	0.0453	0.0260	47.73	26.07	0.0219	40.18	21.94	
	151.4	67.96	0.0323	0.0323	47.12	32.03	0.0217	31.68	21.53	
	192.0	71.67	0.0283	0.0305	42.56	30.50	0.0245	34.28	24.57	
	251.4	77.76	0.0224	0.0326	41.67	32.41	0.0209	26.70	20.76	
	307.0	78.70	0.0213	0.0308	39.23	30.88	0.0221	28.08	22.10	
420	16.1	45.75	0.0546	0.0319	69.32	31.71	0.0099	21.48	9.82	
	32.1	59.98	0.0370	0.0438	78.95	47.35	0.0121	21.77	13.06	
	51.0	71.54	0.0263	0.0511	77.25	55.26	0.0116	17.51	12.53	
	64.2	78.10	0.0203	0.0526	72.78	56.84	0.0130	17.95	14.02	
	101.2	82.05	0.0166	0.0530	69.75	57.23	0.0164	21.57	17.70	
	101.8	89.20	0.0100	0.0512	62.07	55.36	0.0116	14.02	12.50	
	179.4	95.74	0.0039	0.0515	58.09	55.62	0.0091	10.30	9.86	
	205.0	94.15	0.0054	0.0568	65.16	61.34	0.0112	12.87	12.11	
	245.3	94.24	0.0053	0.0571	65.44	61.67	0.0117	13.42	12.65	
	320.7	97.19	0.0026	0.0526	58.52	56.88	0.0078	8.72	8.47	

Aging of a new pipe reactor

Feed: Lactic acid 0.1 mol l ⁻¹ ; Pressure: 350 bar; Temperature: 385 °C; Residence time: 100 seconds								
Aging time /hours	Conv. /%	Conc. Lac /mol l ⁻¹	Conc. Ald /mol l ⁻¹	Sel. Ald /%	Y. Ald /%	Conc. Acr /mol l ⁻¹	Sel. Acr /%	Y. Acr /%
1.5	74.64	0.0284	0.0310	37.08	27.68	0.0449	53.67	40.06
3.8	74.22	0.0289	0.0324	38.97	28.92	0.0458	55.06	40.87
17.3	74.44	0.0286	0.0335	40.12	29.87	0.0465	55.83	41.56
23.1	73.46	0.0297	0.0341	41.41	30.42	0.0462	56.14	41.25
24.6	73.39	0.0298	0.0332	40.38	29.64	0.0461	56.05	41.13
27.6	73.54	0.0296	0.0343	41.60	30.60	0.0463	56.23	41.35

Influence of the concentration

Pressure: 350 bar; Temperature: 385 °C; Residence time: 100 seconds; Feed: Lactic acid								
Feed Conc. /mol l ⁻¹	Conv. /%	Conc. Lac /mol l ⁻¹	Conc. Ald /mol l ⁻¹	Sel. Ald /%	Y. Ald /%	Conc. Acr /mol l ⁻¹	Sel. Acr /%	Y. Acr /%
0.0678	58.00	0.0285	0.0183	46.61	27.03	0.0151	38.32	22.22
0.0720	55.73	0.0337	0.0207	54.08	28.75	0.0149	38.84	20.65
0.0843	52.08	0.0404	0.0228	-	27.00	0.0292	-	34.69
1.0079	82.29	0.0431	0.0278	48.24	27.63	0.0147	25.43	14.57
0.1011	59.54	0.0409	0.0302	50.09	29.82	0.0302	50.09	29.82
0.1330	58.93	0.0546	0.0360	45.87	27.03	0.0292	37.30	21.98
0.1794	69.66	0.0420	0.0272	-	37.93	0.0184	-	25.68
0.2077	61.21	0.0403	0.0297	46.68	28.58	0.0296	46.53	28.48
0.2084	58.20	0.0436	0.0282	-	33.46	0.0315	-	30.23
0.2200	59.55	0.0445	0.0265	40.47	24.10	0.0219	33.49	19.94
0.3038	61.52	0.0390	0.0288	46.29	28.48	0.0287	46.09	28.36
0.4123	62.60	0.0386	0.0329	50.97	31.91	0.0273	42.34	26.50
0.4178	60.33	0.0504	0.0337	-	40.37	0.0195	-	23.29
0.4368	61.43	0.0421	0.0275	41.01	25.19	0.0181	27.01	16.59
0.5250	63.39	0.0384	0.0339	50.86	32.24	0.0273	41.00	25.99
0.6499	81.76	0.0296	0.0254	46.41	30.09	0.0221	16.65	13.61
1.0010	59.01	0.0410	0.0281	47.59	28.08	0.0145	24.55	14.49

Influence of the pressure

Feed: Lactic acid 0.1 mol/l; Temperature: 385 °C									
R.t. /s	p /bar	Conv. /%	Conc. Lac /mol l ⁻¹	Conc. Ald /mol l ⁻¹	Sel. Ald /%	Y. Ald /%	Conc. Acr /mol l ⁻¹	Sel. Acr /%	Y. Acr /%
156.6	118	82.29	0.0177	0.0262	31.97	26.31	0.0009	1.13	0.93
83.7	150	60.33	0.0396	0.0226	37.64	22.71	0.0008	1.26	0.76
98.2	200	69.66	0.0303	0.0267	38.47	26.80	0.0021	3.04	2.12
105.6	250	55.73	0.0441	0.0244	43.93	24.48	0.0044	7.95	4.43
100.3	300	59.99	0.0399	0.0261	43.67	26.20	0.0142	23.72	14.23
101.2	350	61.54	0.0383	0.0259	42.20	25.97	0.0176	28.75	17.69

Influence of the temperature

Feed: Lactic acid 0.1 mol l ⁻¹ ; Pressure: 350 bar; Residence time: 100 seconds								
T /°C	Conv. /%	Conc. Lac /mol l ⁻¹	Conc. Ald /mol l ⁻¹	Sel. Ald /%	Y. Ald /%	Conc. Acr /mol l ⁻¹	Sel. Acr /%	Y. Acr /%
150	0.31	0.0987	0	0	0	0	0	0
200	0.12	0.0989	0	0	0	0	0	0
250	0	0.0990	0	-	0	0	-	0
300	1.47	0.0975	0.0016	112.53	1.66	0.0010	67.39	0.99
350	22.05	0.0772	0.0134	61.26	13.51	0.0101	46.32	10.22

Screening for catalyst

Feed: Lactic acid 0.1 mol l ⁻¹ ; Pressure: 350 bar									
Catalyst	R.t. /s	Conv. /%	Conc. Lac /mol l ⁻¹	Conc. Ald /mol l ⁻¹	Sel. Ald /%	Y. Ald /%	Conc. Acr /mol l ⁻¹	Sel. Acr /%	Y. Acr /%
-	50.4	36.54	0.0765	0.0211	47.82	17.47	0.0230	52.16	19.06
	102.0	61.52	0.0464	0.0348	46.99	28.91	0.0354	47.71	29.35
	204.0	85.41	0.0176	0.0424	41.20	35.19	0.0389	37.79	32.28
MgSO ₄ 200 ppm	49.7	35.83	0.0680	0.0182	47.84	17.14	0.0194	51.11	18.31
	99.8	66.00	0.0360	0.0296	42.25	27.88	0.0283	40.48	26.71
	214.8	91.98	0.0085	0.0433	44.46	40.89	0.0304	31.22	28.71
MgSO ₄ 800 ppm	50.4	37.74	0.0660	0.0208	51.93	19.60	0.0199	49.66	18.74
	99.5	62.28	0.0400	0.0325	49.16	30.62	0.0311	47.13	29.35
	207.7	87.80	0.0129	0.0422	45.35	39.82	0.0342	36.72	32.24
ZnSO ₄ 200 ppm	49.6	32.98	0.0710	0.0235	67.31	22.20	0.0140	39.91	13.16
	97.8	72.27	0.0294	0.0454	59.21	42.79	0.0292	38.06	27.51
	202.1	91.30	0.0092	0.0615	63.52	57.99	0.0332	34.28	31.30
ZnSO ₄ 800 ppm	50.8	44.92	0.0593	0.0318	65.69	29.51	0.0173	35.72	16.04
	100.0	83.39	0.0179	0.0603	67.18	56.02	0.0226	25.20	21.01
	203.7	96.82	0.0034	0.0681	65.30	63.22	0.0219	21.02	20.36
	510.6	99.05	0.0010	0.0697	65.38	64.76	0.0128	12.01	11.90
KHCO ₃ 200 ppm	50.4	52.18	0.0513	0.0174	31.02	16.19	0.0154	27.46	14.33
	100.2	75.69	0.0261	0.0262	32.19	24.36	0.0239	29.40	22.25
	203.7	93.66	0.0068	0.0321	31.96	29.93	0.0239	23.75	22.24
Na ₂ SO ₄ 1000 ppm	50.4	27.47	0.0860	0.0122	37.41	10.28	0.0223	68.43	18.80
	100.8	50.45	0.0588	0.0197	32.89	16.59	0.0349	58.25	29.39
	201.3	75.52	0.0290	0.0299	33.35	25.19	0.0372	41.54	31.37
K ₂ HPO ₄ 3000 ppm	34.8	25.30	0.0792	0.0092	34.29	8.68	0.0178	66.35	16.79
	99.7	45.04	0.0583	0.0130	27.33	12.31	0.0271	56.72	25.55
	210.5	68.58	0.0333	0.0208	28.59	19.60	0.0262	35.99	24.68
K ₂ HPO ₄ 5000 ppm	49.5	23.38	0.0825	0.0080	31.64	7.40	0.0157	62.32	14.57
	101.1	42.82	0.0616	0.0113	24.55	10.51	0.0226	49.03	21.00
	203.7	65.39	0.0373	0.0209	29.70	19.42	0.0184	26.18	17.12
	431.4	85.52	0.0156	0.0237	25.70	21.97	0.0030	3.28	2.80

Feed: Lactic acid 0.1 mol l ⁻¹ ; Pressure: 350 bar; Temperature: 385 °C									
Catalyst	R.t. /s	Conv. /%	Conc. Lac /mol l ⁻¹	Conc. Ald /mol l ⁻¹	Sel. Ald /%	Y. Ald /%	Conc. Acr /mol l ⁻¹	Sel. Acr /%	Y. Acr /%
-	50.4	46.07	0.0534	0.0354	77.69	35.79	0.0142	31.23	14.39
	103.2	63.19	0.0364	0.0469	75.03	47.41	0.0168	26.82	16.95
	247.2	84.26	0.0156	0.0678	81.25	68.46	0.0156	18.74	15.79
MgSO ₄ 1000 ppm	50.5	38.78	0.0606	0.0390	-	39.44	0.0142	37.09	14.39
	100.7	59.99	0.0396	0.0719	-	72.58	0.0193	32.43	19.45
	254.4	81.62	0.0182	0.1035	-	104.56	0.0208	25.76	21.02
Na ₂ SO ₄ 1500 ppm	51.9	29.91	0.0690	0.0151	51.36	15.36	0.0153	51.99	15.55
	100.6	50.75	0.0485	0.0229	45.78	23.24	0.0170	34.06	17.29
	203.0	67.83	0.0317	0.0353	52.86	35.85	0.0149	22.27	15.10

Various phosphate catalysts

Feed: Lactic acid 0.1 mol l ⁻¹ ; Pressure: 350 bar; Residence time: 100 seconds									
Catalyst	Conv. /%	Conc. Lac /mol l ⁻¹	Conc. Ald /mol l ⁻¹	Sel. Ald /%	Y. Ald /%	Conc. Acr /mol l ⁻¹	Sel. Acr /%	Y. Acr /%	
-	56.72	0.0427	0.0287	51.26	29.07	0.0230	41.11	23.32	
K ₂ HPO ₄ 1000 ppm	46.10	0.0531	0.0180	39.59	18.25	0.0206	45.41	20.93	
KH ₂ PO ₄ 1000 ppm	47.33	0.0519	0.0193	41.42	19.61	0.0229	49.10	23.24	
Cs ₂ HPO ₄ 1000 ppm	46.24	0.0530	0.0181	39.65	18.33	0.0208	45.67	21.12	
CsH ₂ PO ₄ 1000 ppm	47.71	0.0515	0.0193	41.15	19.63	0.0223	47.38	22.61	

Titration of KOH and CsOH with phosphoric acid

Feed: Lactic acid 0.1 mol l ⁻¹ + 1500 ppm KOH; Pressure: 350 bar; Temperature: 385 °C; Residence time: 100 seconds									
A = _m H ₃ PO ₄ /C _m KOH	Conv. /%	Conc. Lac /mol l ⁻¹	Conc. Ald /mol l ⁻¹	Sel. Ald /%	Y. Ald /%	Conc. Acr /mol l ⁻¹	Sel. Acr /%	Y. Acr /%	
0	48.11	0.0502	0.0169	36.40	17.51	0.0137	29.33	14.11	
0.0001	49.20	0.0492	0.0189	39.67	19.52	0.0159	33.33	16.40	
0.001	43.00	0.0552	0.0156	37.49	16.12	0.0169	40.64	17.47	
0.01	43.04	0.0551	0.0155	37.31	16.06	0.0169	40.64	17.49	
0.1	38.82	0.0592	0.0119	31.77	12.33	0.0182	48.56	18.85	
0.33	43.86	0.0543	0.0148	34.98	15.34	0.0211	49.63	21.77	
0.66	47.36	0.0509	0.0146	31.96	15.14	0.0233	50.88	24.10	
1	50.47	0.0479	0.0167	34.11	17.22	0.0240	49.21	24.84	
2	57.41	0.0412	0.0213	38.39	22.04	0.0232	41.69	23.94	

Feed: Lactic acid 0.1 mol l ⁻¹ +1500 ppm CsOH; Pressure: 350 bar; Temperature: 385 °C; Residence time: 100 seconds								
A = C _m H ₃ PO ₄ /C _m CsOH	Conv. (%)	Conc. Lac (mol/l)	Conc. Ald mol/l)	Sel. Ald (%)	Y. Ald (%)	Conc. Acr (mol/l)	Sel. Acr (mol/l)	Y. Acr (%)
0	51.47	0.0486	0.0190	36.87	18.97	0.0157	30.49	15.69
0.000145	51.12	0.0490	0.0191	37.29	19.06	0.0163	31.82	16.27
0.10015	44.34	0.0558	0.0138	31.04	13.77	0.0196	44.18	19.59
1.065	47.44	0.0527	0.0175	36.88	17.50	0.0222	46.72	22.17

Variation of KH₂PO₄ concentration

Feed: Lactic acid 0.1 mol l ⁻¹ ; Pressure: 350 bar									
KH ₂ PO ₄ Conc. /ppm	T /°C	Conv. /%	Conc. Lac /mol l ⁻¹	Conc. Ald /mol l ⁻¹	Sel. Ald /%	Y. Ald /%	Conc. Acr /mol l ⁻¹	Sel. Acr /%	Y. Acr /%
0	350	23.77	0.0759	0.0129	54.55	12.97	0.0110	46.56	11.07
50	350	20.01	0.0797	0.0107	53.45	10.70	0.0108	54.35	10.88
200	350	18.89	0.0808	0.0122	-	12.30	0.0114	-	11.41
1000	350	15.76	0.0839	0.0059	37.49	5.91	0.0101	64.15	10.11
2000	350	16.36	0.0833	0.0057	34.90	5.71	0.0103	63.45	10.38
0	385	56.36	0.0435	0.0296	52.70	29.70	0.0239	42.53	23.97
50	385	51.64	0.0482	0.0230	44.63	23.05	0.0258	50.16	25.90
200	385	49.29	0.0505	0.0206	42.00	20.70	0.0245	49.88	24.59
1000	385	47.03	0.0528	0.0199	42.40	19.94	0.0225	48.05	22.60
2000	385	47.13	0.0527	0.0194	41.43	19.53	0.0215	45.78	21.58
0	420	85.16	0.0148	0.0588	69.27	58.99	0.0154	18.19	15.49
50	420	82.82	0.0171	0.0574	69.62	57.66	0.0166	20.11	16.66
200	420	81.63	0.0183	0.0561	69.04	56.36	0.0156	19.17	15.65
1000	420	83.21	0.0167	0.0563	67.94	56.53	0.0146	17.60	14.64
2000	420	83.21	0.0167	0.0545	65.73	54.69	0.0142	17.11	14.23

Stability of acrylic acid

Variation of temperature and residence time

Feed: Acrylic acid 0.05 mol l ⁻¹ ; Pressure: 350 bar				
R.t. /s	T /°C	Conv. /%	Conc. Acr /mol l ⁻¹	Conc. Lac+Hpa* /mol l ⁻¹
100.2	350	15.91	0.0422	0.0043
153.7	350	19.11	0.0406	0.0048
206.2	350	22.61	0.0388	0.0052
304.2	350	28.22	0.0360	0.0057
50.2	385	15.33	0.0425	0.0029
101.3	385	20.92	0.0397	0.0034
149.9	385	26.68	0.0368	0.0036
199.4	385	33.00	0.0336	0.0036
320.9	385	38.77	0.0307	0.0035
22.6	420	15.66	0.0423	0.0036
50.0	420	21.99	0.0391	0.0037
105.6	420	28.09	0.0361	0.0032
160.9	420	33.99	0.0331	0.0025
219.4	420	38.74	0.0307	0.0023
344.7	420	47.09	0.0265	0.0020

* quantification using the same response factor for lactic acid and 3-hydroxypropionic acid

Influence of KH₂PO₄

Feed: Acrylic acid 0.1 mol l ⁻¹ ; Pressure: 350 bar; Temperature: 385 °C						
Catalyst	R.t. /s	Conc. Lac+Hpa* /mol l ⁻¹	Conv. /%	Conc. Acr /mol l ⁻¹	Sel. Lac /%	Y. Lac /%
KH ₂ PO ₄ 5000 pppm	49.2	0.0092	41.43	0.0728	13.64	6.54
	100.7	0.0059	67.43	0.0397	5.84	4.18
	148.7	0.0039	80.25	0.0237	3.37	2.80
	203.3	0.0029	86.76	0.0156	2.33	2.07
-	100.5	0.0093	19.17	0.0998	26.46	6.90

* quantification using the same response factor for lactic acid and 3-hydroxypropionic acid

Feed: Acrylic acid 0.05 mol l ⁻¹ ; Pressure: 350 bar; 200 ppm KH ₂ PO ₄				
R.t. /s	T /°C	Conv /%	Conc. Acr /mol l ⁻¹	Conc. Lac+Hpa* /mol l ⁻¹
20.5	350	8.65	0.0459	0.0030
40.9	350	15.06	0.0427	0.0042
80.4	350	25.18	0.0376	0.0051
150.8	350	28.09	0.0362	0.0065
201.7	350	30.20	0.0351	0.0069
508.4	350	47.37	0.0265	0.0069
25.6	385	16.22	0.0421	0.0037
38.9	385	20.93	0.0398	0.0042
103.2	385	32.70	0.0338	0.0046
156.0	385	37.19	0.0316	0.0045
204.2	385	43.45	0.0284	0.0044
365.2	385	60.99	0.0196	0.0037
25.5	420	14.94	0.0428	0.0031
50.9	420	19.15	0.0407	0.0031
106.1	420	34.39	0.0330	0.0027
159.8	420	40.20	0.0301	0.0025
207.8	420	51.27	0.0245	0.0022
312.8	420	61.69	0.0193	0.0019

* quantification using the same response factor for lactic acid and 3-hydroxypropionic acid

Reactants with similar structure to lactic acid

Feed: Methyl lactate 0.1 mol l ⁻¹ ; Pressure: 350 bar										
T /°C	R.t. /s	Conv. /%	Conc. Lac /mol l ⁻¹	Conc. LacMe /mol l ⁻¹	Conc. Ald /mol l ⁻¹	Sel. Ald /%	Y. Ald /%	Conc. Acr /mol l ⁻¹	Sel. Acr /%	Y. Acr /%
350	31.6	9.63	0.0789	0.0117	0.0062	63.84	6.15	0.0037	38.24	3.68
	69.8	20.04	0.0757	0.0045	0.0108	53.72	10.77	0.0077	38.22	7.66
	150.8	36.83	0.0633	0	0.0161	43.59	16.06	0.0132	35.65	13.13
	227.2	44.58	0.0555	0	0.0179	40.13	17.89	0.0152	33.95	15.13
385	35.8	33.63	0.0575	0.0090	0.0160	47.51	15.98	0.0115	34.05	11.45
	74.3	55.81	0.0443	0	0.0240	42.93	23.96	0.0181	32.38	18.07
	146.3	69.51	0.0306	0	0.0292	41.86	29.10	0.0210	30.15	20.96
	228.2	77.64	0.0224	0	0.0297	38.14	29.61	0.0207	26.56	20.62

Feed: 2-hydroxy-isobutyric acid 0.1 mol l ⁻¹ ; Pressure: 350 bar; Temperature 385 °C			
R.t. /s	Conv. /%	Conc. Hba /mol l ⁻¹	Conc. Maa /mol l ⁻¹
50	93.19	0.0068	0.0881
100	92.69	0.0073	0.0799
200	93.29	0.0067	0.0702

Feed: Methacrylic acid 0.1 mol l ⁻¹ ; Pressure: 350 bar; Temperature 385 °C			
R.t. /s	Conv. /%	Conc. Maa /mol l ⁻¹	Conc. Hba* /mol l ⁻¹
50	12.01	0.0441	0.0028
100	17.19	0.0415	0.0033
200	25.25	0.0375	0.0031

*isomery has been neglected in HPLC analysis

Feed: 2-hydroxy-3-methylbutyric acid 0.1 mol l ⁻¹ ; Pressure: 350 bar; Temperature 385 °C			
R.t. /s	Conv. /%	Conc. Hmb /mol l ⁻¹	Conc. Mba /mol l ⁻¹
50	92.19	0.0079	0.0005
100	88.76	0.0113	0
200	86.63	0.0135	0

Feed: 2-methyl-3-butenic acid 0.1 mol l ⁻¹ ; Pressure: 350 bar; Temperature 385 °C			
R.t. /s	Conv. /%	Conc. Hmb* /mol l ⁻¹	Conc. Mba /mol l ⁻¹
50	93.70	0.0066	0.0032
100	98.89	0.0102	0.0006
200	99.04	0.0116	0.0005

*isomery has been neglected in HPLC analysis

Feed: 2-Methoxypropionic acid 0.1 mol l ⁻¹ ; Pressure: 350 bar; Temperature: 385 °C								
R.t. /s	Conv. /%	Conc. Lac /mol l ⁻¹	Conc. Ald /mol l ⁻¹	Sel. Ald /%	Y. Ald /%	Conc. Acr /mol l ⁻¹	Sel. Acr /%	Y. Acr /%
50	41.70	0.0585	0.0203	48.52	20.23	0.0149	35.61	14.85
100	65.74	0.0344	0.0326	49.44	32.50	0.0232	35.17	23.12
200	84.92	0.0151	0.0427	50.15	42.58	0.0267	31.38	26.64

Feed: Lactic acid 0.1 mol l ⁻¹ ; Pressure: 350 bar; Temperature: 385 °C								
R.t. /s	Conv. /%	Conc. Lac /mol l ⁻¹	Conc. Ald /mol l ⁻¹	Sel. Ald /%	Y. Ald /%	Conc. Acr /mol l ⁻¹	Sel. Acr /%	Y. Acr /%
50	34.11	0.0653	0.0190	56.32	19.21	0.0159	47.02	16.04
100	58.53	0.0411	0.0300	51.74	30.28	0.0253	43.58	25.51
200	82.42	0.0174	0.0402	49.21	40.56	0.0290	35.48	29.24

Feed: 3-hydroxypropionic acid (Hpa) 0.1 mol l ⁻¹ ; Pressure: 350 bar; Temperature: 385 °C								
R.t. /s	Conv. /%	Conc. Hpa /mol l ⁻¹	Conc. Ald* /mol l ⁻¹	Sel. Ald* /%	Y. Ald* /%	Conc. Acr /mol l ⁻¹	Sel. Acr /%	Y. Acr /%
49.9	34.11	0.0126	0.0026	3.00	2.6218	0.0472	53.98	47.18
102.1	58.53	0.0178	0.0015	1.88	1.5471	0.0586	71.31	58.60
206.6	82.42	0.0257	0	0	0	0.0605	81.38	60.46

* "Ald"- can not be acetaldehyde as shown by ¹H-NMR analysis; there is a peak, however, corresponding to the retention time of acetaldehyde.

Feed: Methyl lactate 0.1 mol l ⁻¹ ; Pressure: 350 bar; Temperature: 385 °C; Residence time: 100 seconds								
Conc. KOH /ppm	Conv. /%	Conc. Lac /mol l ⁻¹	Conc. Ald /mol l ⁻¹	Sel. Ald /%	Y. Ald /%	Conc. Acr /mol l ⁻¹	Sel. Acr /%	Y. Acr /%
500	61.55	0.0430	0.0153	30.69	16.50	0.0115	23.01	12.37
1000	62.29	0.0423	0.0172	33.92	18.48	0.0089	17.67	9.63

Influence of acids

Acetic acid

Feed: Lactic acid 0.1 mol l ⁻¹ ; Pressure: 350 bar; Temperature: 385 °C; Residence time: 100 seconds								
Conc. AcOH /mol l ⁻¹	Conv. /%	Conc. Lac /mol l ⁻¹	Conc. Ald /mol l ⁻¹	Sel. Ald /%	Y. Ald /%	Conc. Acr /mol l ⁻¹	Sel. Acr /%	Y. Acr /%
0.01	60.17	0.0397	0.0244	40.69	24.48	0.0195	32.56	19.59
0.03	59.95	0.0399	0.0267	44.66	26.77	0.0198	33.04	19.81
0.07	60.02	0.0399	0.0269	44.88	26.94	0.0201	33.56	20.14
0.18	61.43	0.0385	0.0327	53.40	32.80	0.0198	32.32	19.85

Phosphoric acid

Feed: Lactic acid 0.1 mol l ⁻¹ ; Pressure: 350 bar; Residence time: 100 seconds									
T /°C	Conc. H ₃ PO ₄ /mol l ⁻¹	Conv. /%	Conc. Lac /mol l ⁻¹	Conc. Ald /mol l ⁻¹	Sel. Ald /%	Y. Ald /%	Conc. Acr /mol l ⁻¹	Sel. Acr /%	Y. Acr /%
350	0.14	54.13	0.0450	0.0447	84.16	45.55	0.0054	10.11	5.47
385	0.01	63.20	0.0361	0.0401	64.68	40.88	0.0179	28.86	18.24
385	0.03	71.69	0.0278	0.0498	70.80	50.76	0.0143	20.26	14.52
385	0.07	81.49	0.0182	0.0638	79.67	64.92	0.0100	12.48	10.17
385	0.14	86.12	0.0136	0.0708	83.67	72.06	0.0080	9.41	8.11

Influence of bases

Feed: Lactic acid 0.1 mol l ⁻¹ ; Pressure: 350 bar; Temperature: 385 °C; Residence time: 100 seconds								
Conc. LiOH /ppm	Conv. /%	Conc. Lac / mol l ⁻¹	Conc. Ald / mol l ⁻¹	Sel. Ald /%	Y. Ald /%	Conc. Acr /mol l ⁻¹	Sel. Acr /%	Y. Acr /%
100	61.28	0.0388	0.0121	19.76	12.11	0.0148	24.09	14.76
500	57.46	0.0426	0.0168	29.16	16.76	0.0095	16.48	9.47
1000	53.40	0.0467	0.0168	31.39	16.76	0.0055	10.24	5.47
Conc.KOH /ppm	Conv. /%	Conc. Lac / mol l ⁻¹	Conc. Ald / mol l ⁻¹	Sel. Ald /%	Y. Ald /%	Conc. Acr /mol l ⁻¹	Sel. Acr /%	Y. Acr /%
100	53.40	0.0467	0.0130	24.33	13.00	0.0165	30.89	16.50
500	58.91	0.0412	0.0166	28.13	16.58	0.0134	22.69	13.37
1000	58.23	0.0418	0.0167	28.66	16.69	0.0109	18.72	10.90
Conc. CsOH /ppm	Conv. /%	Conc. Lac / mol l ⁻¹	Conc. Ald / mol l ⁻¹	Sel. Ald /%	Y. Ald /%	Conc. Acr /mol l ⁻¹	Sel. Acr /%	Y. Acr /%
100	57.47	0.0426	0.0206	35.85	20.60	0.0168	29.15	16.75
500	58.45	0.0416	0.0162	27.69	16.19	0.0157	26.78	15.65
1000	56.58	0.0435	0.0151	26.64	15.08	0.0141	24.93	14.11

Gas phase analysis

Feed: Lactic acid 0.1 mol l ⁻¹ ; Pressure: 350 bar					
T /°C	R.t. /s	CO /% mol	CO ₂ /% mol	C ₂ H ₄ /% mol	CO/CO ₂ Ratio
350	50	0.8589	0.0728	0.0132	11.80
350	50	0.8272	0.0654	0.0106	12.65
350	100	0.8219	0.0701	0.0258	11.72
350	200	0.8568	0.1073	0.0447	7.99
385	50	0.8527	0.0741	0.0294	11.51
385	100	0.7774	0.1001	0.0559	7.77
385	200	0.6755	0.1623	0.0873	4.16
420	50	0.8342	0.0657	0.0121	12.70
420	100	0.7338	0.0996	0.0185	7.37
420	200	0.6435	0.1296	0.0250	4.97

Feed: Acetaldehyde 0.05 mol l ⁻¹ ; Pressure: 350 bar					
T /°C	R.t. /s	CO /% mol	CO ₂ /% mol	C ₂ H ₄ /% mol	CO/CO ₂ Ratio
425	150	0.3735	0.0207	0.0003	18.04

¹H-NMR Analysis of the Lactic acid/3-hydroxypropionic acid molar ratio and regressions used to determine the concentrations of the two isomers

Feed: Lactic acid 0.1 mol l ⁻¹ ; Pressure: 350 bar		
T /°C	R.t. /s	Lac/Hpa molar ratio
350	25	-
	50	-
	100	-
	890	9.52
385	65	66.67
	80	33.33
	150	22.22
420	50	66.67
	100	33.33
	200	13.33

Feed: Acrylic acid 0.05 mol l ⁻¹ ; Pressure: 350 bar		
T /°C	R.t. /s	Lac/Hpa molar ratio
350	25	0.09
	50	0.16
	100	0.28
385	25	0.24
	80	0.59
	100	0.69
	150	0.74
420	25	0.10
	80	0.29
	200	0.27

Feed: Lactic acid 0.1 mol l ⁻¹ ; Pressure: 350 bar; 200 ppm KH ₂ PO ₄		
T /°C	R.t. /s	Lac/Hpa molar ratio
350	25	133.33
	150	13.33
	300	5.56
385	16.5	296.30
	150	22.22
	350	9.52
420	50	66.67
	100	33.33
	200	13.33

Feed: Acrylic acid 0.05 mol l ⁻¹ ; Pressure: 350 bar; 200 ppm KH ₂ PO ₄		
T /°C	R.t. /s	Lac/Hpa molar ratio
350	20	0.11
	200	0.36
	500	0.55
385	25	0.23
	150	0.60
	350	0.78
420	25	0.19
	150	0.31
	300	0.32

Feed	Catalyst /g g ⁻¹	Temp. /°C	Regression: Lac/Hpa molar ratio at residence time τ
Lac 0.1 M	200 ppm KH ₂ PO ₄	385	$7008.9 \cdot \tau^{-1.1351}$
Acr 0.05 M	200 ppm KH ₂ PO ₄	350	$-2 \cdot 10^{-6} \cdot \tau^2 + 0.0017 \cdot \tau + 0.0806$
Acr 0.05 M	200 ppm KH ₂ PO ₄	385	$0.2072 \cdot \ln(\tau) - 0.4402$
Acr 0.05 M	200 ppm KH ₂ PO ₄	420	$-3 \cdot 10^{-6} \cdot \tau^2 + 0.0015 \cdot \tau + 0.1535$
Acr 0.05 M	-	385	$0.2833 \cdot \ln(\tau) - 0.668$
Acr 0.05 M	-	420	$\frac{9.26 \cdot 10^{-5} \cdot \tau^3 + 0.6346 \cdot \tau^2 + 1.571 \cdot \tau + 1.0295}{9.26 \cdot 10^{-5} \cdot \tau^3 + 0.1582 \cdot \tau^2 + 1.527 \cdot \tau + 0.867}$

Data used for the simulation

Concentrations are given in mol/l and are calculated at the conditions from reactor; "-1" as a concentration refers to concentrations which are not to be taken into account by the software

Data from experiments without catalyst

	R.t. /s	Lac /mol l ⁻¹	Ald /mol l ⁻¹	Acr /mol l ⁻¹	D /mol l ⁻¹	Acr1 /mol l ⁻¹	Hpa1 /mol l ⁻¹	D1 /mol l ⁻¹
350 °C	0	0.0663	0	0	0	0.0330	0	0
	18.0	0.0635	0.0023	0.0014	-1	-1	-1	-1
	25.6	-1	-1	-1	-1	0.0297	0.0011	0.0023
	32.2	0.0612	0.0035	0.0026	-1	-1	-1	-1
	50.0	0.0579	0.0049	0.0038	-1	-1	-1	-1
	51.2	-1	-1	-1	-1	0.0279	0.0017	0.0034
	65.3	0.0564	0.0057	0.0048	-1	-1	-1	-1
	100.1	0.0515	0.0076	0.0074	-1	-1	-1	-1
	100.2	-1	-1	-1	-1	0.0278	0.0028	0.0024
	101.2	0.0505	0.0082	0.0069	0.0007	-1	-1	-1
	150.8	0.0464	0.0099	0.0083	0.0016	-1	-1	-1
	153.7	-1	-1	-1	-1	0.0267	0.0032	0.0032
	190.5	0.0443	0.0092	0.0106	0.0021	-1	-1	-1
	206.2	-1	-1	-1	-1	0.0256	0.0034	0.0040
	253.5	0.0398	0.0131	0.0104	0.0030	-1	-1	-1
	304.2	-1	-1	-1	-1	0.0237	0.0038	0.0055
305.7	0.0392	0.0111	0.0124	0.0036	-1	-1	-1	

	R.t. /s	Lac /mol l ⁻¹	Ald /mol l ⁻¹	Acr /mol l ⁻¹	D /mol l ⁻¹	Acr1 /mol l ⁻¹	Hpa1 /mol l ⁻¹	Lac1 /mol l ⁻¹	D1 /mol l ⁻¹
385 °C	0	0.0509	0	0	0	0.0276	0	0	0
	16.6	0.0462	0.0051	0.0042	-1	-1	-1	-1	-1
	20.2	0.0426	0.0065	0.0050	-1	-1	-1	-1	-1
	31.9	0.0393	0.0083	0.0069	-1	-1	-1	-1	-1
	50.2	-1	-1	-1	-1	0.0234	0.0011	0.0005	0.0026
	64.6	0.0297	0.0130	0.0107	-1	-1	-1	-1	-1
	83.0	0.0265	0.0139	0.0105	0	-1	-1	-1	-1
	98.7	0.0250	0.0151	0.0121	-1	-1	-1	-1	-1
	101.3	-1	-1	-1	-1	0.0218	0.0012	0.0007	0.0039
	149.9	-1	-1	-1	-1	0.0202	0.0011	0.0008	0.0054
	151.4	0.0178	0.0177	0.0119	0.0035	-1	-1	-1	-1
	192.0	0.0156	0.0176	0.0135	0.0043	-1	-1	-1	-1
	199.4	-1	-1	-1	-1	0.0185	0.0011	0.0009	0.0071
	251.4	0.0123	0.0180	0.0115	0.0091	-1	-1	-1	-1
	307.0	0.0117	0.0175	0.0121	0.0096	-1	-1	-1	-1
	320.9	-1	-1	-1	-1	0.0169	0.0010	0.0009	0.0088

	R.t. /s	Lac /mol l ⁻¹	Ald /mol l ⁻¹	Acr /mol l ⁻¹	D /mol l ⁻¹	Acr1 /mol l ⁻¹	Hpa1 /mol l ⁻¹	Lac1 /mol l ⁻¹	D1 /mol l ⁻¹
420 °C	0	0.0300	0	0	0	0.0163	0	0	0
	16.1	0.0176	0.0111	0.0032	-1	-1	-1	-1	-1
	22.6	-1	-1	-1	-1	0.0137	0.0010	0.0001	0.0014
	32.1	0.0120	0.0142	0.0039	-1	-1	-1	-1	-1
	50.0	-1	-1	-1	-1	0.0127	0.0010	0.0002	0.0024
	51.0	0.0085	0.0166	0.0038	0.0035	-1	-1	-1	-1
	64.2	0.0066	0.0171	0.0042	0.0022	-1	-1	-1	-1
	101.2	0.0054	0.0172	0.0053	0.0044	-1	-1	-1	-1
	101.8	0.0032	0.0166	0.0038	0.0064	-1	-1	-1	-1
	105.6	-1	-1	-1	-1	0.0117	0.0008	0.0002	0.0035
	160.9	-1	-1	-1	-1	0.0107	0.0006	0.0002	0.0047
	179.4	0.0013	0.0167	0.0030	0.0091	-1	-1	-1	-1
	205.0	0.0018	0.0184	0.0036	0.0081	-1	-1	-1	-1
	219.4	-1	-1	-1	-1	0.0100	0.0006	0.0002	0.0055
	245.3	0.0017	0.0185	0.0038	0.0079	-1	-1	-1	-1
	320.7	0.0008	0.0171	0.0025	0.0096	-1	-1	-1	-1
	344.7	-1	-1	-1	-1	0.0086	0.0005	0.0001	0.0070

Data from experiments with 200 ppm KH₂PO₄

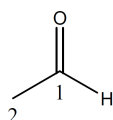
	R.t. /s	Lac /mol l ⁻¹	Ald /mol l ⁻¹	Acr /mol l ⁻¹	D /mol l ⁻¹	Acr1 /mol l ⁻¹	Hpa1 /mol l ⁻¹	Lac1 /mol l ⁻¹	D1 /mol l ⁻¹
350 °C	0	0.0660	0	0	0	0.0331	0	0	0
	20.2	0.0611	0.0025	0.0019	0.0002	-1	-1	-1	-1
	20.5	-1	-1	-1	-1	0.0303	0.0018	0.0002	0.0009
	25.4	0.0599	0.0024	0.0022	0.0012	-1	-1	-1	-1
	40.9	-1	-1	-1	-1	0.0282	0.0024	0.0004	0.0022
	50.7	0.0555	0.0032	0.0043	0.0026	-1	-1	-1	-1
	80.3	0.0524	0.0042	0.0060	0.0029	-1	-1	-1	-1
	80.4	-1	-1	-1	-1	0.0248	0.0028	0.0006	0.0050
	102.3	0.0487	0.0051	0.0074	0.0042	-1	-1	-1	-1
	150.8	-1	-1	-1	-1	0.0238	0.0033	0.0010	0.0050
	152.9	0.0447	0.0054	0.0092	0.0058	-1	-1	-1	-1
	155.5	0.0441	0.0061	0.0093	0.0056	-1	-1	-1	-1
	201.7	-1	-1	-1	-1	0.0231	0.0034	0.0012	0.0054
	205.0	0.0404	0.0066	0.0108	0.0071	-1	-1	-1	-1
	508.4	-1	-1	-1	-1	0.0174	0.0032	0.0014	0.0112
	609.4	0.0258	0.0076	0.0148	0.0155	-1	-1	-1	-1

	R.t. /s	Lac /mol l ⁻¹	Ald /mol l ⁻¹	Acr /mol l ⁻¹	Hpa /mol l ⁻¹	D /mol l ⁻¹	Acr1 /mol l ⁻¹	Hpa1 /mol l ⁻¹	Lac1 /mol l ⁻¹	Ald1 /mol l ⁻¹	D1 /mol l ⁻¹
385 °C	0	0.0550	0	0	0	0	0.0277	0	0	0	0
	16.8	0.0432	0.0040	0.0047	0.0002	0.0029	-1	-1	-1	-1	-1
	25.6	-1	-1	-1	-1	-1	0.0232	0.0017	0.0004	0.0003	0.0021
	38.9	-1	-1	-1	-1	-1	0.0219	0.0018	0.0006	0.0002	0.0032
	50.9	0.0315	0.0081	0.0096	0.0004	0.0054	-1	-1	-1	-1	-1
	81.7	0.0251	0.0104	0.0119	0.0005	0.0071	-1	-1	-1	-1	-1
	103.2	-1	-1	-1	-1	-1	0.0186	0.0017	0.0009	0.0005	0.0060
	103.5	0.0216	0.0108	0.0132	0.0006	0.0087	-1	-1	-1	-1	-1
	154.0	0.0165	0.0119	0.0142	0.0007	0.0117	-1	-1	-1	-1	-1
	156.0	-1	-1	-1	-1	-1	0.0174	0.0016	0.0009	0.0006	0.0072
	186.0	0.0147	0.0139	0.0144	0.0008	0.0113	-1	-1	-1	-1	-1
	197.4	0.0143	0.0135	0.0144	0.0008	0.0120	-1	-1	-1	-1	-1
	204.2	-1	-1	-1	-1	-1	0.0157	0.0015	0.0010	0.0008	0.0089
	361.6	0.0082	0.0127	0.0136	0.0009	0.0195	-1	-1	-1	-1	-1
	365.2	-1	-1	-1	-1	-1	0.0108	0.0011	0.0009	0.0011	0.0138

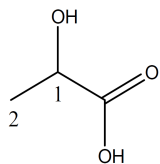
	R.t. /s	Lac /mol l ⁻¹	Ald /mol l ⁻¹	Acr /mol l ⁻¹	Hpa /mol l ⁻¹	D /mol l ⁻¹	Acr1 /mol l ⁻¹	Hpa1 /mol l ⁻¹	Lac1 /mol l ⁻¹	Ald1 /mol l ⁻¹	D1 /mol l ⁻¹
420 °C	0	0.0325	0	0	0	0	0.0164	0	0	0	0
	10.0	0.0199	0.0066	0.0033	0	0.0027	-1	-1	-1	-1	-1
	25.5	-1	-1	-1	-1	-1	0.0139	0.0008	0.0002	0.0002	0.0012
	25.8	0.0126	0.0123	0.0041	0.0001	0.0034	-1	-1	-1	-1	-1
	50.8	0.0093	0.0149	0.0041	0.0002	0.0040	-1	-1	-1	-1	-1
	50.9	-1	-1	-1	-1	-1	0.0132	0.0008	0.0002	0.0003	0.0018
	81.4	0.0056	0.0178	0.0046	0.0002	0.0043	-1	-1	-1	-1	-1
	102.2	0.0038	0.0183	0.0056	0.0002	0.0047	-1	-1	-1	-1	-1
	106.1	-1	-1	-1	-1	-1	0.0107	0.0007	0.0002	0.0006	0.0042
	129.4	0.0029	0.0188	0.0051	0.0002	0.0055	-1	-1	-1	-1	-1
	153.9	0.0025	0.0177	0.0050	0.0002	0.0071	-1	-1	-1	-1	-1
	159.8	-1	-1	-1	-1	-1	0.0098	0.0006	0.0002	0.0006	0.0051
	207.8	-1	-1	-1	-1	-1	0.0080	0.0005	0.0002	0.0008	0.0069
	208.8	0.0022	0.0197	0.0042	0.0003	0.0061	-1	-1	-1	-1	-1
	312.8	-1	-1	-1	-1	-1	0.0063	0.0005	0.0002	0.0009	0.0086
313.9	0.0014	0.0176	0.0037	0.0003	0.0096	-1	-1	-1	-1	-1	

¹H-NMR Data of the reactor samples

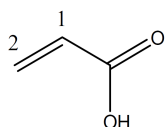
The spectra have been acquired using a Bruker DRX-500 spectrometer. The samples consisted of aqueous solutions to which D₂O has been added. The chemical shift, δ , is given in ppm and is relative to the tetramethylsilane (TMS) internal standard. In brackets, the number of signals (singlet, doublet, triplet, etc.), the number of protons involved as well as an identification label are given in this order. The spin-spin coupling constant, J , is given in Hz with a superscript indicating the number of bonds separating the nuclei. All measurements were carried out at room temperature with a resolution of 500 MHz.



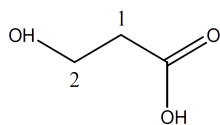
Acetaldehyde: ¹H-NMR (500 MHz, H₂O/D₂O, TMS): $\delta = 2.166$ (d, 3H, 2H), 9.600 (q, 1H, 1H) ppm; ³ $J_{1\text{H},2\text{H}} = 3.0$ Hz.



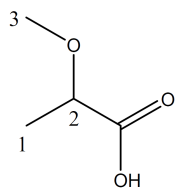
Lactic acid: ¹H-NMR (500 MHz, H₂O/D₂O, TMS): $\delta = 1.345$ (d, 1H, 2H), 4.310 (q, 1H, 1H) ppm; ³ $J_{1\text{H},2\text{H}} = 7.0$ Hz.



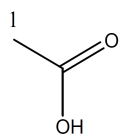
Acrylic acid: ¹H-NMR (500 MHz, H₂O/D₂O, TMS): $\delta = 5.920$ (dd, 1H, 2H_{cis}), 6.105 (dd, 1H, 1H), 6.335 (dd, 1H, 2H_{trans}) ppm; ³ $J_{1\text{H},2\text{H}_{\text{cis}}} = 10.5$ Hz; ² $J_{2\text{H},2\text{H}_{\text{geminal}}} = 0.75$ Hz; ³ $J_{1\text{H},2\text{H}_{\text{trans}}} = 17.5$ Hz.



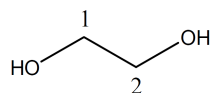
3-Hydroxypropionic acid: ¹H-NMR (500 MHz, H₂O/D₂O, TMS): $\delta = 2.544$ (t, 2H, 1H), 3.785 (t, 2H, 2H) ppm; ³ $J_{1\text{H},2\text{H}} = 6.0$ Hz.



2-Methoxypropionic acid: $^1\text{H-NMR}$ (500 MHz, $\text{H}_2\text{O}/\text{D}_2\text{O}$, TMS): $\delta = 1.292$ (d, 3H, 1H), 3.285 (s, 3H, 3H), 3.943 (q, 1H, 2H) ppm; $^3J_{1\text{H},2\text{H}} = 7.0$ Hz.



Acetic acid: $^1\text{H-NMR}$ (500 MHz, $\text{H}_2\text{O}/\text{D}_2\text{O}$, TMS): $\delta = 2.080$ (s, 3H, 1H) ppm.



Ethylene glycol: $^1\text{H-NMR}$ (500 MHz, $\text{H}_2\text{O}/\text{D}_2\text{O}$, TMS): $\delta = 3.598$ (s, 4H, 1H) ppm.

Chemical substances used in experiments

Substance	CAS No.	Concentration /%	Manufacturer
Acetaldehyde	75-07-0	99.5	Acros
Acetic acid	64-19-7	99.8	Acros
Acrylic acid	79-10-7	99	BASF
DL-2-bromopropionic acid	598-72-1	99+	Acros
Cesium hydroxide, monohydrate	35103-79-8	99.5	Acros
Ethyl acetate	141-78-6	99.5+	Acros
2-hydroxyisobutyric acid	594-61-6	98	Acros
3-hydroxypropionic acid	503-66-2	30	TCI
(S)-(+)-2-hydroxy-3-methylbutanoic acid	17407-55-5	99+	Acros
DL-Lactic acid	50-21-5	85	Acros
Lactic acid, lithium salt	867-55-0	99	Acros
Lithium hydroxide	1310-65-2	98	Merck
Methanol	67-56-1	99+	Acros
Magnesium sulfate, anhydrous	7487-88-9	97	Acros
3-methyl-2-butenic acid	541-47-9	97	Sigma-Aldrich
Methyl-(S)-(-)-lactate	27871-49-4	97	Acros
Phosphoric acid	7664-38-2	85	Acros

Potassium hydroxide	1310-58-3	85	Acros
Potassium hydrogen carbonate	298-14-6	99	Merck
Potassium phosphate, dibasic, anhydrous	7758-11-4	99	Acros
Potassium phosphate, monobasic	7778-77-0	99	Acros
Propionic acid	79-09-4	99	Aldrich
Sodium hydroxide	1310-73-2	99	Merck
Sodium methoxide	124-41-4	99	Acros
Sodium sulfate, anhydrous	7757-82-6	99	Acros
Sulfuric acid	7664-93-9	for standard 0.5 M solution	Merck
Zinc sulfate, heptahydrate	7446-20-0	99	Merck

Zusammenfassung

Acrylsäure findet eine Anwendung in der chemischen Industrie als Zwischenprodukt für die Synthese von Polyacrylaten und Kopolymeren, die in der Formulierung von Farbstoffen, Lacken usw. angewendet werden. Industriell wird Acrylsäure aus Naphta über Propen hergestellt und ist dadurch von der Erdöl- und Erdgasknappheit betroffen.

Eine Möglichkeit für die Herstellung von Acrylsäure aus nachwachsenden Rohstoffen ist die Nutzung von Milchsäure und deren Dehydratisierung in nah- und überkritischem Wasser. Überkritisches Wasser ist ein sauberes, umweltschonendes Reaktionsmedium. Milchsäure kann aus Kohlenhydraten gewonnen werden und steht damit in großen Mengen zur Verfügung, findet allerdings noch wenige industrielle Anwendungen.

Versuche Milchsäurederivate zu Acrylsäurederivaten umzusetzen existieren schon seit ungefähr 70 Jahren. Dennoch hat dieser synthetische Weg bis dato keine industrielle Anwendung gefunden.

Im Rahmen dieser Arbeit wurden Experimente entworfen und durchgeführt, die dem Zweck dienen, die Reaktion zur Herstellung von Acrylsäure näher zu bringen. Insofern wurden die Reaktionskinetik und der Reaktionsmechanismus untersucht, um optimale Reaktionsbedingungen zu finden.

Eine Versuchsanlage für die Durchführung der Experimente im überkritischen Wasser wurde aufgebaut und eine passende Methode für die Quantifizierung der im Reaktionsgemisch anwesenden Substanzen sowohl in der Flüssigphase als auch in der Gasphase entwickelt.

Um optimale Reaktionsbedingungen zu finden, wurde der Einfluss von unterschiedlichen Parametern wie Temperatur, Druck, Konzentration des Eduktes und Verweilzeit auf die Reaktion untersucht. Des Weiteren wurde der Einfluss der Zugabe von Säuren, Basen und Salzen untersucht. Ein Optimum für die Reaktion wurde bei 385 °C, 350 bar und 200 Sekunden Verweilzeit gefunden. Bei denselben Bedingungen sinkt die Selektivität zu Acetaldehyd (dem wichtigsten Nebenprodukt der Reaktion) um 5 bis 6 %, wenn eine Menge von 200 ppm (g g^{-1}) Kaliumdihydrogenphosphat in der Eduktlösung anwesend ist.

Die Stabilität von Acrylsäure in nah- und überkritischem Wasser wurde untersucht. Es wurde festgestellt, dass die Addition von Wasser zu Acrylsäure nicht nur zu 3-Hydroxypropionsäure, dem normalen Produkt einer Markovnikov-Addition, führt, sondern auch zu Milchsäure, insbesondere bei 390 °C, wo sich das Stoffmengenverhältnis von Milch- zu 3-Hydroxypropionsäure einem Wert von eins nähert.

Ein bislang ungeklärtes Problem bei der Aufklärung des Reaktionsmechanismus betrifft die Decarboxylierung von Milchsäure. Es kann zwar Kohlendioxid detektiert werden, aber das erwartete Decarboxylierungsprodukt Ethanol ist im Reaktionsgemisch unter keinen Bedingungen zu finden. Stattdessen findet man nur Acetaldehyd. Demzufolge wurde in der Fachliteratur postuliert, dass die Decarboxylierung von Milchsäure eine radikalische Reaktion ist. In dieser Arbeit wurde gezeigt, dass die Decarboxylierung von Milchsäure nicht stattfindet und die größten Mengen von Kohlendioxid durch die Wassergas-Shift-Reaktion aus Kohlenmonoxid entstehen.

Ein kinetisches Modell basierend auf den experimentellen Daten wurde entwickelt. Die Geschwindigkeitskonstanten für die Reaktionen, in denen Acetaldehyd, Acryl-, Milch- und 3-Hydroxypropionsäure beteiligt sind, wurden mit Hilfe einer Simulationssoftware für drei Temperaturen (350, 385 und 420 °C) ermittelt.

Horea Szedlacsek

Am Pelz 82

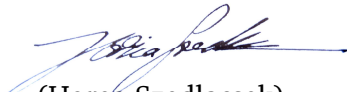
64295 Darmstadt

e-mail: horea.szedlacsek@googlemail.com

Darmstadt, 07.11.2012

Erklärung

Ich erkläre hiermit, dass ich meine Dissertation selbstständig und nur mit den angegebenen Hilfsmitteln angefertigt habe.


(Horea Szedlacsek)

Horea Szedlacsek

Am Pelz 82


64295 Darmstadt

e-mail: horea.szedlacsek@googlemail.com

Darmstadt, 07.11.2012

Erklärung

Ich erkläre hiermit, noch keinen Promotionsversuch unternommen zu haben.



(Horea Szedlacsek)

Lebenslauf

Persönliche Daten

Horea Szedlacsek

Adresse:

E-mail:

Geburtsdag:

Staatsbürgerschaft:

Geburtsort:

Am Pelz 82, 64295 Darmstadt

horea.szedlacsek@googlemail.com

16. November 1981

rumänisch

Bukarest, Rumänien

Berufserfahrung

01.12.2006 – 01.04.2011

Promotion an der TU–Darmstadt

Arbeitskreis Prof. Dr. Vogel

Thema: *Herstellung von Acrylsäure aus nachwachsenden Rohstoffen in überkritischen Medien*

01.04.2005 – 30.09.2005

Diplomarbeit

Jena BioScience GmbH, Jena

Thema: *Synthese eines Guanosinriphosphatderivates und dessen Immobilisierung auf Agar*

Ausbildung

02.10.2000 – 14.02.2006

Studium Chemietechnik

„Politehnica“ Universität, Bukarest, Rumänien

Abschluss: Dipl.-Ing. – Chemietechnik

16.09.1996 – 30.06.2000

Oberstufe: Colegiul Național „Mihai-Viteazul“,
Gymnasium, Bukarest, Rumänien

Abschluss: Abitur



(Horea Szedlacsek)

Darmstadt, 7. November 2012